CHARACTERIZATION OF FUNCTIONAL AND MOLECULAR PROPERTIES OF CIRCULATING EXTRACELLULAR VESICLES OF CHILDHOOD IDIOPATHIC NEPHROTIC SYNDROME PATIENTS

A DISSERTATION SUBMITTED TO
THE GRADUATE SCHOOL OF ENGINEERING AND SCIENCE OF
BILKENT UNIVERSITY
IN PARTIAL FULLFILMENT OF THE REQUIREMENTS
FOR THE DEGREE OF
DOCTOR OF PHILOSOPHY
IN
MOLECULAR BIOLOGY AND GENETICS

By
Fehime Kara Eroğlu

OCTOBER 2021

CHARACTERIZATION OF FUNCTIONAL AND MOLECULAR PROPERTIES OF CIRCULATING EXTRACELLULAR VESICLES OF CHILDHOOD IDIOPATHIC NEPHROTIC SYNDROME PATIENTS

By Fehime Kara Eroğlu

October 2021

We certify that we have read this dissertation on and that in our opinion it is fully adequate, in scope and in quality, as a dissertation for the degree of Doctor of Philosophy.

İhsan Gürsel (Advisor)

Hasan Tayfun Özçelik

Mayda Gürsel

Ali Düzova

Serkan Belkaya

Approved for the Graduate School of Engineering and Science

Ezhan Karaşan

Director of the Graduate School of Engineering and Science

To my love Mehmet

To my star Ece Feride

To my luck Oğuz Fuat

ABSTRACT

CHARACTERIZATION OF FUNCTIONAL AND MOLECULAR PROPERTIES OF CIRCULATING EXTRACELLULAR VESICLES OF CHILDHOOD IDIOPATHIC NEPHROTIC SYNDROME PATIENTS

Fehime Kara Eroğlu
PhD in Molecular Biology and Genetics
Advisor: İhsan Gürsel
October 2021

Nephrotic syndrome (NS) is one of the most common causes of glomerular disease in children and is characterized by the triad of proteinuria, hypoalbuminemia, and edema. The major molecular event in the pathogenesis of NS is the disruption of the glomerular filtration barrier, which is primarily driven by podocyte injury. The most common clinical presentation of NS in children is steroid-sensitive nephrotic syndrome (SSNS), characterized by complete remission within 4 weeks of steroid therapy and no apparent glomerular change in the light microscopic evaluation of kidney biopsies, thereby named as Minimal Change Disease (MCD). Since previous research suggests a role of a circulating factor in the pathogenesis of steroid-sensitive nephrotic syndrome (SSNS), we speculated that circulating plasma extracellular vesicles (EVs) are a candidate source of such a soluble mediator. Here, we aimed to characterize and try to delineate the effects of these EVs *in vitro*. Plasma EVs from 20 children with SSNS in relapse and remission, 10 healthy controls and 6 disease controls were obtained by serial ultracentrifugation. Characterization of these EVs was performed by electron microscopy, flow cytometry and western blotting. The major proteins from the plasma EVs were identified via mass spectrometry. A Gene Ontology classification analysis and ingenuity pathway analysis were performed on selectively expressed EV proteins during relapse. Immortalized human podocyte culture was used to detect the effects of EVs on podocytes. The protein content and the particle number of plasma EVs were significantly increased during NS relapse. Relapse NS EVs selectively express proteins which involved actin cytoskeleton rearrangement. Among these, the level of RAC-GTP was significantly increased in relapse EVs compared to remission and disease control EVs. Relapse EVs were efficiently internalized by podocytes and induced significantly enhanced motility and albumin permeability. Moreover, relapse EVs induced significantly higher levels of RAC-GTP and phospho p38 (p-p38) and decreased levels of synaptopodin in podocytes. Circulating relapse EVs are biologically active molecules that carry active RAC1 as cargo and induce recapitulation of the nephrotic syndrome phenotype in podocytes *in vitro*.

Keywords: Nephrotic syndrome, children, extracellular vesicles, RAC1, phospho-p38

ÖZET

ÇOCUKLUK ÇAĞI İDİYOPATİK NEFROTİK SENDROM HASTALARININ DOLAŞIMDA BULUNAN HÜCRE DIŞI KESECİKLERİNİN FOKSİYONEL VE MOLEKÜLER ÖZELLİKLERİNİN KARAKTERİZASYONU

Fehime Kara Eroğlu
Moleküler Biyoloji ve Genetik, Doktora Tezi
Tez Danışmanı: Ihsan Gursel
Ekim 2021

Nefrotik sendrom çocukluk çağında en sık görülen glomerüler hastalık olup, proteinuri, ödem, hipoalbuminemi ile karakterizedir. Hastalığın patogenezinde en önemli etken podosit hasarı sonucu glomerüler filtrasyon bariyerinin hasar görmesidir. Çocukluk çağında nefrotik sendromun olgularının büyük çoğunluğu steroid yanıtlı nefrotik sendrom (SYNS) olarak tanımlanır ki bu hastalar 4 haftalık steroid tedavisi ile tamamen remisyona girerler ve böbrek biyopsisi ışık mikroskobik incelemesinde belirgin patolojik bulgu yoktur. Daha önceki çalışmalarda SYNS patogenezinde dolaşımda bulunan bir patolojik faktör suçlanmıştır, fakat bu faktör henüz net olarak ortaya konulamamıştır. Hücre dışı kesecikler bütün vücut sıvılarında bulunan ve taşıdıkları protein ve diğer biyolojik aktif moleküller sayesinde birçok hastalık patogenezinde son yıllarda gittikçe daha da çok araştırılan hücre parçacıklarıdır. Bu çalışmada dolaşımda bulunan hücre dışı keseciklerin SYNS patogenezinde rol oynayabileceğini öngördük ve bu keseciklerin özelliklerini ortaya koyarak, *in vitro* etkilerini araştırmayı amaçladık. Bu amaçla çocukluk çağındaki 20 SYNS hastası, 10 sağlıklı kontrol ve 6 diğer glomerüler hastalığı olan çocukların plazma hücre dışı kesiciklerini izole ederek elektron mikroskopi, akım sitometrisi ve immün blotlama yöntemi ile karakterize ettik. Ayrıca kütle spektormetresi ile proteinlerini tanımlayarak, hastalık aktif dönemde eksprese edilen proteinleri 'Ingenuity Pathway Analysis' veri analizi ile inceledik. Hücre dışı keseciklerin podositler üzerindeki etkilerini insan podosit kültürü ile inceledik. Sonuçlarımız ile SYNS hastalarının dolaşımında bulunan hücre dışı keseciklerinin sayısının ve protein miktarlarının arttığını gözlemledik. Ayrıca bu keseciklerde hastalığın aktif dönemlerinde daha çok aktin ve hücre iskelet düzenlemesi yapan proteinler selektif eksprese ediliyordu. Bu kesecikler podositlerin içine girebiliyor ve podositlerin hareketlenmesine ve albümin geçirgenliğinin artmasına sebep oluyorlardı. Ayrıca bu kesecikler podositlerin daha çok RAC-GTP ve fosforile p38 eksprese etmesine, sinaptopodin miktarının ise azalmasına neden oluyorlardı. Bu sonuçlar neticesinde nefrotik sendrom hastalarının dolaşımında bulunan hücre dışı kesciklerinin biyolojik olarak aktif olduklarını ve *in vitro* deney ortamında podositlerde hastalık bulgularının ortaya çıkmasına neden olduklarını gösterdik.
Anahtar kelimeler: Nefrotik sendrom, çocukluk çağı, hücre dışı kesecikler, RAC1, fosfo-p38

ACKNOWLEDGEMENTS

First and foremost, I have to thank my supervisor Prof Ihsan Gursel to give me, a clinician the opportunity to experience and work in laboratory. In these six years he has offered me advice, support and encouragement not only in science but also in my difficult times. Without his help, understanding and respect in every step throughout this work, this paper would have never been accomplished. I am proud of and grateful for working with him and wish to express my sincere thanks for his support and understanding over these past years.

I would also like to show my gratitude to Prof Mayda Gursel. Her way of thinking and enthusiasm for immunology made a strong impression on me. I feel me very lucky to meet her and to work with her. I would like to thank Prof Gursel for valuable feedbacks about my experiments.

I would also like to Prof Tayfun Ozcelik for his valuable time and suggestions during my thesis work. I have also learnt a lot from him and from other Faculty members during my classes.

Without knowing anything about the lab work, the first few years were very difficult for me. In these years Dr Bilgi Gungor, Ersin Gül and Naz Sürücü from METU encouraged me a lot. I would also thank to Dr Tamer Kahraman, Muzaffer Yıldırım, Göksu Gökberk Kaya from Bilkent THORLAB for their help and support. Tuğçe Canavar Yıldırım and Nilsu Turay also helped me with my experiments. I will always remember the joy and kindness of the 'the best team': İrem Evcili, Naz Bozbeyoğlu, Berfu Saraydar, Aslı Gülce Bartan, Bilgehan İbibik, Tugçe Bildik, Pınar Gur Cetinkaya and Artun Bulbul. I want to express my gratitude to the lab technicians Okan Erşahan and Abdullah Ünnü, lab managers Pelin Makas and Seda Şengül Birkan, to our veterinary physician Gamze Aykut and to our Faculty secretary Yıldız Kahyaoğlu and to Yavuz Ceylan for their invaluable help and support. I usually worked at nights and I would also specially thank to all of Bilkent Security Staff for enabling a trustworthy environment.

I would like to thank to Mehmet M. Altıntaş, PhD from Rush University for valuable suggestions about podocyte culture; Dr Ulku Guler and Prof Dr Bekir Salih from Hacettepe University for proteomics; to Volkan Yazar from THORLAB for proteomics analyses.

I wish to express my sincere thanks to the patients and families; to my colleagues, to our very special nurses and supporting staff from the Department of Pediatric Nephrology in Dr Sami Ulus Childrens' Hospital. Their support, help and kindness were very valuable for me.

Most importantly, none of this could have happened without my family. My mother and father take care of my children when I was in laboratory. Most importantly they did not question me, why I was struggling with that much work, and always trusted me. And my husband Mehmet was the greatest support to me in all those years. We have sacrificed a lot from our private life but he did not complain even once. Every time I was ready to quit, did not let me and I am forever grateful.

And finally, I would like to dedicate this work to all of the 'Women in Science'. As a mother, doctor and PhD student I know I could not be the 'perfect'. I have always been 'multitasker'. But, anyway, I did not give up and did it. As a mother, this dissertation stands the best testament to my unconditional love for my children. This is one of the best that I can do to provide them and to the other children a better future.

Contents

List of Figures

List of Tables

ABBREVIATIONS

Nephrotic syndrome	NS
Idiopathic Nephrotic syndrome	INS
Glomerular filtration barrier	GFB
Glomerular basement membrane	GBM
Minimal Change Disease	MCD
Focal segmental glomerulosclerosis	FSGS
Membranoproliferative glomerulonephritis	MPGN
Membranous nephropathy	MN
Steroid sensitive nephrotic syndrome	SSNS
Steroid resistant nephrotic syndrome	SRNS
Frequent relapsing nephrotic syndrome	FRNS
End stage renal disease	ESRD
Mesenchymal-to-epithelial transition	MET
Pre-tubular aggregate	PA
S-shaped body	SSB
Foot processes	FPs
Rho-guanosine triphosphatases	Rho-GTPases
Guanine nucleotide exchange factors	GEFs
GTPase activating proteins	GAPs
GDP dissociation inhibitors	GDIs
Mitogen activating protein kinase	MAPK
Foot process effacement	FPE
Chronic kidney disease	CKD
Human leucocyte antigen	HLA
Phospholipase c gamma 2	PLCγ2
T helper	Th
Immune dysregulation, polyendocrinopathy, enteropathy, X-linked	IPEX
Regulatory T cells	Tregs
Cluster of differentiation	CD
Interleukin	IL
Interleukin 13	IL13
Antibody-secreting cells	ASC

Antigen presenting cells	APCs
Lipopolysaccharide	LPS
Toll-like receptor 4	TLR4
Soluble urokinase plasminogen activator receptor	SUPAR
Puromycin aminonucleoside	PAN
Corticosteroid	CS
Calcineurin inhibitors	CNIs
Azathioprine	AZA
Mycophenolate mofetil	MMF
Steroid-dependent nephrotic syndrome	SDNS
Nuclear factor κB	NF-κB
Cyclosporine A	CsA
Sphingomyelin phosphodiesterase acid like 3B	SMPDL-3b
Extracellular vesicles	EVs
Multivesicular bodies	MVBs
Intraluminal vesicles	ILVs
Early-sorting endosome	ESE
Endosomal sorting complexes required for transport	ESCRT
Tumor susceptibility gene 101	TSG101
Apoptosis-linked gene 2-interacting protein X	ALIX
Phospholipase D2	PLD2
ADP-ribosylation factor 6	ARF6
Diacylglycerol kinase α	DGKα
Late-sorting endosomes	LSEs
Soluble *N*-ethylmaleimide- sensitive factor attachment protein receptors	SNAREs
Phosphatidylethanolamine	PE
Phosphatidylserine	PS
Tubuloepithelial cells	TECs
Macrophages	MQs
Bovine serum albumin	BSA
Angiotensin-converting enzyme	ACE
Enzyme-linked Immunosorbent Assay	ELISA
Room temperature	RT
Dulbecco's Phosphate-Buffered Saline	DPBS
Phosphate-Buffered Saline	PBS
Peripheral mononuclear cells	PBMCs

Roswell Park Memorial Institute	RPMI
Fetal bovine serum	FBS
Phorbol 12-myristate 13-acetate	PMA
Fluorescence Activated Cell Sorting	FACS
Interferon	IFN
Relative Centrifugal Force	RCF
p-Nitrophenly Phosphate	PNPP
Ultracentrifugation	UC
Transmission electron microscopy	TEM
Dithiothreitol	DTT
Iodoacetamide	IAA
Ingenuity Pathway Analysis	IPA
Insulin Transferrin Selenium	ITS
Sodium dodecyl sulfate–polyacrylamide gel electrophoresis	SDS–PAGE
C3 botulinum toxin substrate 1	RAC1

1. CHAPTER 1

INTRODUCTION

1.1. Definition of Nephrotic Syndrome

Nephrotic syndrome is massive loss of plasma proteins in urine, characterized by edema, proteinuria and hypoalbuminemia. This common chronic renal disease develops mostly from the alterations of the perm selectivity barrier of the glomerular filtration barrier (GFB) which normally prevents the loss of plasma proteins to leak into urine (Figure 1.1). This barrier is consisted of mainly three parts: fenestrated endothelium, the glomerular basement membrane (GBM) and podocytes. Podocytes are 'octopus-like' highly specialized renal cells of this filter and of the glomeruli which is the smallest functioning unit of kidney. Proteinuria and proteinuria-related symptoms are the only or the main clinical presentation of diseases affecting podocytes [1]. Recent developments in genetics and podocyte biology had greatly improved the understanding of the podocyte pathology and diseases which are initiated with podocyte damage or dysfunction have been termed as 'podocytopathies' irrespective of the pathological pattern or cause of podocyte injury [1]. Here, we will discuss the main topic of this thesis work, childhood steroid sensitive nephrotic syndrome, under the umbrella term 'podocytopathies'.

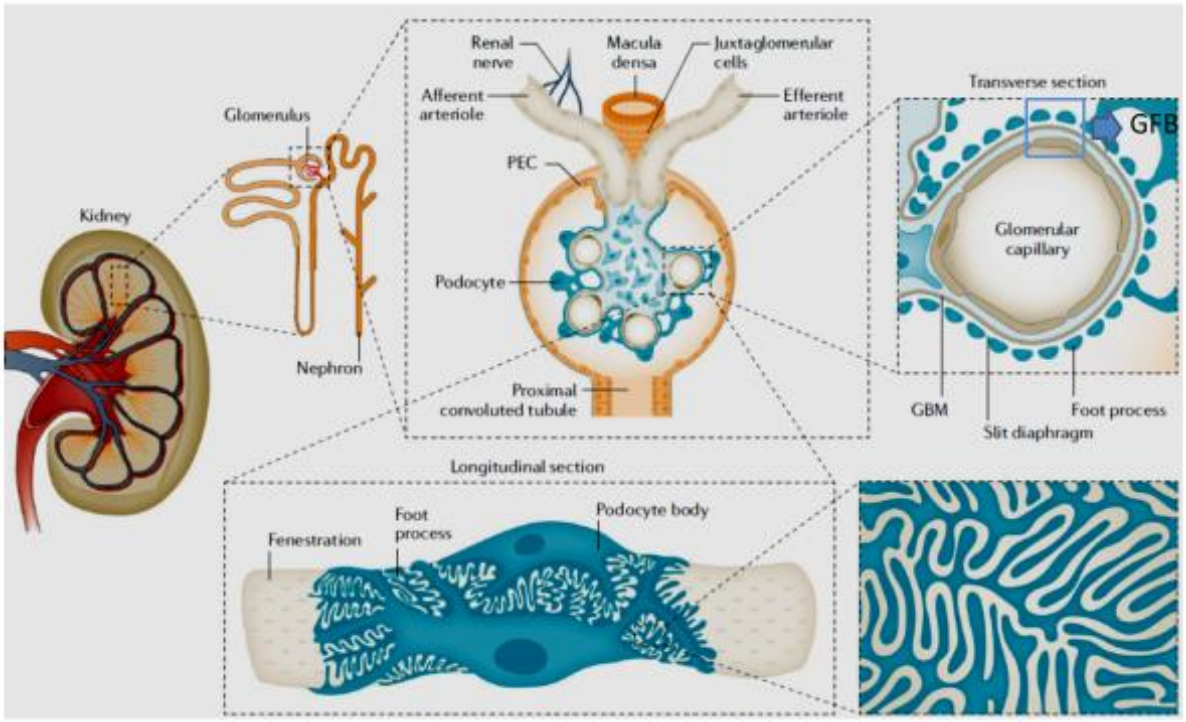

Figure 1.1. The structure of the kidney, nephron, glomerulus and glomerular filtration barrier (GFB). Nephron is the functional unit of the kidney and comprised of glomerulus and tubule. The glomerulus is composed of a tuft of capillaries covered by podocytes adhering the glomerular basement membrane (GBM) which interdigitate in slit diaphragm (SD) (Adapted from Ref. 1).

1.2. Clinical Presentation

Nephrotic syndrome (NS) is a clinical term, mainly characterized by massive proteinuria, hypoalbuminemia and edema (Figure 1.2). Physiologically, NS develops when the loss of protein in urine exceeds the rate of albumin synthesis in the liver, resulting in hypoalbuminemia and edema. Hyperlipidemia with marked elevations in the plasma levels of cholesterol, low density lipoproteins, triglycerides and lipoprotein A is also another feature of childhood nephrotic syndrome due to compensation of the excessive loss of plasma protein with increased protein and lipoprotein synthesis by the liver. Another factor may be decreased plasma oncotic pressure stimulating hepatic lipoprotein synthesis, resulting in hypercholesterolemia [2].

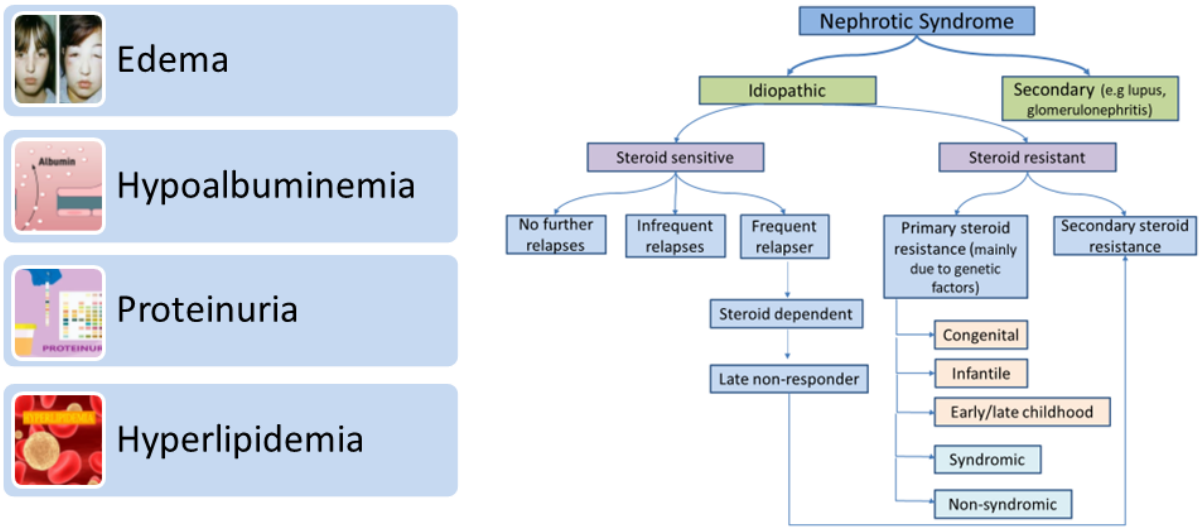

Figure 1.2. Clinical features and classification of nephrotic syndrome in children (Adapted from Ref. 3).

Nephrotic syndrome may be caused by a variety of glomerular and systemic diseases which is called secondary nephrotic syndrome. But in children the cause of nephrotic syndrome is to usually not known and this subtype is called as idiopathic nephrotic syndrome (INS) (Figure 1.2). Nearly in all of the cases, the clinical diagnosis of INS is often very simple. The clinician can quickly diagnose a child with periorbital or generalized edema by making a urine test. In infants and small children, periorbital swelling and generalized edema may not be prominent. Significant proteinuria with more than 2+ albumin on urine dipstick or a spot urine protein/ creatinine ratio greater than 2 mg/mg and serum albumin of less than 2.5 g/dl are diagnostic.

The clinical evaluation of the patients is different according to age and the clinician should be aware of these clinical definitions associated with nephrotic syndrome. In children with the ages of between 2-8 years, the main cause of nephrotic syndrome is idiopathic, on biopsy there is no apparent microscopic change and namely 'Minimal Change Disease (MCD)'. These children generally give perfect response to steroids and the clinician can start steroid therapy without further evaluation with kidney biopsy and guide further diagnosis with response to steroid therapy. In that sense, INS is a diagnosis of exclusion

and is managed by clinician after careful examination of the child for the clues of inherited, systemic diseases and toxic causes of proteinuria particularly visual and hearing problems [3].

1.3. Definitions and Epidemiology

The approach to the clinical entity, nephrotic syndrome is different according to age. In adults and adolescents, the diagnostic algorithm usually starts with kidney biopsy and pathological classification; however the classification of nephrotic syndrome start with clinical response to steroids in children based on the multicenter International Study of Kidney Diseases in Children study which showed that almost 80% of children diagnosed with NS entered remission following an initial 8-week course using prednisone [4]. When these children were analyzed based on histology, steroid responsiveness was found in 93% of those with MCD which is characterized by no apparent histological change on light microscopic examination of the kidney [4]. On electron microscopy, MCD biopsies were shown to have extensive podocyte foot process effacement, a sign of podocyte injury. However, 30% of those children who did not give response to steroids, were most commonly showed to have focal segmental glomerulosclerosis (FSGS) which reflects long lived podocyte damage and accompanying fibrosis in kidney. The incidence of other glomerular diseases such as membranoproliferative glomerulonephritis (MPGN) and membranous nephropathy (MN) are characterized by immune complex deposition on glomerular basement membrane and their incidences also increase with age. MCD and FSGS are pathological diagnoses, however in literature MCD and steroid sensitive nephrotic syndrome (SSNS) were often used interchangeably to describe patients, who respond to steroids and have better prognosis (Figure 1.2) [5]. However, some steroid resistant patients may be diagnosed as MCD in initial biopsy and develop FSGS later on. The pathogenesis of these two entities is still unclear and there is continuing discussion on whether these two pathological diagnoses represent different stages of one common pathophysiological process or whether they are two different disease entities [6].

Idiopathic nephrotic syndrome is seen in all parts of the world. The annual incidence of nephrotic syndrome was reported to be 1.15 to 2.1 new cases per 100,000 children, based on the prospective epidemiological studies from French, New Zealand, Australia and Netherlands [7]. The prevalence is about 10-50 cases per 100.000 children [5]. There is a male preponderance among young children, at a ratio of 2:1 to females whereas this ratio equals in adolescence and adults. The estimated incidence of INS in Japan was reported to be higher, 6.49 cases/100,000 children per year which is approximately 3-4 times higher than that in Caucasians [8]. Moreover, INS was found to be 6 times more common in children with Asian descent compared to their European counterparts in United Kingdom [9]. These findings support genetic preponderance of nephrotic syndrome in childhood. However, the percentage of children diagnosed with NS was found similar among ethnic groups in Houston, USA [10]. The pathological and clinical diagnosis also differs by geographic location and ethnic origin. In a recent

report from Nigeria among black children in Lagos, the proportion with SSNS (%80) is comparable to proportions described in children of Asian and European descent whereas some older studies with smaller cohorts have showed much lower proportions (only 9% to 50%) [11]. Such differences underline the role of genetic as well as environmental factors in the pathogenesis of the disease [10]. The genetic factors in pathogenesis of NS were detailed in the following sections. However, there is little information about the environmental factors. A prospective study from French had showed seasonal variation with a winter peak within an area of Paris and suggested the hypothesis of an infectious or transmissible agent as a trigger of the disease and the possibility of an epidemic course, suggesting that environmental factors play a central role in the physiopathology of the disease [7]. However, an observational study from USA did not show seasonal variation with either the incidence of nephrotic syndrome or timing of relapses, but had showed a coincidence with allergies and asthma [12].

1.4. Prognosis and complications

Before the introduction of antibiotics, NS prognosis usually depends on the severity of infections and the mortality rate was reported to be as high as 67%. The first significant improvement in mortality was seen in 1939 after the introduction of sulfonamides and then penicillin [10]. In the current era, the mortality is 1.9% and infections are still the most important cause of mortality [4].The introduction of adrenocorticotropic hormone and cortisone in the 1950s contributed to dramatic resolution of proteinuria and with the current treatment protocols, nowadays the most important factor contributing to NS patient prognosis is steroid responsiveness. While steroid resistant patients have %50 of having chronic kidney disease and ESRF; steroid responsive patients have much lower risk of end stage renal disease (ESRD) [1, 5, 10]. However, 80-90% of children experience one or more relapses, 50% percent become steroid dependent and are exposed to long term side effects of steroids as obesity, hypertension and diabetes [13]. Moreover, during the course of NS relapses, there is an increased risk of thromboembolism due loss of anticoagulant factors in plasma.

1.5. Pathogenesis

Podocytes play the major role in pathogenesis of nephrotic syndrome, in this regard firstly podocyte development and physiology will be discussed in this section.

1.5.1. Podocyte development

The embryonic kidney, metanephros develops from intermediate mesoderm which is constituted mainly from two tissues, the ureteric bud and metanephric mesenchyme. Starting at approximately the 5th week of gestation in humans, reciprocal inductive signals cause the ureteric bud to grow out from the caudal portion of the mesonephric duct which later on forms renal pelvis and urinary tract [14]. The metanephric

mesenchyme condenses around the ureteric bud to form nephron progenitor cells. These cells transform from mesenchymal-to-epithelial transition (MET) and elongate to form the pre-tubular aggregate (PA), followed by formation of the renal vesicle and S-shaped body (Figure 1.3). Podocyte precursors are found at the proximal domain of S-shaped body. In this epithelization process, ureteric bud derived Wnt/catenin signaling plays an important role. As podocytes differentiate, forming foot processes and slit diaphragms, they lose their proliferative capacity. At the same time, GBM composition changes from laminin-1 to laminin-11 and from α -1 and α -2 type IV collagen chains to α -3, α -4, and α -5 type IV collagen chains [15]. The formation of glomerulus and nephrons in human declines by 32–34 weeks of gestation, however in mice and rats it continues till postnatal 7–10 day. In newborns the glomeruli located at the cortex are mostly immature and smaller compared to the deeply localized juxtamedullary glomeruli. There is no new glomeruli development after birth, but they continue to grow and mature postnatally, reaching their adult size at approximately three and a half years of age [15].

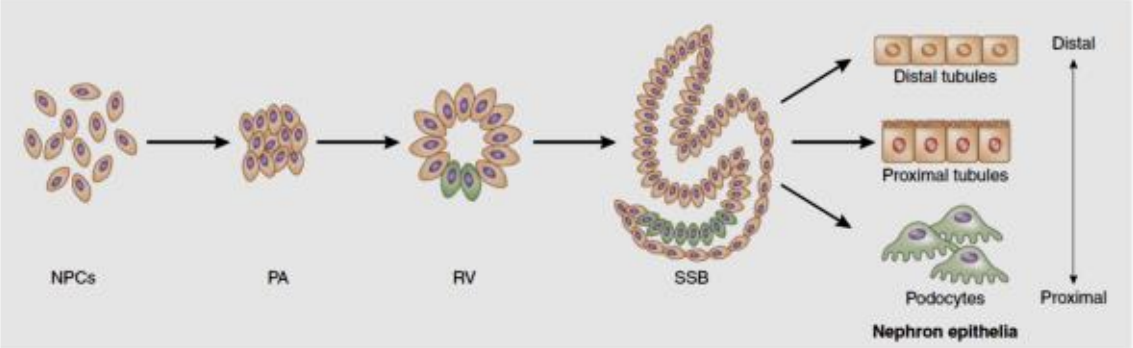

Figure 1.3. Development of nephron. Nephron progenitor cells (NPC) in the metanephric mesenchyme aggregate and form peritubular aggregate (PA) then renal vesicle (RV) which then forms S-shaped body (SSB). Podocyte precursors are found at the proximal domain of S-shaped body (SSB) (Ref. 14).

Podocytes localize on the outside of glomerular capillary wall. Even during healthy conditions, they withstand a tremendous amount of circumferential and shear stress, which further increase in case of podocyte loss on the remaining podocytes [1]. Podocytes bear this stress by having a sophisticated cell cytoskeleton and cell polarity organization. They wrap glomerular endothelium and mediate efficient attachment to GBM by their cellular processes. During development, these processes detect and avoid interlinking with their own cellular protrusions, they make interdigitating process with another [16]. There is a dynamic and reciprocal relationship between neighboring podocytes and GBM. Podocytes have mainly three processes: primary, secondary and tertiary foot processes. Primary and secondary processes are mainly regulated by microtubules and intermediate filaments, whereas tertiary processes or foot processes (FPs) depend mainly on actin cytoskeleton. Foot processes are the main processes of podocytes since they form two important structure of kidney (Figure 1.1). Firstly, the part of FP which binds to GBM is called focal adhesions, which supply accommodation of the podocytes to changes occurring in the surrounding. Secondly, the interdigitating FPs of the neighbouring podocytes bridged basolaterally by specialized, trilaminar intercellular structures called slit diaphragm (SD), which has ~200 nm diameter, serving as a ~60 kDa size-selective filter [4]. The barrier is selective for both

molecular size and electric charge, hold back the passage of anionic proteins [1, 17]. This anionic charge is due to anionic glycocalyx that contains sulphated molecules such as glycosamminoglycans and sialysated glycoconjugates, including podocalyxin covering podocytes. Podocytes also produce proteo-glycans, such as glypican-1 and syndecan-4. Damage to focal adhesions and SD has been implicated in the initiation and progression of podocytopathies [18].

1.5.2. Actin cytoskeleton

Foot processes are the main part of podocytes that react to environmental stimuli. Podocytes usually respond to immunologic or toxic stimulus with increased or decreased motility which sometimes end with podocyte loss. Actin proteins form the main cytoskeleton of the foot process, but are also involved in anchoring the podocyte to its environment [17]. Beneath the plasma membrane of the foot process, the cortical actin network binds to unique proteins of the slit diaphragm and focal adhesion complexes thereby prevent their detachment by interacting with the neighboring podocytes and underlying GBM (Figure 1. 4) [18, 19].

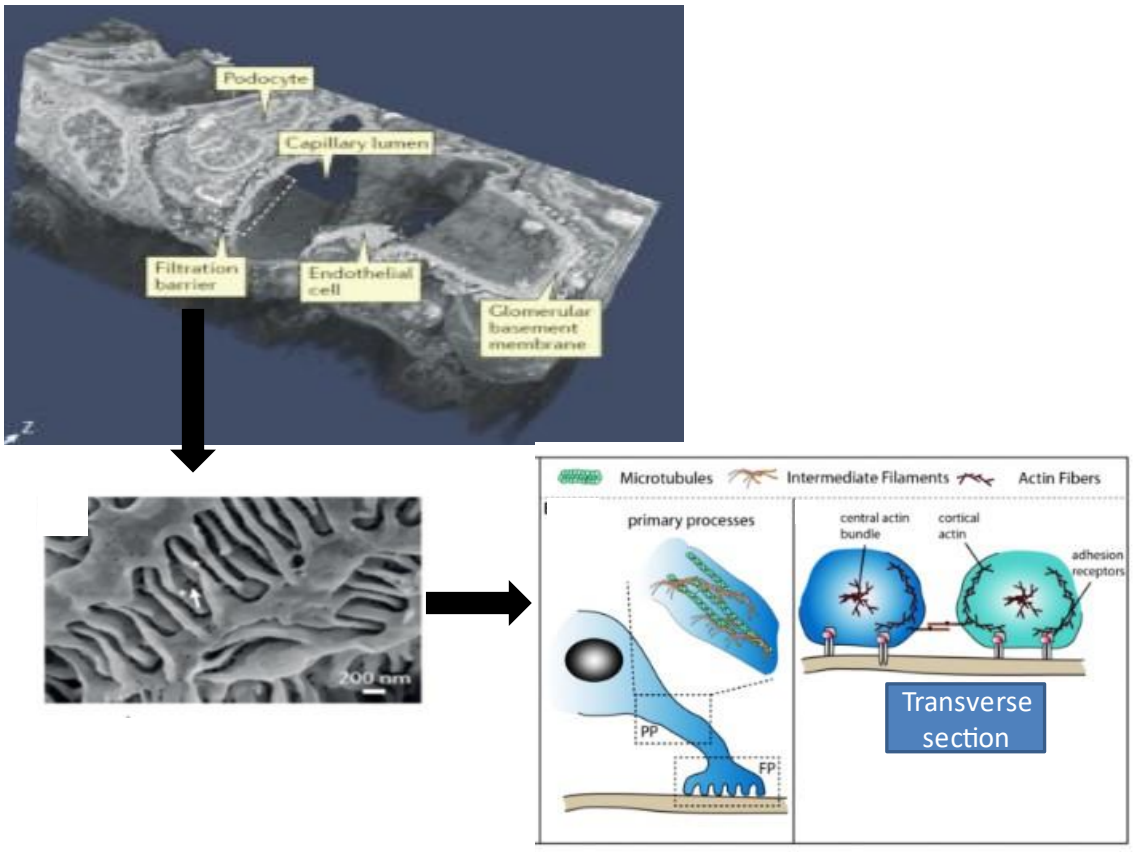

Figure 1.4. Podocytes have mainly three processes: primary, secondary and tertiary foot processes. Primary and secondary processes are mainly regulated by microtubules and intermediate filaments whereas tertiary processes or foot processes (FPs) depend mainly on actin cytoskeleton (Adapted from Ref. 18 and 19).

1.5.3. Rho GTPases and the Actin Cytoskeleton

Rho-guanosine triphosphatases (Rho-GTPases), with 22 members, have long been known for their involvement in actin cytoskeletal remodeling, cell motility, and podocyte disease [20]. A functional imbalance of Rho GTPases, either increased or decreased activities can result in foot process effacement (FPE) and proteinuria. The activities of various Rho GTPases must be kept in a delicate balance for the normal morphology and physiological processes of podocytes. The functions of Rho GTPases are controlled by the molecular switches. They are inactive in GDP-bound form and active in GTP-bound form. This GDP/GTP cycle is majorly kept in balance by guanine nucleotide exchange factors (GEFs), GTPase activating proteins (GAPs) and GDP dissociation inhibitors (GDIs). GEFs indorse the exchange of GDP to GTP and activate Rho GTPases in response to stimuli. On the other hand, GAPs promote the intrinsic GTPase activity. GDIs isolate GDP-bound Rho GTPases and inhibit GDP dissociation, thus inhibit activation of Rho GTPases [20] (Figure1.5).

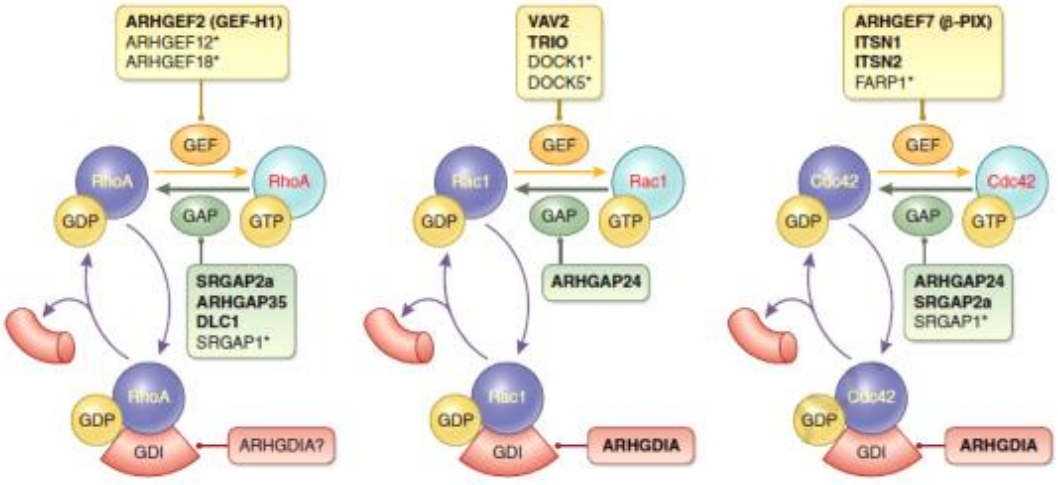

Figure 1.5. The functions of Rho GTPases are controlled by the molecular switches. They are inactive in GDP-bound form and active in GTP-bound form. This GDP/GTP cycle is majorly kept in balance by guanine nucleotide exchange factors (GEFs), GTPase activating proteins (GAPs) and GDP dissociation inhibitors (GDIs). GEFs indorse the exchange of GDP to GTP and activate Rho GTPases in response to stimuli. On the other hand, GAPs promote the intrinsic GTPase activity. GDIs isolate GDP-bound Rho GTPases and inhibit GDP dissociation, thus inhibit activation of Rho GTPases (Ref. 20).

Among Rho GTPases, RAC1 activity promotes the formation of a branched actin network especially in the podocyte lamellipodia (Figure 1.6). RhoA activity favors actin polymerization and the formation of actin bundles, mainly in the filopodia. By deleting podocyte GTPases (specifically each GTPase), it was demonstrated that only CDC42 loss resulted in a profound podocyte damage, characterized by massive proteinuria and dramatic ultrastructural abnormalities (Figure 1.6). On the contrary, loss of RhoA and RAC1 did not result in any overt phenotype under physiologic conditions. However, *in vitro* and *in vivo* studies had showed that overexpression of RAC1 cause proteinuria and podocyte foot process effacement. Moreover, loss function mutations in ARHGDIA gene, a Rho GDI (GDP dissociation

inhibitor) which causes of familial nephrotic syndrome in human, had RAC1 overactivation and inhibition of RAC 1 activity in ARHGDIA null mice suppressed proteinuria. Moreover, Robins et al had showed that RAC1 was overexpressed in kidney biopsies from patients with MCD and idiopathic FSGS and the sera of same patients activated RAC1 downstream p38 in cultured podocytes [21]. They also studied the dose dependent effects of RAC1 activation in a transgenic mouse model expressing a doxycycline-inducible active form of RAC1. Constitutive activation of RAC1 caused glomerulosclerosis resembling FSGS, however transient activation of RAC1 caused transient proteinuria. Pathway analysis revealed that RAC1 activation leads to p38 mitogen activating protein kinase (MAPK) activation and redistribution of Beta1 integrin that RAC-P38 MAPK activation was surged as useful bioassays to measure the activity of potential permeability factors [21].

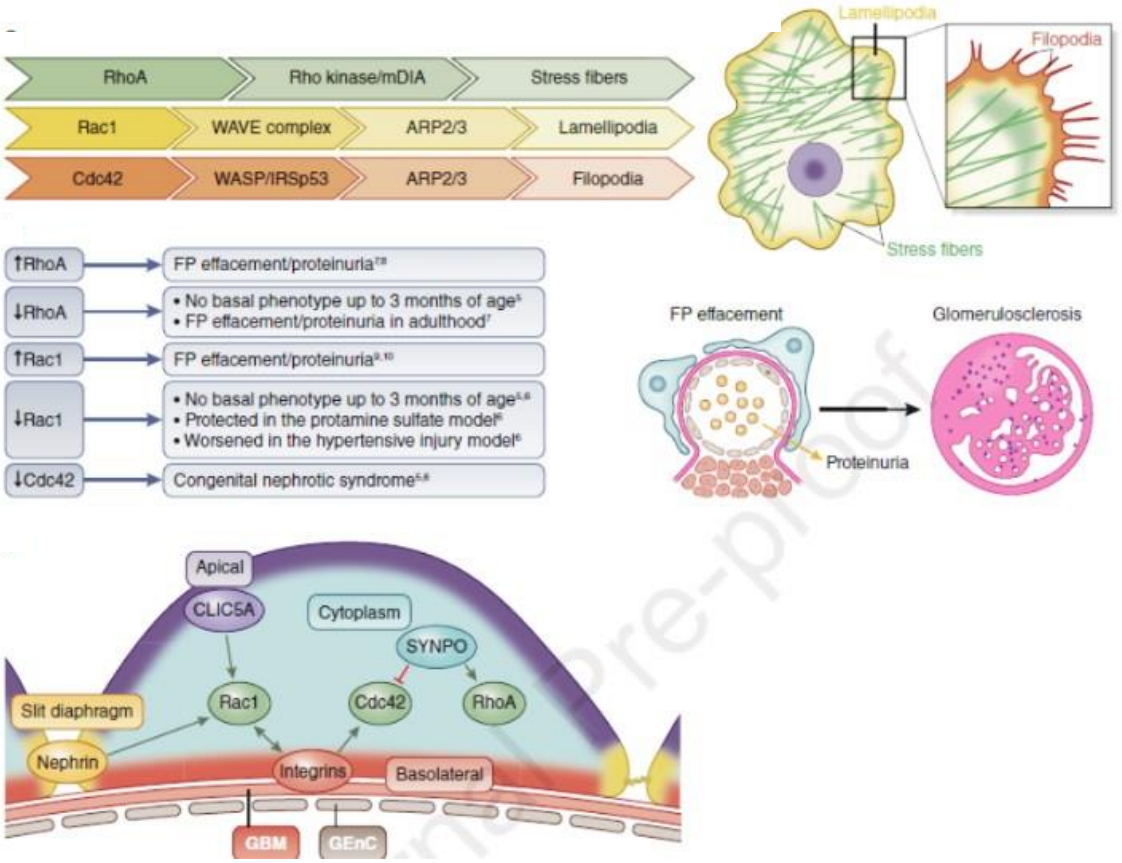

Figure 1.6. A functional imbalance of Rho GTPases, either increased or decreased activities can result in foot process (FP) effecement and proteinuria. The activities of various Rho GTPases must be maintained in a precise balance for the normal morphology and function of podocytes (Adapted from Ref. 20).

1.5.4. Podocyte effacement, detachment and loss

Podocytes are accepted as non-motile cells, at least under normal physiologic conditions. However, recent studies showed a migrating podocyte phenotype under stressed conditions as unilateral ureteral obstruction and adriamycin nephropathy [22]. By damaging insult, FP exhibit various actin-based

structures namely lamellipodia (broad membrane protrusions) and filopodia (long, thin, sharp structures) (Figure 1.6). The focal adhesion complex tethers the foot processes to the GBM and plays role in movement. The foot processes use opposing forces, they drag the cell as the protrusions such as lamellipodia move forward. Each movement is composed of break-down an existing adhesion point and reinstallation of a new one (Figure 1.6) [16].

As podocytes become more injured, they undergo a process called '*effacement'* (Figure 1.7). This process can only be detected at electron microscopy, which could be defined as loss of distinctive interdigitating pattern of foot processes, resembling immature podocytes of the developing kidney at the ultrastructural level (Figure 1.7 a and b) [1, 18, 23]. Podocytes become more diffuse, spreading out which leads to a reduction in filtration barrier function. During the initial phase of FPE, slit diaphragms are displaced from their physiologic distribution and replaced by occluding junctions (Figure 1.7.d) [18, 24]. Foot processes pull back to the primary processes; podocyte cell bodies approach and adhere to the GBM, causing a reduction in the space between podocytes and endothelium which suggest that effacement might be an adaptive strategy of podocytes to increase their adhesive strength at the expense of glomerular filtration capacity, and thereby prevent the formation of multiple flow resistances that could finally contribute to cell detachment and loss (Figure 1.7c) [18, 25].

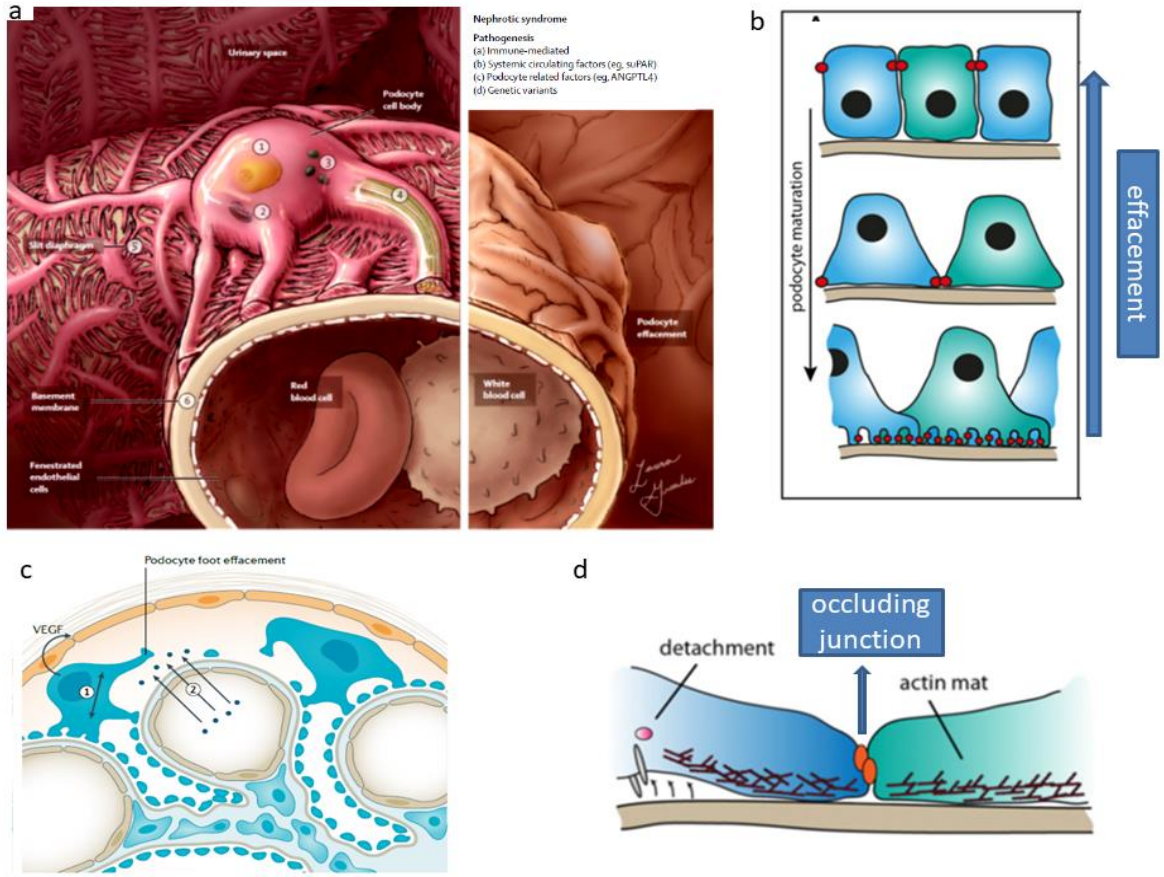

Figure 1.7. Foot process effacement. (Adapted from 1, 19,23)

Effacement can also be described as foot process simplification that podocytes to resemble immature podocytes of the developing kidney at the ultrastructural level and accepted as the very initial step of

proteinuria *in vivo* (Figure 1.7b) [26]. Foot process effacement (FPE) is a reversible process which can be restored with treatment or clearance of toxic substances. However, if the injury continues, podocyte detachment and loss can also occur and has been found to correlate with the development of glomerular sclerosis and chronic kidney disease [1, 25].

1.5.5. Causes of podocyte injury

During childhood NS can be divided majorly into three categories based on the pathophysiological mechanisms: congenital/infantile NS, steroid sensitive NS and steroid resistant NS [10]. Congenital nephrotic syndrome (CNS) is defined as proteinuria manifesting in the first 3 months of life. NS appearing later during the first year (4–12 months) is defined as infantile NS, and NS manifesting thereafter is called childhood NS which can be divided into SSNS and steroid resistant nephrotic syndrome (SRNS) according to steroid response at the 4^{th} week of steroid therapy [10] (Figure 1.2). The discoveries in next-generation sequencing technologies have changed the approach to NS in the last decade. Genetic forms of nephrotic syndrome had considered as infrequent disorders [27]; however, recent researches had showed that at least 66 % of the cases presenting with SRNS during the first year of life [28] and up to 30 % of SRNS cases with an onset below 25 years of age have an underlying monogenic defect [29]. In familial and infant-onset NS, this percentage increases to 57%–100%, as compared with 10%–20% of sporadic cases during childhood. Despite the advances in the genetic era, there are still lots of unknown about the pathogenesis of SRNS with unknown genetic causes and SSNS [30]. The effectiveness of glucocorticoids and other immunosuppressive drugs in some cases of SRNS and in all cases of SSNS had suggested a major role of the immune system in the pathogenesis of these disorders. However recent studies have suggested that the immunosuppressives have also a direct effect on podocytes apart from their immunologic effects.

In adulthood nephrotic syndrome usually presents clinically differently, with progressive proteinuria, kidney dysfunction and fibrosis and FSGS phenotype in biopsy. The common environmental/ multigenetic diseases such as obesity and diabetes mellitus play also an important role in the development and further progress of nephrotic syndrome [1]. Moreover, genome wide association studies in adults showed several susceptibility genes associated with nephrotic syndrome. Among these genes, *APOL1* (encoding apolipoprotein L1), which involves protein-changing mutations (G1 and G2 alleles), have an unusually large effect for common genetic variants. This variant is associated with development of FSGS, chronic kidney disease and hypertension [31]. Low nephron mass due to congenital kidney hypoplasia, reflux nephropathy or renal agenesis may cause nephrotic syndrome in adulthood by progressive hyperfiltration injury. The causes of podocytopathies across life span was showed in Figure 1.8.

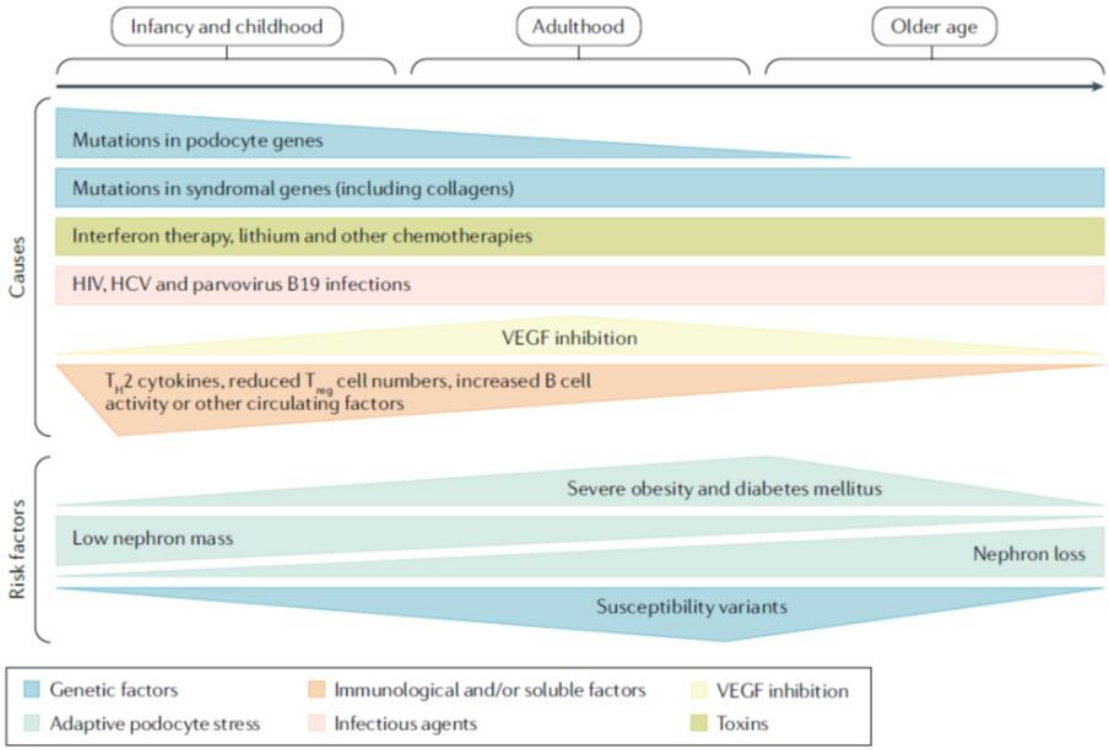

Figure 1.8. The causes of podocyte injury across life span (Adapted from Ref.1)

1.5.5.1. Genetic causes of podocyte injury

Up to now more than 50 genes have been associated with inherited NS which encode proteins critical for the proper function of podocytes and the glomerular filtration barrier [1]. These discoveries greatly increased the knowledge on the pathophysiological mechanisms of the podocytes and glomerular filtration barrier placing the podocyte at the center of NS pathogenesis [1]. Patients with these mutations most commonly have SRNS phenotype, do not fully respond to immunosuppressive drugs and have high probability to develop chronic kidney disease (CKD). With whole exome sequencing (WES) technology, nearly 30% of children are now diagnosed with a monogenic disease [32]. Mutations in podocin (NPHS2), Wilms tumor (WT1), and nephrin (NPHS1) are the most common genetic SRNS causes in European patients, however the frequency of genetic mutations may change according to population [33]. The likelihood of identifying a causative mutation is inversely related to age at disease onset and is increased with either a positive family history or the presence of extrarenal manifestations [33]. Recently, mutations encoding COQ10, an enzyme having role in oxidative phosphorylation in mitochondria was shown to respond oral COQ10 therapy [34]. The gene list showing their locations on podocytes were shown in Figure 1.9.

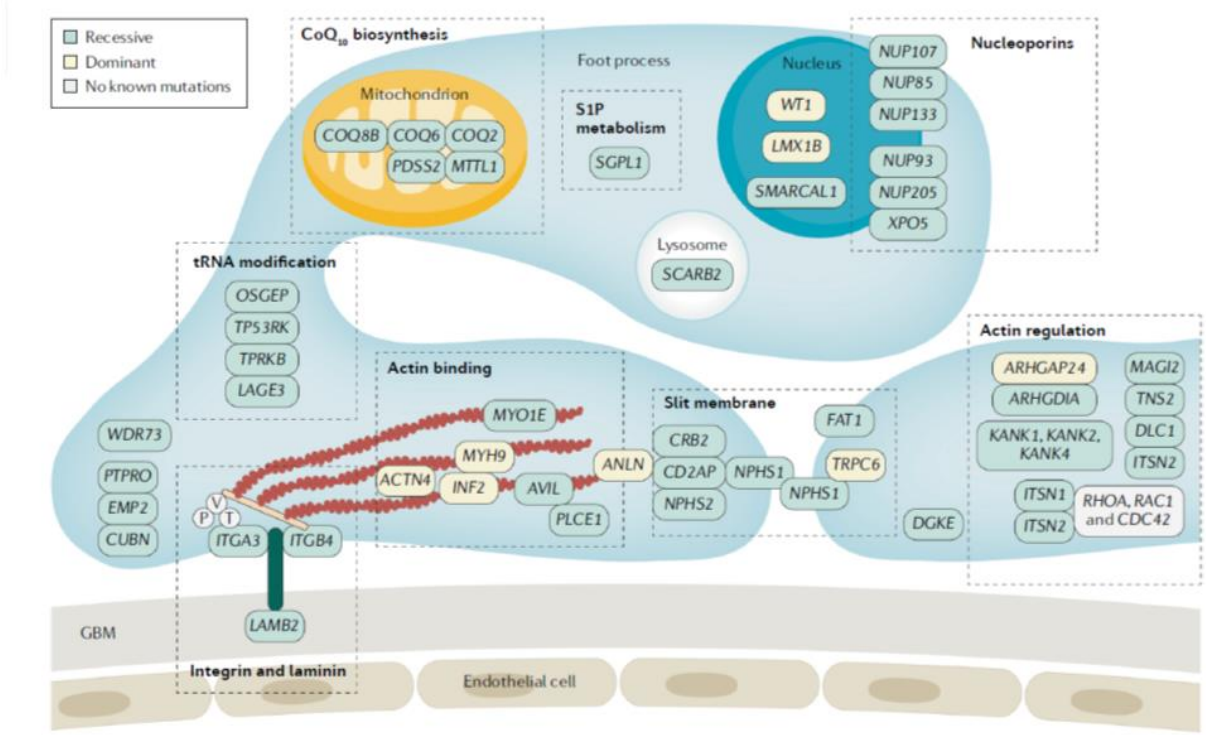

Figure 1.9. Monogenic causes of NS (Adapted from Ref 1).

However, up to now there is no known monogenic cause of SSNS. But evidence suggests that genetics may contribute to pathogenesis of SSNS. Firstly, some children with mutations in SRNS genes such as PLCE1 and NPHS1 have been reported to have steroid responsive disease [30, 35, 36]. In addition, about 3% of children with SSNS have a first degree relative with SSNS [30, 37]. Moreover, there are reports of children with NS with mutations in single genes KANK 1 or 2 or EXT 1 who responded to corticosteroids or have minimal change histology [30, 38-40]. In a Turkish family with SSNS, loss of function mutation in epithelial membrane protein 2 (EMP2) gene was detected [39]. However, analysis of a large cohort of 131 patients with familial SSNS (59 unrelated families) did not identify pathogenic variants in EMP2 [41].

The second issue in genetic background of SSNS is that race implicates the incidence of SSNS which is more common in South Asians than Caucasians and other races in both Europe and North America [30, 42]. Genome wide association studies (GWAS) had suggested the strongest association with the loci human leucocyte antigen (HLA) class II specifically HLA-DR/DQ loci which encode MHC class II molecules required for extracellular antigen presentation [30, 43-45]. These HLA-DQ and HLA-DR regions are highly polymorphous and play an important role in pathogenesis of multiple autoinflammatory and autoimmune diseases. In multiple studies with different ethnic groups, the association of between HLA-DR/DQ alleles and SSNS was confirmed, that this region plays a critical role in SSNS pathogenesis [30]. However, as discussed in Section 1.3, there is evidence that suggest the involvement of environmental factors and ethnic variation. Moreover, in various immunologic disorders associated with HLA variants, there is no clinical finding of NS. These findings suggest the presence of

additional genetic factors outside of the HLA region that increase the susceptibility to renal disease. Recent reports have also found two rare variants in PLCG2 and BTNL2 genes as SSNS candidate loci outside the HLA region [43, 44, 46]. The rare variants (minor allele frequency <5 %) in the gene PLCG2 encode the protein phospholipase c gamma 2 (PLCγ2) and were found to be associated with SSNS in South Asian children. PLCG2 is involved in adaptive immunity and B cell signaling making it another reasonable risk locus for SSNS. Based on these studies, the combination of variations in HLA-DQ and DR and other MHC genes combined with rare variants in other genes mentioned above may light the pathogenesis of SSNS. In this scenario, environmental factors could play as a second-hit for the disease [43, 44, 46].

Moreover, Ashraf et al. sequenced more than 1000 families with high-throughput exon sequencing and discovered recessive mutations of six genes (MAGI2, TNS2, DLC1, CDK20, ITSN1, ITSN2) as novel causes of nephrotic syndrome in 17 families [47]. The patients with these mutations were characterized as partially treatment-sensitive nephrotic syndrome [47]. These six proteins were shown to interact with each other and have role in podocyte migration with Rho-like small GTPase activity. The knockdown of MAGI2, DLC1, or CDK20 in cultured podocytes increased RhoA activation and reduced the migration rate which was reversed with the treatment with dexamethasone. These findings partly explained the effect of steroid treatment in a model of genetic NS independent of their immunological effects and underlined the importance of Rho-like small GTPase regulatory cluster in pathogenesis of SSNS. However, in only 17 of 1000 families, the genetic mutations may clarify the pathogenesis and it is yet unclear the detailed mechanisms of the steroid actions on podocytes.

1.5.5.2. Immunological and Soluble Factors causing podocyte injury

1.5.5.2.1. T cells

Historically, INS was hypothesized to be caused by (a) circulating factor/s. These hypotheses go back to the year 1974, Shaulb hypothesis which suggested that this circulating factor(s) were originated from T cells [48]. The main observation of this hypothesis were (1) remission of disease after measles infection, which causes cell-mediated immunosuppression (2) co-occurrence of MCD and Hodgkin disease, a kind of lymphoma (3) the response of MCD immunosuppressives and (4) the absence of immunoglobulin and complement deposition in glomeruli which is a frequent finding seen in most of other proteinuric kidney diseases [5].

Supernatants of T cell hybridoma lines obtained from patients with MCD were shown to induce foot process effacement and proteinuria in rats [49]. Moreover imbalance of T cell subset distribution was suggested, with increased expression of $CD8^+$ T cytotoxic T cells and decreased $CD4^+$ circulating helper T cells, and strengthened the role of T cells in pathophysiology of INS [50]. However, the patient groups were not homogeneous, including SSNS and SRNS patients. Another study has showed increased CD8

T cell subset in SSNS patients during remission [51]. However, some studies did not find any difference in the $CD4^+$ and $CD8^+$ T-cell subsets [52] (Figure 1.10). Also, an increase in Th17 cells, Th17-related circulating cytokines and in IL-17 deposition in kidney biopsies with a reduction of $CD4^+CD25^+FoxP3^+$ Tregs was observed in INS patients [53]. Moreover, supernatants of healthy Th17 cells were shown to induce p38 MAPK and JNK pathways as well as an increase in motility of cultured podocytes [54].

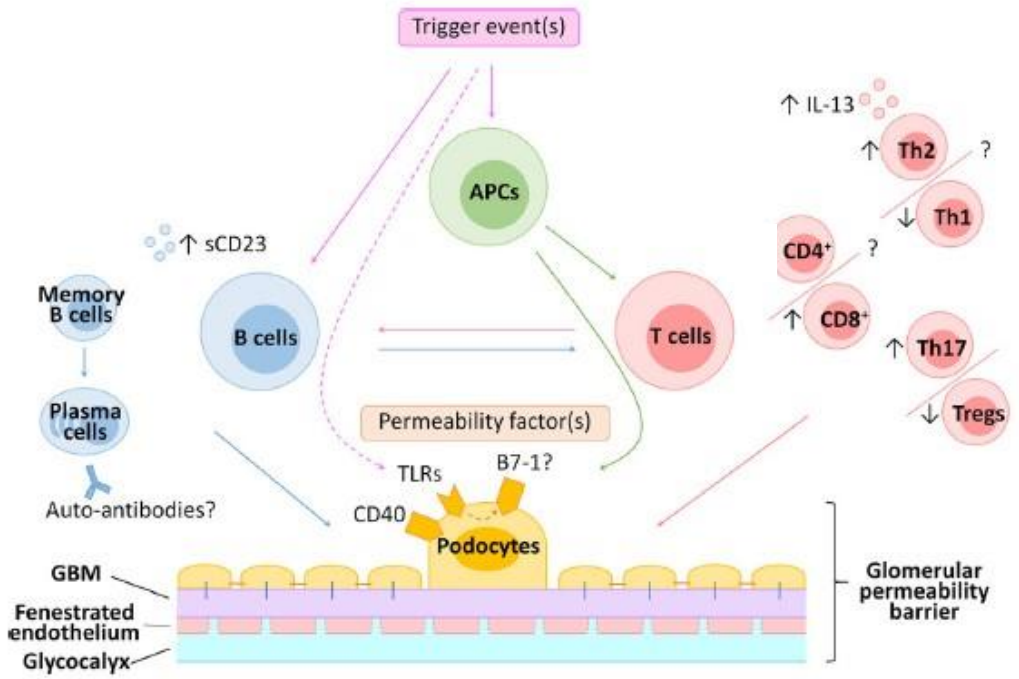

Figure 1.10. Immunologic and soluble factors causing nephrotic syndrome (Adapted from Ref 65).

INS was also associated with with decreased activity of Tregs. This observation was also supported with the observation that some IPEX (immune dysregulation, polyendocrinopathy, enteropathy, X-linked) syndrome patients, a disease driven by a genetic defect of Foxp3 leading to defective T-cell regulatory functions, were shown to develop INS [55] (Figure 1.10). Furthermore Bertelli *et al.* demonstrated that amplified neutrophil-induced oxidative burst during infection caused down regulation of an inhibitory enzyme expressed by Tregs during INS relapse [56]. Moreover, in animal models of nephrotic syndrome, infusion of Tregs or Treg expansion by IL2 and adenosine have been shown to cause improvement of nephrotic syndrome [57, 58]. Recently Tsuji S *et al.* has showed that in FRNS patients has decreased rate of Treg expansion during nephrotic relapse. The authors have also studied 16s RNA of patients' gut microbiota and found decreased proportion of butyric acid producing bacteria in frequently relapsing nephrotic syndrome (FRNS) patients [59] which suggested relapse of NS could be prevented by probiotics [60, 61].

Some clinical observations suggest association of atopy, asthma and other allergic diseases with INS. In a longitudinal cohort of children with NS, a total of 64% children have lifetime allergies, 20% have asthma, 33% have wheezing, 27% have eczema and 24% have rhinitis [12]. These diseases are characterized by preponderance of Th2/Th1 cells (Figure 1.10). An increased expression and production

of the Th2-specific IL-13 in patients with INS was also described [30]. In a rat model of IL13 overexpression, IL-13 transfected rats showed proteinuria, hypoalbuminemia and foot process effacement on electron microscopy [62]. Gene expression analysis of IL-13 overexpressed rats showed increased expression of IL13R, IL4R and B7-1 whereas downregulated expression of podocin, nephrin and dystroglycan. In another model of Buffalo/Mna rats, which develop spontenous proteinuria and FSGS, Le Berre L *et al.* has showed increased Th2 signature in kidneys [63]. Moreover, IL13 was shown to induce disrupted cytoskeletal connections on podocytes which is reversed by montelucast, a leukotriene receptor antagonist used to treat allergic diseases [64].

1.5.5.2.2. B cells

Although there is lack of immune deposits in renal biopsies from FSGS and MCD patients, B cells were also shown to have role in pathogenesis of INS of childhood. Similar to T cell subsets, B cell subsets were also shown to be changed during NS relapse in children. Also, rituximab, which is an anti-CD20 antibody, depleting all B cells except long-lived plasma cells and stem cells is effective in maintenance of SSNS remission in steroid dependent and frequent relapsing patients [1, 65]. Rituximab deplete mature and memory B-cells and short-lived antibody secreting cells (ASCs), thereby hampering majorly autoantibody production [65, 66].

Recent studies also suggest a link between B and T cells in pathogenesis of MCD. Colucci M *et al.* observed atypical IgM on the surface of T cells, which were found more profoundly in steroid dependent patients compared to infrequent relapse SSNS patients. These IgM molecules on T cells were found to be antigen non-specific and less glycosylated, bind more profoundly to T cell surface, causing more profound T cell activation. The authors showed unaffected levels of aberrant T cells with steroid therapy but their levels significantly decreased after rituximab [67]. B cell-targeted treatment may also affect the autoreactive T-cell pool, since B cells can efficiently present antigens and provide costimulatory signals to T cells which has been suggested as a potential mechanism of autoreactive T-cell depletion following anti-CD20 therapy [68, 69].

Kemper MJ *et al* had studied the level of soluble CD25, which is soluble IL2 receptor, a marker of T cell activation and soluble CD23, a soluble low-affinity IgE receptor, a marker B-cell stimulation and showed that both of these markers were markedly increased during relapses of INS [70] (Figure 1.10). Colucci *et al* showed significantly increased levels of total, transitional, memory, and switched memory B cells compared to controls in 51 children with steroid sensitive NS during relapse whereas B cell subsets were comparable to controls in children with steroid resistant NS patients with genetic mutations [71]. The duration of remission after rituximab therapy has been proposed to be estimated by $CD19^+$ B cells and particularly memory B cell levels [72, 73].

Apart from antibody secretion, B cells have also role in antigen presentation, activation of T cells and cytokine secretion [65]. To decipher the role of antibody independent role of B cells, Kim AHJ *et al*. studied the role of IL4, which is secreted by B cells and TH2 cells [74]. They showed that IL4 can induce podocyte membrane ruffling and detachment which are signs of podocyte injury *in vitro*. Moreover, using a method of *in vivo* gene delivery, they confirmed that IL-4 overexpression in mice is sufficient to induce foot process effacement and proteinuria. They also showed that antigen-specific B cells could induce foot process effacement in an IL-4–dependent fashion when planted a B cell antigen on the glomerular basement membrane (GBM) [74].

Lastly several autoantibodies were accused for causing GBM injury. Jamin *et al.* showed anti UCHL1 antibodies obtained from SSNS patients caused podocyte injury *in vitro* in immortalized human podocyte culture and podocyte effacement in mice *in vivo* [75]. In adult recurrent FSGS patients, autoantibodies against CD40, a costimulatory molecule of the TNF receptor superfamily and highly expressed by antigen-presenting cells, were shown as the strongest impact on the prediction of FSGS recurrence [76]. This findings may also explain the therapeutic efficacy of plasma exchange in prevention and treatment of FSGS relapse after transplantation.

1.5.6. Podocytes as modulators of immune response

Historically podocytes as epithelial cells had been considered as passive target for immunological injury. However recent studies suggested that podocytes had active immunological mechanism that surge inflammation. Podocytes were shown to internalize IgG and antigens [77]. They remove immunoglobulins that accumulate at the GBM by the neonatal Fc receptor (FcRn), an IgG and albumin transport receptor, expressed on podocytes. Additionally, podocytes were shown to present antigens to CD4+ and CD8+ T cells by MHC II and MHC I and induce their proliferation [78]. Podocytes also express various costimulatory molecules as CD80 and CD40 which are increased in response to various infectious stimuli and inflammatory milieu (Figure 1.10) [79, 80]. These findings suggested that podocytes act as non-hematopoietic antigen presenting cells [78]. CD80 or B7-1, which is a costimulatory molecule expressed on most of antigen presenting cells (APCs), is also expressed on podocytes in response to lipopolysaccharide (LPS) stimulation and its cytoplasmic tail was shown to block β1 integrin activation by competing with talin [81, 82]. Urinary CD80 level was shown to be increased during MCD relapse compared to MCD remission and FSGS [83-85]. It had been hypothesized that during MCD relapse ineffective circulating Treg response or ineffective autoregulatory mechanism of podocytes to express CTLA-4 may perpetuate increased CD80 expression and podocyte motility [57, 86-88] but exact molecular mechanisms of CD80-CTLA-4 interaction and clinical response to abatacept is still debatable [89-91].

Podocytes were also shown to express various toll-like receptors as toll-like receptor 4 (TLR4) and TLR3 and their expression were shown to be up-regulated in response to TLR3 ligand, polyIC [92].

These stimuli induce expression of CD80 and actin reorganization which provides a mechanism why infections are frequent stimulators of INS relapses.

1.5.6.1. Effect of circulating permeability factors on podocytes

Apart from cytokines and immunologic factors, several circulating plasma permeability factors were accused in pathophysiology of INS especially FSGS. However, the role of circulating permeability factors in MCD so SSNS is unclear. The circulating permeability factor hypothesis is based on the clinical observations that nearly one third of FSGS cases after transplantation recurred in transplanted kidneys [93] and decreased levels proteinuria was observed in these patients with plasma exchange or plasmapheresis [94]. One of the most persuasive evidence for a circulating permeability factor arose from a case report, in which a renal allograft that was removed at 14 days of post transplantation due to the recurrence of FSGS and was retransplanted to another patient (with Type 2 diabetes) after which it recovered its function and did not show proteinuria [95].

Haemopexin is one of the permeability factors which was shown to affect glomerular sialo-glycoproteins in patients with MCNS. It is a haem-scavenging plasma protein and its purified human or recombinant haemopexin form was shown to induce reversible proteinuria accompanied by podocyte FPE in rats [94, 96]. Haemopexin was also shown to induce nephrin-dependent cytoskeletal rearrangement in cultured podocytes. It is suggested that various isoforms of haemopexin exist. In in physiological conditions perhaps circulating haemopexin is inactive but that in certain conditions it can become activated and act as serine protease [97-99]. However, these observations thus far have not been validated.

Another permeability factor is soluble urokinase plasminogen activator receptor (suPAR). Wei *et al.* had showed that this factor activated podocyte β3 integrin, resulting in reorganization of the actin cytoskeleton of podocytes [100]. *In vivo* high-dose recombinant mouse suPAR was shown to induce proteinuria, increased podocyte β3 integrin activity and foot process effacement in mice [100]. However, experimental data were not supported by clinical data. The authors have showed that when adjusted for renal function suPAR levels did not differentiate between FSGS and other kidney diseases [101]. Wada T *et al.* also showed that there is no correlation between serum suPAR and degree of proteinuria [102]. Moreover, Sinha *et al*. has showed that suPAR levels did not distinguish FSGS and MCD [103].

1.5.7. Modelling of NS *in vitro* and *in vivo*

Cultured podocytes are frequently used to investigate the presence and toxicity of immunologic factors and other factors *in vitro* [104]. Characteristics of podocytes exposed to nephrotic factors change by means of actin cytoskeleton, increased motility in scratch test and cytoplasmic redistribution of nephrin and podocin [104]. However, these changes are qualitative based on the subjective observations. Albumin influx assay is based on the amount of albumin transit across podocytes cultured on transwell filters. Increased albumin amount in the upper part of trans well system indicates change in podocyte

morphology and disruption of slit diaphragm *in vitro* [105]. Koshikawa *et al.* studied the role of p38 mitogen-activated protein kinase (MAPK) signalling pathway in rat puromycin aminonucleoside nephropathy and mouse adriamycin nephropathy. They showed increased phosphorylated p38 (p-p38) MAPK in podocyte nuclei in these models and in biopsies from minimal change nephropathy, membranous nephropathy and focal segmental glomerulosclerosis patients relative to healthy controls [106]. Additionally, they found that marked p38 MAPK phosphorylation preceded proteinuria in experimental models of NS and that the proteinuria could be blocked by the administration of a p38 MAPK inhibitor [106].

1.6. Treatment of Nephrotic Syndrome

As stated above, a substantial portion (80-90%) of children with INS gives perfect response to corticosteroids with complete remission [5, 107]. However, 40-50% of those patients have frequent relapses or steroid dependency. Most of these children have remission with lower dose of steroid but continuous steroid therapy makes them vulnerable to corticosteroid (CS) related complications as obesity, growth delay, diabetes and hypertension. In these patients, immunosuppressives as cyclophosphamide, calcineurin inhibitors (CNIs), azathioprine (AZA) or mycophenolate mofetil (MMF) have been used as steroid sparing agents (Figure 1.11). More recently, recurrent rituximab or ofatumumab (another anti-CD20 antibody), have been shown to be helpful in inducing remission in patients with FRNS or SDNS (Figure 1.11) [5, 108]. All of these drugs were suggested to control immune dysfunction as the above studies showed immune dysregulation especially effecting T cells. However, recent studies showed that those immunosuppressive drugs had also direct effects on podocytes [109-111].

Glucocorticoids (GC) are, like other steroid hormones, lipophilic molecules that can easily diffuse across the cell membrane and bind to the glucocorticoid receptors (GRs) in the cytoplasm. After binding to GR, GC/GR translocates to nucleus and bind to DNA or interact with co-activator complexes. This mechanism of GC function is called genomic mechanism and GR/GC complex exerts most of its anti-inflammatory and immunosuppressive effects by this mechanism [112]. They increase expression of anti-inflammatory genes and decrease expression of pro-inflammatory genes. Furthermore, the GR/GC complex can, either directly or indirectly, interact with pro-inflammatory transcription factors nuclear factor κB (NF-κB), which is a key transcription factor responsible for T-cell activation and activator protein 1 (AP-1) and thus reduce their activity. Non-genomic mechanisms of GCs include changing the physicochemical property of cell membranes, directly or through binding to intracellular or membrane-bound GRs [112]. This mechanism has also showed to inhibit T cell receptor signaling. Corticosteroids at low doses induce apoptosis and inhibit early activation and the proliferation of B cells. But antibody secreting plasma cells require higher doses of steroids to inhibit antibody production and cytokine

production [65, 113]. Corticosteroids have also direct effects on podocytes. Dexamethasone increases actin filament stability by increasing the activity of the actin-regulating RhoA GTPase, inhibits podocyte apoptosis by restoring the PI3K/Akt pathway and downregulates vascular endothelial growth factor and IL-6 cytokine production by podocyte cell lines [114, 115].

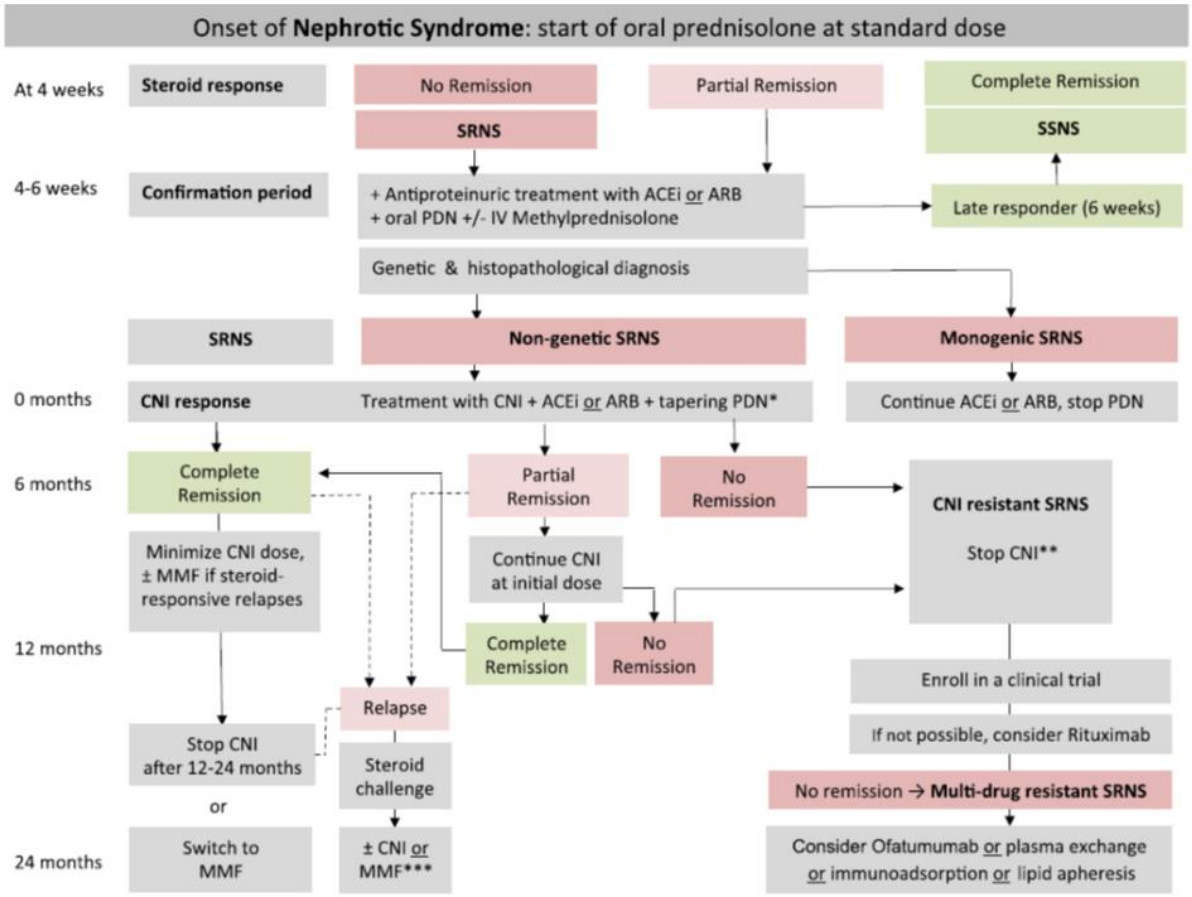

Figure 1.11. Management of nephrotic syndrome in children (Adapted from Ref 107).

Calcineurin inhibitors (CNI) are widely used in steroid dependent NS cases to decrease relapse frequency of NS in children. CNIs bind intracellular proteins called immunophilins; cyclophilins in the case of cyclosporine A (CsA), and the FK-binding proteins in the case of tacrolimus (also known as FK506). This complex then binds to an intracellular molecule called calcineurin, a phosphatase and regulator of intracellular calcium. By inhibition of calcineurin, its downstream effector cytoplasmic nuclear factor of activated T cells (NFATc) is also inhibited causing decreased expression of multiple cytokines and costimulatory molecules including IL-2, which stimulates the growth and differentiation of T cells, IL-4 and CD40 ligand [116]. As glucocorticoids, CNIs inhibit naive B cells, but not plasma cell differentiation and surface immunoglobulin expression. Their inhibitory effect on antibody responses was suggested to depend on their indirect suppressive effect on T helper cells [65]. CNIs have also direct effect on podocytes. CNIs were shown to stabilize the actin cytoskeleton by preventing

cathepsin mediated degradation of synaptopodin and subsequent RhoA mediated stabilization of actin stress fibers [117]. Moreover CNIs restore expression of podocyte specific proteins as zonula occludens and synaptopodin under cellular stress [111]. In addition, tacrolimus may also exert a protective effect by reducing calcium influx mediated by the podocyte cell membrane-associated transient potential cation channel 6 (TRPC-6), whose mutations have been reported in genetic forms of FSGS [118].

As mentioned above rituximab is anti-CD20 monoclonal antibody inhibit differentiation stages of B lymphocytes and effect T cells by inhibiting APC or directly depleting $CD20^+$ T cells [119]. Rituximab has hypothesized to reduce Th17 responses and restores the frequency and function of Tregs in other autoimmune disorders. Rituximab is a potent immunosuppressive drug with risk of hypogammaglobulinemia and resulting opportunistic infections [65]. Surprisingly, rituximab can also exert a direct protective effect on the podocyte actin cytoskeleton by binding to and preventing sphingomyelin phosphodiesterase acid like 3B (SMPDL-3b) downregulation [120]. However, the efficacy of ofatumumab, which binds a different epitope of the CD20 molecule and inhibit CD20, is against this hypothesis [65].

As a summary, INS of childhood is a podocytopathy however the exact mediators of the disease that 'hit' the podocytes are not yet known. Treatment is successful in steroid sensitive patients however relapses occur in a substantial portion of patients which make children vulnerable to side effects of immunosuppressive drugs.

1.7. EXTRACELLULAR VESICLES

1.7.1. Definition

In addition to classical signaling through cell-cell contact and soluble factors, intercellular communication also occurs through cellular release of extracellular vesicles (EVs) which have the potential to deliver a particularly diverse array of messages to cells at a level beyond that of soluble factor signaling. Nomenclature of extracellular vesicles has not fully described yet. International Society of Extracellular Vesicles defines extracellular vesicles as the particles released from the cell that are delimited by a lipid bilayer, cannot replicate and do not have a functional nucleus. EVs can be categorized in many different ways: according to size (microvesicles, exosomes, apoptotic bodies), sub cellular (endosomal or ectosomal) origin or cell of origin [121]. Exosomes are usually defined as vesicles that are of endosomal origin, released through reverse budding late endosomes, multivesicular bodies containing intraluminal vesicles and 30-150 nm in size. Microvesicles are usually defined as vesicles that are of ectosomal origin that pinch off the surface of the plasma membrane via outward budding and 100-1000 nm in size. Apoptotic bodies are 1-5 um in size and released by apoptotic cells through caspase dependent pathways and characterized by the presence of histone complexes. EVs reflect the protein and genomic content of parent cells and are composed of nucleic acids, several proteins, chemical, and structural substances derived from the cell of origin [122]. They are enriched in not only membrane proteins as trafficking and adhesion molecules, but also cytoskeleton proteins as enzymes, heat shock proteins, cytoplasm and signal transduction molecules, cytokines, chemokines, proteinases and cell specific antigens. In addition to these EVs carry important messenger RNAs (mRNAs) and non-coding RNA (ncRNAs) including miRNAs. These functional substances differ in relation to the cell type of origin and mirror the certain physiological and pathological conditions of the cells at the time of their packaging and secretion [122]. Almost all cell types release EVs. They are found majorly in plasma but also other bodily fluids including urine, semen, breast milk, saliva and sputum. EVs take place in important biological functions acting as mode of communication between cells. Once suggested as cell debris, now it is discussed if particular cells secrete EVs delineated with particular signals to manipulate target cell, indicating a functionally aimed mechanism-driven buildup of specific cellular structures in exosomes, suggesting that they have a major role in regulating intercellular communication.
EVs act on local or distant cells from cell-of-origin. Recent studies have shown that EV signaling can significantly immune response to infections, rheumatological diseases and various cancers [122].

1.7.2. Biogenesis of Extracellular vesicles

As stated above EVs was proposed to define all lipid bilayer-enclosed extracellular structures. EVs can be generated in two ways: By outward budding of the plasma membrane or by an intracellular endocytic

trafficking pathway involving fusion of multivesicular bodies (MVBs) with the plasma membrane. EVs are very heterogeneous in respect to their size, cargo, functional effect on recipient cells and cell of origin. There are various ways to obtain EVs. By most of the current isolation methods the obtained EVs contain a mixture of small EVs, which are of endosomal origin and called as exosomes and relatively bigger vesicles which are of plasma membrane or non-endosomal origin, namely microvesicles. Moreover, during EV isolation not only these vesicles but also lipoproteins and the newly identified exomeres are also obtained. Because of this heterogeneity nowadays new techniques are tried to be developed to overcome this difficulty [122].

Exosome formation starts with invagination of bilayered plasma membrane and the formation of intracellular multivesicular bodies (MVBs) containing intraluminal vesicles (ILVs), thereby this cup-shaped structure that contains many cell-surface proteins as well as soluble proteins from the extracellular milieu. The second step is de novo formation of an early-sorting endosome (ESE), which sometimes may directly merge with a preexistent ESEs. The trans-Golgi network and endoplasmic reticulum have an endosomal sorting complexes required for transport (ESCRT) proteins such Sytenin-1, TSG101 (tumor susceptibility gene 101), ALIX (apoptosis-linked gene 2-interacting protein X), syndecan-1, tetraspanins (CD9, CD82), sphingomyelinases, phospholipase D2 (PLD2), ADP-ribosylation factor 6 (ARF6) GTPase, diacylglycerol kinase α (DGKα) and contribute to the formation and the content of the ESE (Figure 1.12)[123].

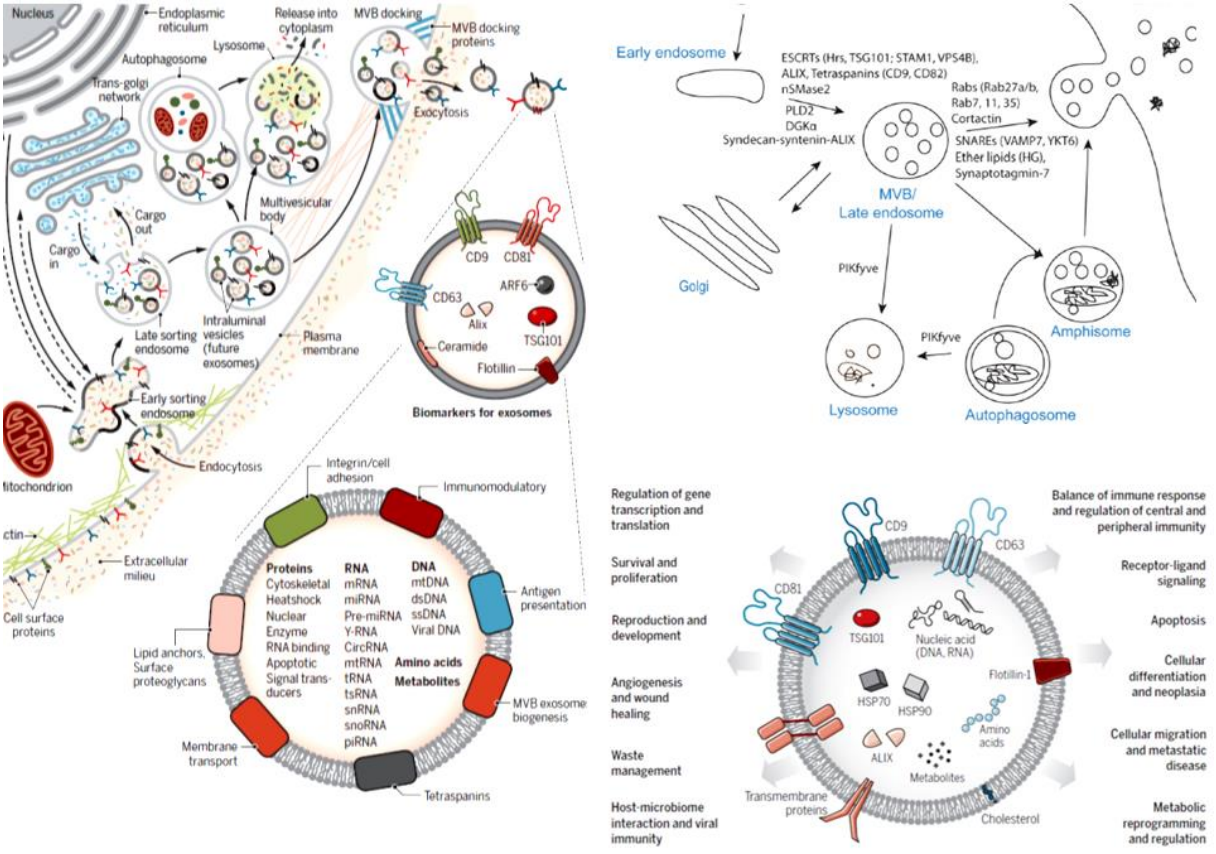

Figure 1.12. EV biogenesis, content and functions (Ref 121, 122).

Lastly, these ESEs mature to late-sorting endosomes (LSEs) and MVBs, then either fuse with lysosomes to be degraded or fuse with the plasma membrane to be released as exosomes. Transport of MVBs to the plasma membrane is mediated by actin and the microtubule cytoskeleton. In this process Rab GTPases have important roles as membrane trafficking, vesicle budding, transport of vesicles along actin and tubulin and membrane fusion. Moreover, other small GTPase families as Rho/Rac/ CDC42 have shown to play a role in exosome release. Another protein group that have role in membrane fusion is soluble *N*-ethylmaleimide- sensitive factor attachment protein receptors (SNAREs) which help fusion of vesicles with their recipient plasma or organelle membranes. Moreover, ether lipids, cholesterol, calcium and calcium sensing proteins as synaptotagmin, V-ATPase-mediated acidification of MVBs have been shown to have role in MVB fusion with plasma membrane and release of exosomes. Externalization of phosphatidylethanolamine (PE) and phosphatidylserine (PS) may be more specifically involved in plasma membrane-derived EV secretion [121].

1.7.3. The role of EVs in kidney diseases

The role of EVs in kidney physiology and pathophysiology is in its infancy. The smallest functional unit of kidney is nephron which is formed by various cell types with complex relations (Figure 1.13). EVs may have various roles both in intranephrotic communication and also other organ-kidney communication [124]. Kidney cells were designated to adapt circulatory and nutritional changes of the body. The filtered plasma is concentrated and its electrolyte concentration is regulated by various hormones and circulating factors. Recent evidence has suggested that exosomes have role in communication between cells during physiological and pathological state [125]. However, these studies are mostly based on *in vitro* evidence. The first study by Street JM *et al.* studied the role of EVs in water absorption form kidneys. They showed that desmopressin, which controls the regulation of water retention, increases exosomal aquaporin 2 which is a water channel located on the membrane of kidney collecting ducts. The stimulation of murine kidney collecting duct cells with these aquaporin 2 rich exosomes significantly increased water transport [126]. Also, exosomes were shown to have role in physiologic regulation of acid base load. Pantare *et al.* showed that acid load changed the B1 subunit of an apical vacuolar-type H^+-adenosine triphosphatase (V-ATPase) on exosomes, which regulate fine tuning of blood acid-base balance [127]. Supporting these findings, urinary exosomal cargo was demonstrated to be changed in hereditary tubular diseases as Bartter and Gitelman syndromes and distal renal tubular acidosis and was suggested as a biomarker for diagnosis of these diseases [128]. Additionally, Gildea *et al.* stimulated distal and collecting duct cells with EVs derived from fenoldopam stimulated proximal tubular cells and showed increased reactive oxygen species production in recipient cells [129]. Moreover, Oosthuyzen *et al* showed that vasopressin increased the uptake of EVs by collecting duct cells *in vitro* and *in vivo* and exosomes induce mi-RNA regulated gene changes [130].

Gracia T *et al.* confirmed miRNA and subsequent tubular channel expression change via exosomes between different tubular epithelial cells *in vitro* [131].

Tubulointerstitial inflammation and subsequent fibrosis play a pivotal role in pathogenesis of chronic kidney disease (CKD) due to various common glomerular and tubular diseases. Tubular epithelial cell (TEC), endothelial cells and macrophages (MQ) secrete many bioactive molecules reciprocally during toxin or systemic inflammatory injury such as immunologic reaction to graft during transplant glomerulopathy, various glomerulonephritis, diabetic nephropathy and focal segmental glomerulosclerosis. Tubular injury may subside with tissue regeneration and reorganization, with the help of the signals that come from stem cells or interstitial cells or may progress to fibrotic changes with ongoing inflammation. Mice and human studies suggest that IL1, IL6, TGFβ and TNFα are the major proinflammatory signals that surge tubulointerstitial injury. Moreover, recent data suggest that EVs may regulate immune responses via transferring diverse class of signaling molecules including cytokines, chemokines, enzymes and growth factors [132]. *In vivo* and *in vitro* studies on this topic are very few however, have suggested that EVs may have both anti-inflammatory and pro-inflammatory role [133-136].

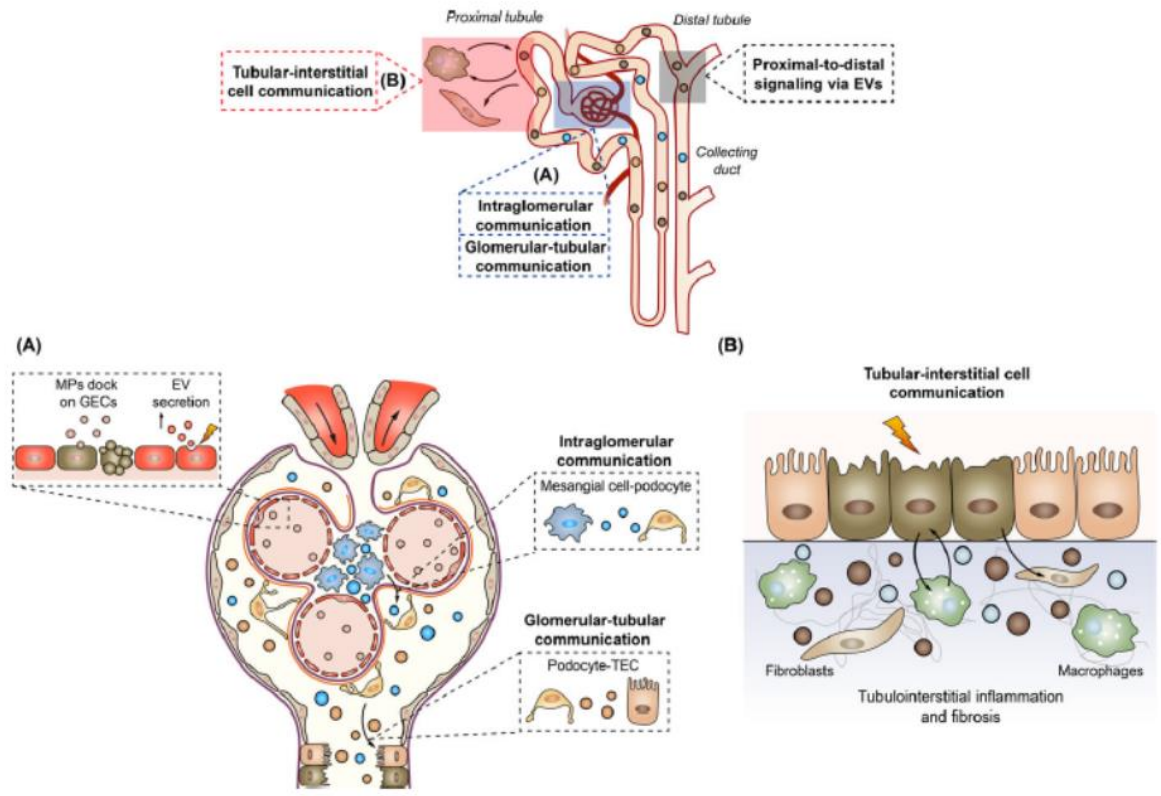

Figure 1.13. The role EVs in intranephronic communication (Adapted from Ref. 123)

The first study by Borges FT *et al.* demonstrated that injured epithelial cells produced more exosomes which carry TGFβ mRNA and promote proliferation, α-smooth muscle actin expression, F-actin expression, and type I collagen production in fibroblasts [137]. Recently, Liu *et al.* has confirmed their findings by showing EVs derived from TGFβ stimulated renal proximal tubular cells induced fibroblast activation which was inhibited by pharmacologic inhibition of exosome production [133]. Moreover, they showed that exosomes mediated profibrotic changes by inducing sonic hedhegog pathway and blockade of exosome secretion *in vivo* ameliorated renal fibrosis after ischemic or obstructive injury. Moreover, Guan L *et al.* showed that hypoxic tubuloepithelial cells (TECs) exhibit increased miR-150 and fibroblast develop more profibrotic characteristics upon uptake of these exosomes [135].

There is also evidence that tubular cells communicate with MQs via exosomes. Lv LL *et al.* studied exosome cytokine mRNAs in rat models of acute and chronic kidney disease and showed exosomes of injured tubular cells carry CCL2 mRNA [138]. Moreover, they showed that proximal TECs exposed to albumin also secreted exosomes with increased CCL2 mRNA, which may explain the pathogenesis of 'proteinuria induced kidney injury' in glomerulopathies especially fibrosis during course of proteinuric kidney diseases. They also showed that macrophages exposed bovine serum albumin (BSA) treated proximal tubular cells had increased inflammatory response and migration *in vitro* and mice exposed to these exosomes developed tubular injury with renal inflammatory cell infiltration [138]. Patients with IgA nephropathy were showed to have increased excretion of exosomes with increased expression of CCL2 mRNA, which supported *in vitro* and *in vivo* findings [139].

Hypoxia is another factor that promotes tubulointerstitial inflammation. In mice models of ischemia-reperfusion injury Li ZL *et al.* demonstrated a higher content of miR-23a [140] whereas Ding C *et al.* demonstrated a higher content of miR-374b-5p in EVs released by tubular cells [141]. In both studies EVs were shown to induce activate proinflammatory macrophage polarization. Li ZL demonstrated that miR-23a downregulated the protein A20, a negative regulator of NF-kB signaling leading to macrophage activation [140].

The reciprocal interaction of podocytes with other glomerular cells via EVs was mostly studied in models of diabetic nephropathy. Li M *et al.* had showed that high glucose provoked microvesicle production from podocytes via NOX4/ROS pathway [142]. Interestingly, Munkonda *et al.* showed that microvesicles obtained from untreated human podocyte culture induce proximal tubule fibrotic signaling via p38 MAPK and CD36 [143]. Huang Y *et al.* showed that high glucose treated podocytes secrete EVs that promote apoptosis of proximal TEC. They showed that EVs derived from high glucose treated podocytes carry five differentially expressed miRNAs which were shown to be related to biological processes and pathways of pathogenesis of diabetic kidney disease [144]. Moreover, two studies had showed that high glucose treated mesangial cells and endothelial cells affect podocytes via exosomes [145, 146]. Wu X *et al.* showed that high glucose exposed glomerular endothelial cells cause EMT of podocytes via TGFβ containing exosomes [146].

In the light of these studies and their preponderance in urine, extracellular vesicles serve as a rich source of biomarkers in kidney diseases. Early diagnosis is difficult and takes time in most of kidney diseases in which invasive kidney biopsy is the only method to diagnose. In this regard, 'omics' of the urine EVs is the candidate source of biomarkers. Recently, Chen T *et al*. had studied urinary exosomal miRNA profile of 129 childhood nephrotic syndrome patients and 129 age matched healthy controls and identified upregulated miR-194-5p, miR-146b-5p, miR-378a-3p, miR-23b-3p, and miR-30a-5p correlated with proteinuria [147]. However, their cohort consists of heterogeneous nephrotic syndrome patients with various histological and clinical presentation as well as patients on treatment. In another study, the detection of WT-1 on exosomes was suggested to be a marker of podocyte injury and may help to differentiate FGSG from SSNS [148].

Moreover, there are plenty of mice studies that suggest that stem cell EVs (mostly mesenchymal stem cells) and EVs loaded with anti-inflammatory molecules may play therapeutic role in acute kidney injury [125, 149].

As a summary, EVs are the 'snap-shot' of the cellular mechanisms ongoing in the organism and are one of the main mediators of intracellular communication. Many studies have suggested that they have important roles in intranephronic communication including intraglomerular, glomerulotubular, proximal to distal tubular signaling and tubulointerstitial signaling. Moreover, they may serve as biomarkers in kidney diseases showing glomerular and tubular damage.

1.8. Aims and Outline of the Study

INS of childhood is a podocytopathy, however the exact mediators of the disease that 'hit' the podocytes are not yet known. Treatment is successful in steroid sensitive patients however relapses occur in a substantial portion of patients which make children vulnerable to side effects of immunosuppressive drugs. As previous research suggests a role of a circulating factor in the development of SSNS, we speculated that EVs are a candidate source of such a soluble mediator. Once suggested as cellular garbage, recent studies showed that extracellular vesicles are abundant in body fluids, released virtually by all known cell types during physiological and upon pathological states and mediate cell to cell communication. In this thesis, we aimed to characterize the circulating EVs of NS patients and try to delineate the effects of these EVs on healthy PBMCs and podocytes *in vitro*.

The patient group was consisted of primarily children with SSNS. But as disease controls, children with FSGS and other glomerular diseases that is characterized by proteinuria but have other immunopathologic mechanisms were recruited. Healthy controls were tested for proteinuria in urine.

T and B cell subsets were shown to be changed during NS relapse in children. In the light of previous findings, firstly we planned to characterize T and B subsets as well as monocyte and dentritic cell subsets and compare the results between patients and controls. Secondly, we planned to characterize

the plasma EVs. Extracellular vesicles were isolated by serial ultracentrifugation from healthy controls and nephrotic syndrome patients in relapse and remission. In order to be sure that if they carry EV characteristics and from which cell types they originate from, we planned to visualize EVs with electron microscopy and characterize EVs for EV specific proteins and cell-of-origin with flow cytometry and western blotting. Moreover, the protein contents of the EVs and their individual particle sizes and numbers were measured in order to show the effect of disease status (proteinuria) on EV quantity and content. The major proteins from the plasma EVs were identified via mass spectrometry. A Gene Ontology classification analysis and ingenuity pathway analysis were performed on selectively expressed EV proteins during relapse. Thirdly, the effects of EVs on healthy PBMCs and podocytes were studied in order to show if they transfer a pathological phenotype to these cells *in vitro*. PBMCs were stimulated with EVs, supernatant cytokine concentration and T helper cell phenotype after and before stimulation were compared.

Modeling NS *in vitro* is in its infancy and we have limited parameters to quantify changes in podocyte culture. However human immortalized podocyte culture which differentiates at 37^{o}C, expresses a slit diaphragm-like structure and the vast majority of the podocyte specific proteins. EVs were not internalized by all the cell types equally, therefore we first assessed the kinetics of EV binding and internalization by podocytes. Foot process effacement and increased motility of podocytes are the key events in the development of nephrotic syndrome. *In vitro* podocyte motility was assessed by scratch assay. After scratching the well, the podocytes were stimulated with plasma, plasma fractions from which EVs were depleted (supernatant collected after ultracentrifugation at 100,000 *g*) and EVs from patients and healthy controls. Moreover, the albumin influx assay provides information about the integrity of the slit diaphragm *in vitro*. Podocytes seeded on collagen-coated Transwells were exposed to EVs from NS patients and healthy controls for 4 hours, and then, the albumin influx was measured. Finally, according to relapse EV proteomics characterization, the possible proteins and pathways were studied more deeply on podocyte culture.

2. CHAPTER 2

MATERIALS AND METHODS

2.1. Participants

This study was approved by the local ethics committee of the Dr Sami Ulus Children's Hospital and Human Ethics Committee of Bilkent University. The patient group consisted of 20 children with SSNS, 12 patients with FSGS, 3 patients with membranous glomerulopathy and 3 patients with Henoch-Schönlein Purpura (HSP) nephritis. Blood for the isolation of relapsed NS EVs was taken at the time of the patient's first attack, and EVs were used in experiments after the patients experienced a complete response to steroids within 4 weeks of the treatment. As seen in Table 1, on follow-up of mean 3.8±0.8 years, five of our SSNS patients were diagnosed as frequent relapser and 15 of them were diagnosed as infrequent relapser. None of our SSNS patients developed secondary steroid resistance nor had high suspicion of different underlying pathology during the follow-up period. Remission SSNS EVs were isolated from the same patients when they are non-proteinuric with normal albumin levels, after the cessation of steroid treatment or once they were prescribed low-dose steroids (<0.2 mg/kg/day). PBMCs and plasma EVs of 12 FSGS patients were used in PBMC characterization and stimulation. All of the FSGS patients were diagnosed with biopsy. Two of 8 relapse FSGS patients were taking angiotensin-converting enzyme (ACE) inhibitors but the others were not using drugs. Three of 4 FSGS remission patients were on low dose steroids and one was on steroid and cyclosporine treatment. As other glomerular disease controls, samples from 3 patients with membranous nephropathy and 3 patients with HSP nephritis confirmed by biopsy were used. Blood from these patients was taken at their initial admission to Dr Sami Ulus Children's Hospital, and these patients were not on immunosuppressive treatment at the time of blood withdrawal. All healthy controls (n=10) had negative protein with urinary dipstick and normal urine microscopy. Fasting blood from patients and healthy donors was collected in EDTA-coated tubes after informed consent obtained. Clinical and demographic characteristics of patients and controls were shown in Table 1.

Table 2.1. Clinical and Demographic Characteristics of Patients and Controls

	Healthy Controls	SSNS Patients	Disease Control Patients	FSGS patients
n	10	20	6	12
Diagnosis		SSNS Frequent relapser (n=5) Infrequent relapser (n=15)	Membranous Nephropathy (n=3) HSP nephritis (n=3)	FSGS relapse (n=8) FSGS remission (n=4)
Mean follow-up time		3.8±0.8 years	1.7±0.4 years	4.2±2.3
Gender (Male/Female)	5/5*	11/9*	3/3	7/5
Age (Mean±SD)	6.8±3.2**	5.9±1.8**	8.8±4.7	12.2±3.9
Laboratory Findings at Relapse				
Albumin (Mean±SD)	NA	1.62±0.27	1.71±0.25	2.7±1.0
Spot protein/creatinine (mg/mg creatinine) (Mean±SD)	NA	6.97±2.89	8.31±2.16	4.97±4.87

The statistical significance of gender ratios is insignificant between healthy controls and SSNS patients (The Fischer's exact test, p=0.860).

**The statistical significance of the mean values of ages is insignificant between healthy controls and SSNS patients (Student's T test, p=0.335).

2.2. Materials

2.2.1. Cell Culture Media and Buffers

RPMI 1640 with L-glutamine and phenol red (Biological Industries, #BI01-100-1A), FBS (Gibco, #10270-106, Lot 42G6172K), Penicillin-Streptomycin (10,000 U/mL, #15140-122), 10X Trypsin-EDTA without phenol red (0.5%, #15400-054), DPBS (#14190-250) were obtained from Gibco, Thermo Fisher Scientific (Waltham, MA, USA). Pyrogen Free Cell Culture Water (#LM-T1707/500) was from Biosera (Nuaille, France). Complete RPMI for podocytes was prepared by supplementing the base media with %10 FBS and Penicillin-Streptomycin and Normocin (Invivogen, # ant-nr-2). During proliferation supplemental Insulin Transferrin Selenium (ITS) 100x (Gibco #41400-045) was used. For podocyte passaging trypsin-EDTA (Biowest, #X0930-100) was at a concentration 0.05% used. Lymphocyte Separation Medium (density 1.077 g/ml, #LSM-A) for PBMC isolation was purchased from Capricorn (Ebsdorfergrund, Germany).

2.2.2. Toll-like receptor (TLR) ligands and cytokines used in *in vitro* stimulation experiments

Types of TLR ligands and cytokines used in cell culture experiments and their *in vitro* working concentrations and vendors are listed in Table 2.2.

Table 2.2. Toll-like receptor (TLR) ligands and Cytokine Receptor ligands used in in vitro stimulation experiments

Ligand or Cytokine Name	**Brand Name (Country)**	**Catalogue Number**	**Working Concentration**	**Receptor/Signalling Pathway**
Phorbol-12-myristate 13-acetate	Sigma Aldrich (Germany)	P1585	50 ng/ml	Protein Kinase C
Ionomycin	Calbiochem (Germany)	407950	1 µg/ml	Ca^{+2} Channels on Endoplasmic Reticulum
LPS (Isolated from *E.coli*)	Sigma Aldrich (Germany)	L-2880-100mg	25 µg/ml	Non-Canonical Inflammasome
Human recombinant IL-13	Biolegend (USA)	571104	40 ng/ml	IL13R/STAT6

2.2.3. ELISA Reagents and Kits

Antibodies, recombinant standards and reagents used for cytokine ELISA experiments and their working conditions are listed in Table 2.3.

Table 2.3. Antibodies, recombinant standards and reagents used for cytokine ELISA experiments

Recombinant Antibody	**Brand Name/ (Country)**	**Catalogue Number**	**Clone**	**Working Concentration**
Anti-human IFN-ɣ	Mabtech (Sweden)	3420-1A-20	1-D1K	2 µg/ml
Biotin anti-human IFN-ɣ	Mabtech (Sweden)	3420-1A-20	7-B6-1	1 µg/ml

Human Recombinant IFN-Ɣ	Mabtech (Sweden)	3420-1A-20	NS	50 ng/ml
Anti-human IL-17	Mabtech (Sweden)	3430-1A-20	MT44.6	2 µg/ml
Biotin anti-human IL-17	Mabtech (Sweden)	3430-1A-20	MT504	1 µg/ml
Human Recombinant IL- 17	Mabtech (Sweden)	3430-1A-20	std	20 ng/ml
Anti-human IL-13	Mabtech (Sweden)	3470-1A-6	25K2	1 µg/ml
Biotin anti-human IL-13	Mabtech (Sweden)	3470-1A-6	MT1318	1 µg/ml
Human Recombinant IL- 13	Mabtech (Sweden)	3470-1A-6	std	10 ng/ml
Anti-human IL-10	Mabtech (Sweden)	3430-1A-20	9D7	2 µg/ml
Biotin anti-human IL-10	Mabtech (Sweden)	3430-1A-20	12G8	1 g/ml
Human Recombinant IL- 10	Mabtech (Sweden)	3430-1A-20	NS	250 ng/ml

2.2.4. Antibodies used in Flow Cytometry

All antibodies used for flow cytometry analyses are listed in Table 2.4.

Table 2.4. The antibodies used for flow cytometry analyses

Target Protein	**Fluorescence Conjugate**	**Catalog #**	**Clone**	**Company**
Human CD4	FITC	300538	RPA-T4	Biolegend (San Diego, CA, USA)
Human CD8	APC/Cy7	344714	SK1	Biolegend
Human CD3	Pacific Blue	34824	SK7	Biolegend
Human CD127	PE	351340	A019D5	Biolegend
Human CD25	APC/Cy7	302614	BC96	Biolegend
Human CD25	APC	302610	BC96	Biolegend

Human CD45	PerCP	368506	2D1	Biolegend
Human CD19	FITC	115506	6D5	Biolegend
Human CD27	BV421	302824	O323	Biolegend
Human IgD	BV785	348242	IA6-2	Biolegend
Human CD274 (PD-L1)	PE	329706	29E.2A3	Biolegend
Human CD123	PE/Cy5	306008	6H6	Biolegend
Human CD303	FITC	354208	201A	Biolegend
Human CD14	APC/Cy7	301820	HCD14	Biolegend
Human CD19	PE/Cy7	552854	SJ25C1	BD Pharmingen (NJ, USA)
Human CD3	BV421	563797	UCHT1	BD Pharmingen
Human CD105	FITC	323203	43A3	Biolegend
Human CD42a	PE	558819	ALMA.16	BD Pharmingen
Human CD81	PE	349506	5A6	Biolegend
Human CD63	PE	353004	H5C6	Biolegend
Human CD9	PE	312106	HI9a	Biolegend
Human podocalyxin	PE	sc-23904 PE	3D3	Santa Cruz
Human IFN-Ɣ	PerCP	502524	4S.B3	Biolegend
Human IL13	PE/Cy7	501913	JES10-5A2	Biolegend
Human IL13	APC	501907	JES10-5A2	Biolegend
Human IL17A	PE	560486	N49-653	BD Pharmingen
Human CD80	FITC	305206	2D10	Biolegend
Human Anti-p38 MAPK (pT180/pY182)	Alexa Fluor 647	51-9006595	36/p38	BD Pharmingen
Human Anti P38 MAPK	PE/Cy7	560241	36/p38	BD Pharmingen

2.2.5. Western Antibodies

All antibodies used for western immunoblotting are listed in Table 2.5.

Table 2.5. Antibodies used for flow cytometry analyses.

Antibody Name	**Brand Name/ (Country)**	**Catalogue Number**	**Clone**	**Dilution Factor**
Alix	Cell Signaling Technology (Germany)	2171	3AG	1:1000
TSG101	Abcam (UK)	ab83	4A10	1:1000
Flotinin-1	Cell Signaling Technology (Germany)	3253S	NS*	1:1000
Grp94 Rabbit	Cell Signaling (Germany)	20292S	D6X2Q	1:1000
Synaptopodin	Santa Cruz (Dallas, Texas, USA)	515842	D-9	1:1000
Phospho-p38	Santa Cruz (Dallas, Texas, USA)	166182	E-1	1:1000
α-Tubulin	Santa Cruz (Dallas, Texas, USA)	5286	B-7	1:1000
HRP-conjugated anti-mouse IgG	Cell Signaling Technology (Germany)	7076S	NS	1:10000
HRP-conjugated anti-rabbit IgG	Cell Signaling Technology (Germany)	7074P2	NS	1:10000

2.3. Methods

2.3.1. Experiments with PBMCs

2.3.1.1. Isolation of Peripheric Blood Mononuclear Cells (PBMCs) from Whole Blood

Peripheral blood 5-20 ml from patients and healthy donors were collected to the EDTA tubes (BD Biosciences, USA) and diluted with the same volume of room temperature (RT) Dulbecco's Phosphate-Buffered Saline (DPBS). The diluted blood samples were slowly layered onto the lymphocyte separation media (Capricorn Scientific, Germany) at a volume ratio of 3:2 and centrifuged at 540x*g* with a deacceleration rate of zero in order to preserve formed layers of cell types for 30 minutes. The layered blood samples contain plasma, PBMCs, erythrocytes and lymphocyte separation media. The upper most layer which is the plasma was collected to another falcon for the experiments and EV purification (explained in Section 2.2.7.1). The cloudy layer containing peripheral mononuclear cells (PBMCs) were collected with sterile Pasteur pipette to another falcon and washed two times with Roswell Park Memorial Institute (RPMI)1640 medium with 2% FBS (Fetal bovine serum) by centrifugation at 400x*g* for 10 minutes. Washed cells were resuspended in 1 ml of complete RPMI-1640 medium containing 5% FBS and were counted in flow cytometry which was explained in the next section.

2.3.1.2. Cell Counting

Podocytes or PMNCs were counted by Novocyte 3000 flow cytometer. The cells diluted 1 ml of appropriate media and 20µl from cell suspension was diluted in 5 ml of isotonic solution (Beckmann Coulter, USA). From this suspension 100 ul was analyzed using flow cytometer. By this was the primary cell suspension was diluted 2500x. Number of the live cells were determined by FSC and SSC gating excluding debris and apoptotic cells. To calculate total number of cells per ml media, numbers of events were multiplied with the dilution factor (2500).

2.3.1.3. Immune Characterization of Peripheral Blood Mononuclear cells with Flow Cytometry

In this study the characterization of B cells, T cells and monocytes were determined on untimulated whole blood. 100-200 µl of whole blood were incubated with 5 µl of fluorochrome labeled antibodies (Table 2.2.4) for 30 minutes at RT in dark. Then erythrocytes were lysed using 1X RBC lysis buffer (Biolegend, USA) for 15 minutes at RT, washed via centrifugation for 10 minutes at 500x*g*, resuspended in 5% RPMI Media and analyzed using Novocyte 3000 flow cytometer.

For immunophenotyping of Th1, Th2, Th17 and Treg cells, frozen cells or exosome stimulated PBMCs were used. For frozen PBMCs, $10x10^6$ DMSO frozen PBMCs were dissolved in 37 ^oC in water bed, washed twice with RPMI media with %2 FBS and then incubated in %20 FBS media for 2 hours. Cells were counted again and $1x10^6$ healthy and patient PBMCs were layered onto 96 well U bottom plates. To induce polyclonal cytokine secretion and better characterize the immune cells, cells were treated with Phorbol 12-myristate 13-acetate (PMA) (50ng/ml) and ionomycin (1µg/ml) or left untreated for 2 hours at 37°C (Ref). In order to stop cytokine secretion, 5 µg/ml Brefeldin A (Sigma Aldrich, Germany) was added into wells to stop cytokine secretion and waited further for 4 hours at 37°C. Then plates were centrifuged at 400x*g* for 10 minutes, supernatants were removed, cells were fixed with 150 µl 1X Cytofix Buffer (BD Biosciences, USA) for 20 minutes at RT in dark, washed twice with FACS buffer then were permeabilized with 150 µl cold 1X Cytoperm Buffer (BD Biosciences, USA) for 15 minutes at RT in dark. After removal of permeabilization buffer with centrifugation at 400x*g* for 10 minutes, cells were stained with cell surface markers (1 µg/ml) and cytokine antibodies (1 µg/ml), which were prepared in Fluorescence Activated Cell Sorting (FACS) buffer (Table 2.3) for 30 minutes at RT in dark. Stained cells were washed twice, resuspended in 150 µl-200 µl FACS Buffer and were analyzed using Novocyte 3000 flow cytometer. At least 40.000 events were acquired within $CD4^+$ gates for each sample.

2.3.1.4. Healthy PBMC stimulation with circulating EVs from patients and healthy controls

Four healthy control PBMCs ($4x10^5$ cells pro well) were stimulated with healthy (n=8) and patient EVs (12 SSNS relapse, 6 SSNS remission, 8 FSGS relapse, 4 FSGS remission) (15 µ pro well) for 36 hours in U bottom duplicates. For intracellular staining and as positive control PBMCs were stimulated with PMA (50 ng/ml) at the 30^{th} hour of stimulation. After 36 hours supernatants were collected from PMA unstimulated cells and the remaining PBMCs were fixed and stained with the antibodies in the same manner as stated above. The supernatant cytokine concentrations were normalized to healthy autologous EV stimulation and represented as fold induction.

2.3.1.5. Naïve T cell isolation and stimulation with healthy and patient EVs

Naïve CD4+ T cells were isolated with Human Naïve CD4+ T cell Isolation Kit II (Miltenyi Biotec, USA) with magnetic depletion of memory $CD4^+$ T cells and non-$CD4^+$ T cells. After isolation PBMCs were incubated in a plastic flask for 90 min at 37^{o}C to get rid of monocytes. Then PBMCs are incubated with a cocktail of biotinylated CD45RO, CD8, CD14, CD15, CD16, CD19, CD25, CD34, CD36, CD56, CD123, anti-TCRγ/δ, anti-HLA-DR, and CD235a (glycophorin A) antibodies. These cells are subsequently magnetically labeled with Anti-Biotin MicroBeads and depleted via LS midi colums (Appendix Figure 4). Subsequently, 2 healthy controls were stimulated with 5 µg EVs with 3 SSNS relapse EV and 2 healthy EVs for 6 days. Four hours before ending the stimulation and intracellular

staining, the cells were stained with PMA (1 µg/ml) and ionomycin (1 µg/ml) then stained with antibodies against CD4, IL13, IL17, IFN gama and IL4. Naive T cells cells were stimulated with 5 µg/ml SPDiOC-stained nephrotic syndrome and healthy EVs for 2, 4, 8, 16 or 24 hours. After incubations were done, cells were centrifuged at 300 RCF for 5 minutes, resuspended in 300 µl PBS and analyzed with NovoCyte flow cytometer. In this reading, first FITC positive cells were accepted as bound and uptake (internalized) EVs.

2.3.2. Cytokine Enzyme Linked Immunosorbent Assay (Cytokine ELISA)

All antibodies, recombinant proteins and their working concentrations that were used in ELISA studies were listed in Table 2.3. HB immuno- plates (SPL Life Sciences, South Korea) were coated with 50 µl of coating antibodies, which were prepared according to the manufactures' instructions in 1X PBS and placed to +4°C for overnight (12- 16 hours). The coating antibodies were removed, and wells were blocked with 200 µl blocking buffer (See Appendix B) for 2 hours at RT. Then plates were washed with washing buffer (See Appendix B) for 5 times for 5 minutes and distilled water for 3 times. After washing, the plates were rigorously dried. Then, wells were incubated with either 50 µl of supernatants that were collected from stimulated PBMCs or plasma samples for overnight at +4°C. The next day, supernatants and standards were removed, and plates were washed, dried and were incubated with 50 µl biotinylated antibodies for 2 hours at RT. The biotinylated antibodies were removed, wells were washed and then incubated with 50 µl SA- ALP (1:1000 diluted (v/v) in blocking buffer) for 1 hour at RT. After washing with the same steps as mentioned before 50 µl *p*-Nitrophenly Phosphate (PNPP) solution (ThermoFischer Scientific, USA), was added onto each well OD values at 405nm of each well were taken with ELISA Plate Reader (Molecular Devices, USA) in every 30 minutes at the first 4-8 hours and overnight when needed. Standard curve was constructed with OD values of serially diluted recombinant proteins with 4-parametric curve.

2.3.3. Experiments with EVs

2.3.3.1. Isolation of Plasma and Plasma EV from Human Blood

Whole blood was mixed with equal volume of phosphate buffered saline (PBS)(Biological Industries, Beit HaEmek, Israel) and slowly layered onto the lymphocyte separation medium with 3:2 (blood:medium) ratio and centrifuged at 540 *g* for 30 minutes. The upper plasma fraction and the cloudy interface containing PBMC were separated. The plasma fraction centrifuged at 2000 *g* to get rid of platelet and dead cells. Supernatants were collected to new tubes, snap-frozen in liquid nitrogen and kept at -80°C for further use. At the time of ultracentrifugation (UC), frozen tubes were thawed very slowly overnight at +4°C in order to prevent EV and/or exosome rupture before isolation and vigorously vortexed before proceeding to UC. If needed, in order to adjust the volume to a fix amount before

centrifugation, some plasma samples were supplemented with cold PBS to 14 ml and centrifuged at 10.000 *g* for 30 min at 4°C. Supernatants were transferred to another UC tube and centrifuged at 100.000 *g* for 90 min at 4°C. At the end of this step, EVs were sedimented. The supernatants were accepted as plasma depleted EV and used at further experiments. In order to get rid of contaminating proteins, EVs were further washed with 14 ml PBS and recentrifuged at 100.000 *g* for 90 minutes at 4 °C. The pellets containing EVs were dissolved with PBS.

2.3.3.2. Determination of EV Protein Content and Number

Protein content of EVs was determined with Pierce BCA Protein Assay Kit (Thermo Fisher Scientific) according to the manufacturer's instructions. Briefly, 25 µl/well BSA standard dilutions and 5 µl/well samples were placed in 96 well plates and were mixed with 200 µl of the working reagent. The plate was incubated in dark at 37°C for 30 minutes and then cooled down at room temperature for 15 minutes. Absorbance at 562 nm was measured with Synergy HT microplate reader (BioTek, Winooski, VT, USA). Particle number of 1µg/ul EV was measured by tunable pulse resistive index system (QNano, Izon Biosciences, USA). Protein amount and particle concentration of EVs were presented as normalized to plasma volume (ml) and plasma albumin concentration (g/dl).

2.3.3.3. Transmission Electron Microscopy

The morphology and the size of EVs were evaluated by transmission electron microscopy (TEM). EV suspensions (5 µl) were dropped onto formvar/carbon-coated nickel mesh grids and incubated for 20 min. Then, the excess suspension on the nickel mesh grids was blotted with filter paper and nickel mesh grids were negatively stained with 2.0% phosphotungstic acid and 2.0% uranyl acetate, respectively. After washing, samples were air-dried for 15 minutes and visualized using a digital camera (Orius, Germany) connected to transmission electron microscope (JEM1400; Jeol, Tokyo, Japan).

2.3.3.4. Analysis of EV Surface Markers by Flow Cytometry

A bead-based detection method was used for surface protein characterization of EVs with flow cytometry. Latex beads were coated with purified anti-human CD63 or CD81 antibody to capture EVs. Carboxyl latex beads (Thermo Fisher Scientific, Carlsbad, CA, USA) were mixed with anti-CD63 or CD81 (Biolegend, San Diego, CA, USA) at a 1µl:1µg (bead:antibody) ratio to capture CD63 or CD81 positive EVs. The volume was completed to 50 µl with PBS and the mixture was incubated for 30 minutes at RT. Then, the volume was increased to 500 µl with PBS and the mixture was incubated on a rotator at a low speed overnight. The bead-antibody mixture was precipitated at 10.000 *g* for 10 minutes,

blocked with 5% BSA (Capricorn Scientific GmbH, Ebsdorfergrund, Germany) for 4 hours at RT, precipitated again at 10.000 *g* for 10 minutes, resuspended in PBS containing 1% BSA and stored at 4°C. For each staining of EVs, 1 µg EV was mixed with 1 µl of the final coated bead solution. Volume was increased with PBS up to 50 µl and the mixture was incubated at RT for 30 minutes. Then the volume was increased to 500 µl and the mixture was slowly rotated overnight to let the EVs and the beads conjugate. After overnight conjugation, EV-bead conjugates were incubated with fluorochrome antibodies for human CD9, CD63, CD81 (Biolegend, San Diego, CA, USA) and PE-Podocalyxin (Santa Cruz, Dallas, Texas, USA) and their appropriate isotype controls at a concentration of 1 µg/ml in 100 µl volume for 1 hour at RT in the dark. After 1 hour of incubation, samples were washed with PBS and centrifuged at 10.000 RCF for 5 minutes, then resuspended in 100 µl of PBS and analyzed with NovoCyte flow cytometer (ACEA Biosciences). For the quantification of cell-surface specific markers of plasma EVs samples, EV-anti-CD81 coated bead conjugates were stained with an antibody against one of the following cell surface markers: PE-CD42a (platelet, BD Pharmingen, Franklin Lakes, NJ, USA), FITC-CD105 (endothelial cells, Biolegend, San Diego, CA, USA), BV421-CD3 (T-cells, BD Pharmingen, Franklin Lakes, NJ,USA), APC/Cy7-CD14 (monocytes, Biolegend, San Diego, CA, USA), PC7-CD19 (BD Pharmingen, Franklin Lakes, NJ, USA) with the same method. The particle counts after a very stringent FSC-SSC gating strategy was divided to the total bead-EV conjugate counts to calculate the percentage of antibody positive beads. Every EV sample was stained in triplicate and the mean percentage of each sample was used in the analysis.

2.3.4. Proteomics Studies

2.3.4.1. Sample Preparation for Proteomics studies

50 µg of protein from each sample was transferred to micro tubes. The proteins were reduced with dithiothreitol (DTT) to adjust the 5 mM final concentration at room temperature and alkylated with iodoacetamide (IAA) to set the 50mM final concentration at room temperature for 1 hour in dark. The additional DTT was added to set the 10 mM final concentration. Proteins were precipitated using methanol/chloroform precipitation protocol and dissolved in solution having 8M urea and 50mM Tris buffer at pH 8.5. The urea concentration was then diluted to 1M with 50mM Tris buffer at pH 8.5. Trypsin was dissolved in 50mM Tris buffer at pH 8.5 and then added to the protein solution in the ratio of 1:100 (w/w, trypsin/protein). Finally, incubation was performed overnight. Trifluoroacetic acid was added to the incubated solution in order to stop the enzymatic digestion setting the final concentration of trifluoroacetic concentration to 0.5% (v/v). The samples were cleaned using Sep-Pak (Waters) according to the manufacturer protocol. Samples were dried using Speed-Vac centrifugal evaporator and then dissolved in MilliQ water (18. 2 MΩ.cm) to make the concentration of protein 0.5 µg/µl.

2.3.4.2.Mass Spectrometry

Peptides were run on a 15 cm column (EASY-Spray column, 15 cm length, 75 µm internal diameter, PepMap C18, 3 µm particles, 100 Å pore size) connected to an Ultimate 3000 RSLnano system (Dionex, Thermo Scientific) in a Q Exactive Plus mass spectrometer. Samples were loaded onto the column with buffer A (0.1% formic acid in water) and eluted with a 260-min gradient time, with 5% to 95% buffer B (95% ACN, 0.1% FA, 5% H_2O) at a flow rate of 250 nl/min. Mass spectra were acquired with an Orbitrap Q Exactive Plus mass spectrometer in the data-dependent mode and the scan range was from 200 to 3000 m/z for four hours. Peptide fragmentation was performed via HCD with the energy set at 29 NCE was used for peptide fragmentation. The MS/MS spectra were acquired at a resolution of 17,500 for every sample. The analysis was run only once.

2.3.4.3.Proteomics Analysis

The raw data from mass spectrometry were run in Proteome Discoverer version 2.2 for peptide and protein identification. Data analysis was performed using Microsoft Excel. Gene symbols of the significant proteins identified were uploaded to the Ingenuity Pathway Analysis (IPA v10.2020) server for in-depth knowledge analysis using the "Core Analysis" function (Fisher's Exact Test (FET) p-value: 1e-03). The venn diagram was generated using the "venn()" function in the R package gplots v3.0.1.1. The gene list enrichment analysis platform, EnrichR v01.07.2020, at https://amp.pharm.mssm.edu/Enrichr/ was used with the following library in this study: GO Cellular Compartments. Information for Top 100 EV proteins from the database Vesiclepedia (http://www.microvesicles.org/extracellular_vesicle_markers) was accessed in July 2020 [150]. The mass spectrometry proteomics data have been deposited to the ProteomeXchange Consortium via the PRIDE partner repository with the dataset identifier PXD024217 [151].

2.3.5. Experiments with human podocyte cell culture

2.3.5.1.Human immortalized podocyte cell culture

Human conditionally immortalized human podocytes (LY8H3) were kindly provided by Prof Moin Saleem (Bristol, UK). For proliferation, they were cultivated at the permissive temperature of 33°C in podocyte medium containing RPMI 1640 supplemented with Insulin Transferrin Selenium (ITS), Penicillin/Streptomycin, Normocin and 10% FBS. For differentiation, they were grown on rat tail Collagen I (100 µq/ml) (Gibco, Thermo Fischer Scientific, Carlsbad, CA, USA) coated wells at 37°C

for ten to fourteen days before used experimentally. On some experiments with EVs, EV-free podocyte medium was used which was prepared by FBS centrifuged at 100.000 *g* for 4 hours. EVs from podocyte culture supernatant were isolated with the protocol mentioned above. Podocytes were grown on collagen coated T75 plates and stimulated with IL13 (40 µg/ml) or LPS (25 µg/ml) or with podocyte medium as control for 24 hours.

2.3.5.2. Determination of EV binding and uptake of human immortalized podocytes

EV surface was stained with the lipophilic dye SP-DiOC18 (Invitrogen, Carlsbad, CA, USA) which can be analyzed at FITC channel on flow cytometry. SP-DiOC was mixed with EVs at a ratio of 1µg:10µg (SP-DiOC:EV). The mixture was incubated for 60 minutes at 37°C in dark. The solution was diluted to 14 ml with PBS and ultracentrifuged for 90 minutes at 100.000 RCF to remove unbound dye. EV pellet was dissolved in PBS and the volume was adjusted according to further applications. In some experiments we have attempted to further purify EVs following ultracentrifugation and applied to size exclusion columns (IZON qEV column, 70 nm). Human immortalized podocytes were seeded to 6 well plates. After 14 days of differentiation, cells were stimulated with 20 µg/ml SP-DiOC-stained nephrotic syndrome and healthy EVs for 2, 4, 8, 16 or 24 hours. After incubations were done, cells were scraped, then washed with PBS and centrifuged at 300 RCF for 5 minutes, resuspended in 500 µl PBS and analyzed with NovoCyte flow cytometer. In this reading, first FITC positive cells were accepted as bound and uptake (internalized) EVs. To determine internalized EV fraction by the cells, the remaining cells were mixed with 30 µl Trypan Blue (0.1%) to quench membrane bound not internalized EVs from podocyte surface and FITC gate was measured again from the same tube. This value was recorded as internalized EV levels by podocytes. Also, fluorescence signals of SP-DiOC stained EVs in the podocytes were visualized with EVOS FL Auto cell imaging system (Thermo Fisher Scientific).

2.3.5.3. PKH26 labeling of EVs and Phalloidin staining of podocytes

Plasma EVs were labeled with the red lipophilic fluorescent dye PKH26 (Sigma-Aldrich, St. Louis, MO) according to the instructions. The suspension, containing 125 µg (125 µl) EVs, was transferred to a conical-bottom polypropylene tube. A 2x EV suspension was prepared by adding 125 µl of Diluent C to the EV suspension, and a 2x dye solution was prepared by adding 0.5 µl of the PKH67 ethanolic dye solution to 250 ul of Diluent C. Then, 250 ml of 2× EV suspension was quickly added to 250 ul of 2x dye solution, and the EVs/dye suspension was incubated for ~1-5 min. Then, 500 ul of 1% BSA was added to bind excess dye. EVs were centrifuged for 90 min at 100.000 g and pellets were suspended in podocyte medium. In some experiments we have attempted to purify EVs following ultracentrifugation and applied to size exclusion columns (qEVoriginal / 70nm SEC Columns, Izon Biosciences, USA).

Podocytes were incubated with 20 µg of PKH26-labeled EVs for 24 h. The podocytes were fixed with 4% paraformaldehyde for 15 min, washed with PBS, then permeabilized with %0.3 Triton X-100 for 10 minutes. Wells were blocked with 5% BSA for 30 min at room temperature. Subsequently, podocytes were stained with a 2 drops/ml fluorescent conjugated phalloidin (ActinGreen™ 488 ReadyProbes™ Reagent, Thermo Fisher) and DAPI (NucBlue™ Fixed Cell ReadyProbes™ Reagent, Thermo Fisher) 2 drops/ml in PBS for 15 min at room temperature. Wells were washed several times in PBS to remove unbound dye and were observed using EVOS FL Auto cell imaging system (Thermo Fisher Scientific).

2.3.5.4.Albumin influx assay

The albumin influx assay was performed to examine the filtration barrier function of podocyte monolayers as previously described [105]. Transwell chambers (6.5 mm, 24 chambers) with a 0.4-µm pore size (Costar, USA) were used in the albumin influx assay. Podocytes (1×10^5) were seeded on the collagen coated upper permeable supports and cultured under differentiating conditions for 10 days. Cells were washed twice with PBS supplemented with 1 mM MgCl2 and 1 mM $CaCl_2$ to preserve the cadherin-based junctions. The podocytes were incubated with patient and healthy EVs (20 µg/ml) for 4 h. Cells were re-washed, then the upper chamber was then filled with 0.1 ml serum-free RPMI, and the lower chamber was filled with 0.5 ml serum-free RPMI 1640 supplemented with 40 mg/ml of BSA (Capricorn Scientific GmbH, Ebsdorfergrund, Germany). Total protein concentration in the upper chamber was examined using the BCA method at 0, 2 and 4th hours.

2.3.5.5. Scratch Assay

Podocytes were cultured on collagen coated (100 µg/ml) 12 well plates and differentiated for 14 days at 37°C. The culture media was aspirated, and two scratches diagonally were inflicted with a 200 µl pipette tip. The podocytes were then washed with PBS thrice to remove any debris and promigratory factors. Then EVs (20 µg/ml) in EV-depleted podocyte medium or plasma (10%) or EV depleted plasma (10%) in RPMI 1640 were added to the wells and the scratch area was imaged immediately (time 0) and 12 hours later using EVOS FL Auto cell imaging system (Thermo Fisher Scientific). The areas of the clear zone at 0 and 12 h were measured by Image J and podocyte migration was assessed by reduction in the area, indicating more motile cells. The experiment was repeated 3 times with EVs of same patients and healthy controls. Each repeat had 2 replicates.

2.3.5.6.G-LISA Rac activation assay

Immortalized cultured human podocytes were differentiated on collagen coated 6 well plates by switching the temperature to 37°C for 10 days and serum starved for 24 days. Next day, they were stimulated with human plasma (10%) or EVs (20 μg/ml) for 4 hours. Then, cells were lysed, and their Rac1 activity was quantified by using a colorimetric G-LISA Rac Activation Assay Biochem kit (Cytoskeleton, Denver, CO, USA), according to the manufacturer's instructions. EVs were lysed by cold lysis buffer of the kit, sonicated, vortexed and supernatant after 10.000 g centrifugation was used for measuring RAC-GTP content.

2.3.5.7. Flow Cytometry of Human Podocytes for phosho p38 (p-p38) and CD80 staining

Immortalized human podocytes were differentiated on collagen coated 6 well plates for 14 days. On the day of experiments, cells were serum starved for 4 hours, then the media was changed with RPMI 1640 media supplemented with 1) 10% FBS 2) 10% human plasma 3) 10% EV depleted-plasma 4) patient or healthy EVs (20 μg/ml) and EV-depleted 10% FBS 2) 10% FBS with 40 ng/ml IL13. After 30 minutes, media was discarded and cells were fixed with 1.5 ml fixation buffer (2% percent formaldehyde) for 15 minutes in 37 C. Cells were scraped, centrifuged at 800 g for 5 minutes, washed 2 times with PBS and permeabilized with 80% cold methanol on ice for 1 hour. After washing, cells were incubated with Anti-p38 MAPK (pT180/pY182) (Alexa Fluor 647 or PE/Cy7) (BD Biosciences, San Jose, CA, USA) or Anti-CD80 FITC (Biolegend, San Diego, CA, USA) for 1 hour at room temperature, washed once with FACS buffer (1% BSA and 0.1% NaN3 sodium azide in PBS) and analyzed with Novocyte flow cytometer.

2.3.6. Western Blotting

Cell lysates or EV lysates were incubated with RIPA buffer containing 2 M NaCl, 1 M Tris (pH = 8), NP-40, 10% SDS, protease inhibitor cocktail (Thermo Fisher) and fresh phosphatase inhibitors (Thermo Fisher). After 30 min of incubation with intermittent vortexing every 5 min, lysates were centrifuged at 10.000 g for 20 min, and supernatants were collected. Protein concentration was determined with Pierce BCA Protein Assay Kit. Twenty-five micrograms of protein were loaded per well and separated by 10% or 12% sodium dodecyl sulfate–polyacrylamide gel electrophoresis (SDS–PAGE), transferred to a PVDF membrane and probed with 1:1000 diluted primary antibodies against anti-p-p38 (Santa Cruz, Dallas, Texas, USA), Anti-GRP94 antibody (Cell Signaling,Germany)Anti TSG-101 antibody (Abcam, Cambridge, UK), anti-α tubulin (Santa Cruz, Dallas, Texas, USA), anti-synaptopodin (Santa Cruz, Dallas, Texas, USA), anti-Flotillin (Cell Signaling Technology, Frankfurt am Main, Germany) and anti-ALIX (Cell Signaling Technology, Frankfurt am Main, Germany). Blots were visualized by an

Amersham Imager 600 (Little Chalfont, UK) after incubating the membranes with 1:5000 diluted HRP linked secondary antibodies.

2.3.7. Statistical Analysis

Data were analysed with GraphPad Prism 6 Software (San Diego, CA, USA). Normality tests of the numerical variables were evaluated with Kolmogorov-Smirnov test. Descriptive analyses were presented as the mean ± SD for numerical variables. The Mann–Whitney U test or Student's t-test were used to compare the two groups. ANOVA test with Dunnet's or Tukey's post-hoc test was used for analyses of repeated experiments. A chi-squared test or Fisher's exact test (when chi-squared test assumptions did not hold due to low expected counts) was used to compare categorical variables. A p value less than 0.05 was considered significant.

3. Chapter 3

RESULTS

3.1. PBMC Characterization of NS patients and healthy controls

T and B cell subsets were shown to be changed during NS relapse in children. In the light of previous findings, we characterized T and B subsets as well as monocyte and dentritic cell subsets. As shown Figure 3.1 we have found no significant difference between T helper ($CD4^+CD8^-$ cells) and cytotoxic T cell ($CD8^+CD4^-$) subsets as well as their ratio (Appendix Figure 1). There is also no significant difference between Th1 ($CD3^+CD4^+IFN\gamma^+$) cells but Th2 ($CD3^+CD4^+IL13^+$) subset percentage in PBMC is significantly higher during SSNS and FSGS relapse patients compared to healthy controls ($p<0.05$). Th1/Th2 ratio was also significantly decreased in SSNS relapse patients. Moreover, serum plasma IL13 level is significantly higher in SSNS relapse patients compare to SSNS remission and other glomerular disease patients ($p <0.05$).

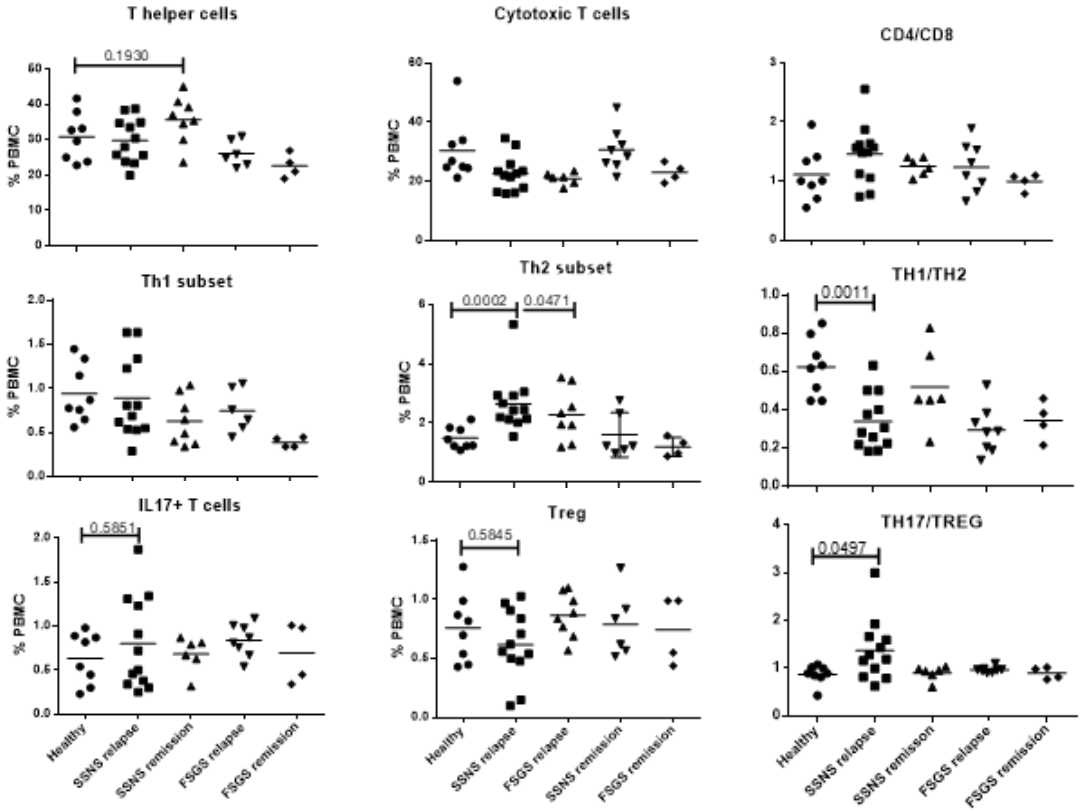

Figure 3.1. T lymphocyte subsets of patients and healthy controls. 1x10^6 frozen PBMCs were stained with antibodies against CD3, CD4 and CD8 to characterize T helper (CD3+CD4+CD8-)(a) and cytotoxic T cells (CD3+CD8+CD4-) (b). For T helper characterization the cells were stimulated with PMA and ionomycin for 6 h and then stained with intracellular cytokines IFNɣ for Th1 (d), with IL13 for Th2 (e), IL17 for TH17 (g) characterization. CD4+CD127dimCD25+ cells were defined as Tregs (h) in this assay. For comparison of T subsets Mann-Whitney U test was used. Mean values were shown.

There was no significant difference in Treg ($CD4^+CD127dimCD25^+$) and Th17 ($CD3^+CD4^+IL17^+$) cell percentages between NS patients and healthy controls. But TH17/Treg percentage was significantly higher in SSNS relapse patients compared to healthy controls (p=0.0497).

B cell ($CD19^+$ cells) percentage is also higher in SSNS relapse patients compared to healthy controls, SSNS remission and FSGS patients ($p < 0.05$) (Figure 3.2). Moreover, memory B cells ($CD19^+CD27^+$ cells) and switched memory B ($CD19^+CD27^+IgD^-$) cells are significantly higher in SSNS relapse patients compared to healthy controls (p=0.006, p=0.045 respectively). Gating strategy is showed in Appendix Figure 2.

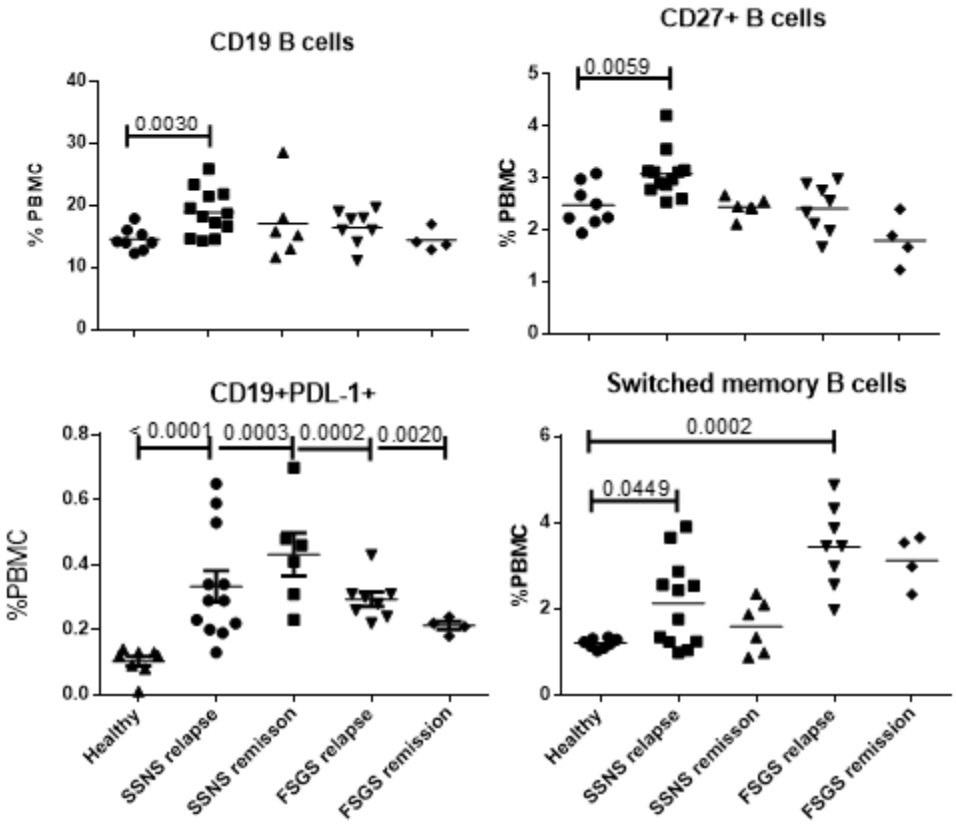

Figure 3.2. B lymphocyte subsets characterization of patients and healthy controls from whole blood. Whole blood was stained with surface marker antibodies against CD19, CD27, IgD and PD-L1 to characterize total B cells ($CD19^+$) (a), memory B cells ($CD19^+CD27^+$) (b), switched memory B cells ($CD19^+CD27^+IgD^-$) (d) and regulatory B cells ($CD19^+PD\text{-}L1^+$) (c). For statistical analysis Mann-Whitney U test were used. Mean values were shown on graph.

We have also studied $CD19^+PD\text{-}L1^+$ cells which were characterized as one of the regulatory B cells [152]. These regulatory B cells were significantly increased in all NS subtypes compared to healthy controls. CD14 positive cells characterize monocytes and significantly increased in SSNS relapse patients compared to healthy controls ($p<0.05$). There was no significant difference among dentritic cell percentage among patient groups (Appendix Figure 3.a and 3.b).

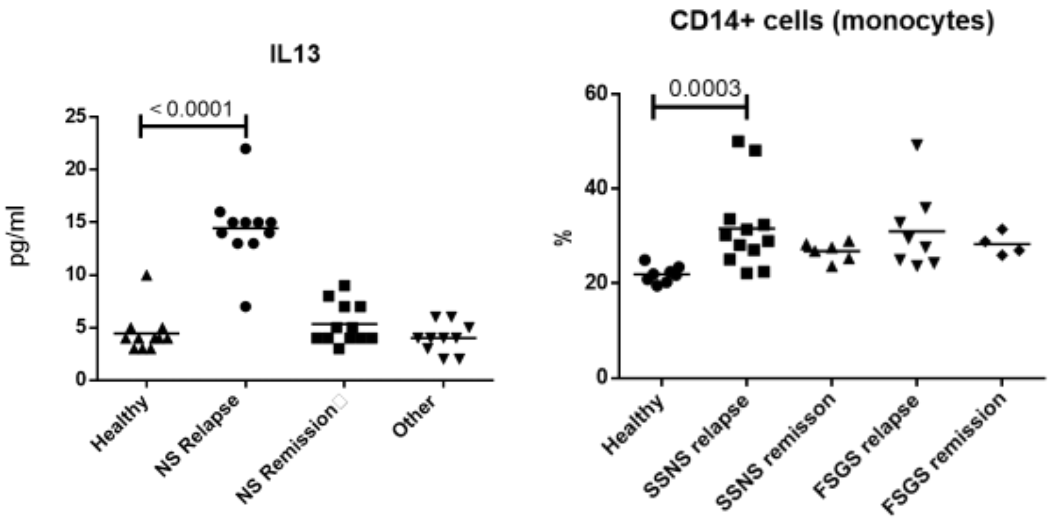

Figure 3.3. Comparison of plasma IL13 and whole blood monocyte percentages of patients and healthy controls. Plasma IL13 was measured by ELISA from plasma. Whole blood was stained with surface marker antibodies against CD45 and CD14 to characterize monocytes. For statistical analysis Mann-Whitney U test were used. Mean values were shown on graph.

3.2. EV Characterization of patients and controls

3.2.1. Transmission Electron Microscopy

Extracellular vesicles were isolated by serial ultracentrifugation from healthy controls and nephrotic syndrome patients in relapse and remission. The International Society of Extracellular Vesicles defines extracellular vesicles as particles released from cells that are delimited by a lipid bilayer, cannot replicate and do not have a functional nucleus [121]. Our TEM images showed the bilayer lipid structure of our EVs (Figure 3.4).

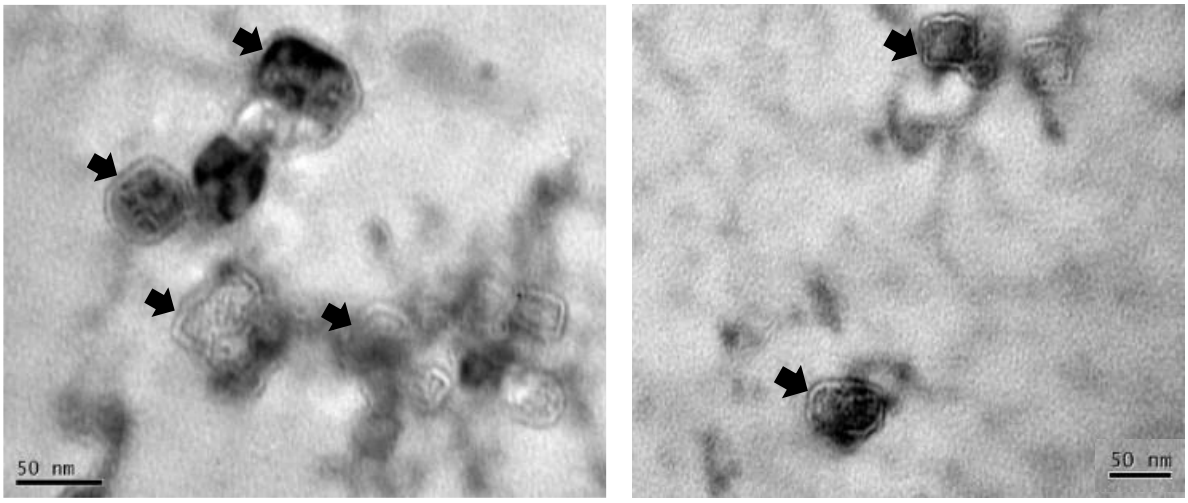

Figure 3.4. Transmission Electron Microscopy (TEM) images of EVs obtained from plasma by serial ultracentrifugation. Arrow heads show typical bilayer membrane of EVs) (Scale bar 50 nm).

3.2.2. Immunoblotting and flow cytometry of EVs with characteristic EV markers

The relapse NS EVs were shown to carry ALIX, TSG 101 and Flotillin by immunoblotting (Figure 1B) and were enriched in tetraspanins, such as CD9, CD63 and CD81 as shown in Supplementary Figure 1,

which play roles in membrane organization and are commonly used as cardinal EV surface markers. As a negative EV marker GRP94, which is endoplasmic reticulum resident protein, was as expected positive on cell lysates and absent on EV samples (Figure 3.5).

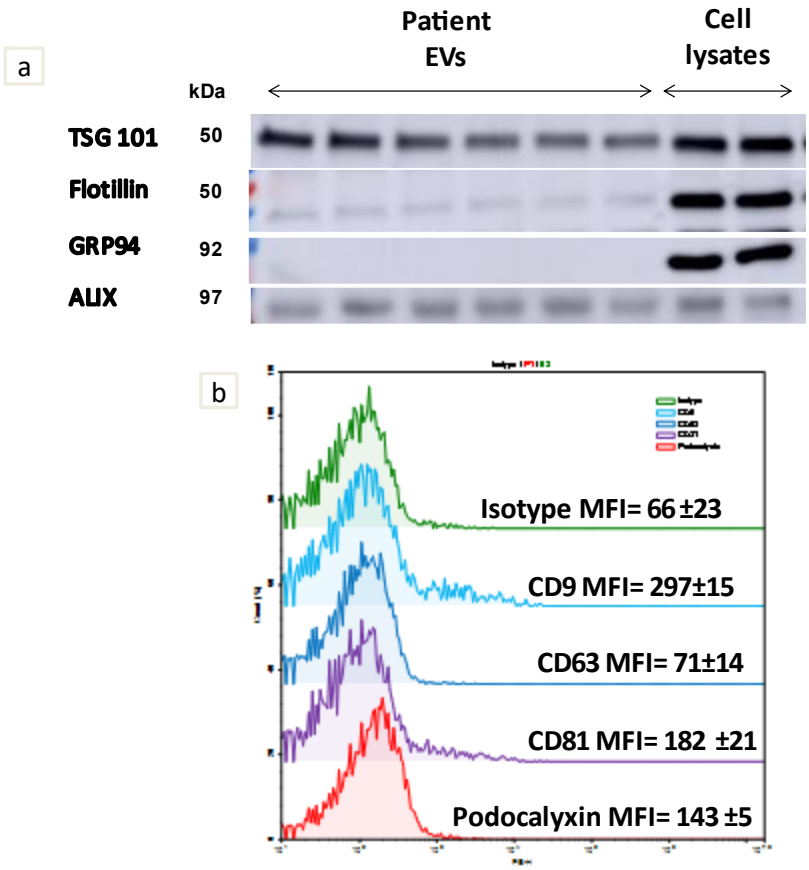

Figure 3.5. EV characterization with specific EV markers. a) Western blot images of expression of EV markers ALIX, TSG 101 and Flotillin on six relapse NS patient EVs and podocyte cell lysates. GRP94 was used as a negative EV marker. b) Histogram plots showing flow cytometry plots of EV markers (CD9, CD63, CD81) and podocyte marker, podocalyxin and appropriate isotypes on NS plasma EVs captured by anti-CD63 coated latex beads.

3.2.3. Bead Based Characterization of EVs with cell specific markers

Plasma EVs constitute particles from a very different cell types. To elucidate the source of NS relapse EVs and to compare with healthy controls, bead captured EVs were stained with cell surface molecules of platelets, endothelium, monocytes, T cells and B cells. As reported previously platelet EVs constitute the major EV pool of our samples [153] and their mean percentage is significantly higher than healthy controls ($p<0.001$). Similarly, the mean percentage of endothelial, monocytes and B cell EV percentages were significantly higher in relapse NS patients compared to healthy controls (Figure 3.6.a). Moreover, the expression of podocalyxin which is expressed on podocytes and endothelial cells, was significantly higher than that on the same amount of healthy control EVs ($p<0.001$, Figure 3.6.b).

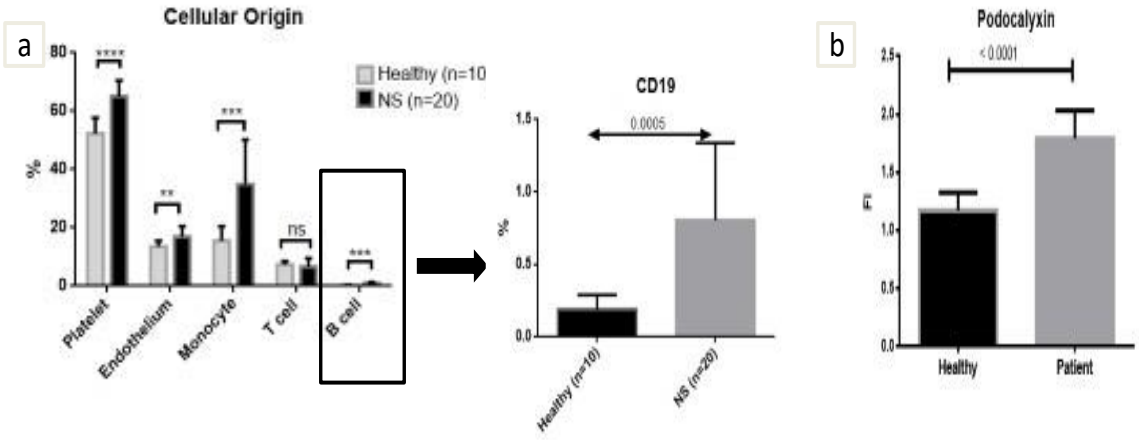

*Figure 3.6 Bead based characterisation of ciriculating EVs of SSNS patients with cell specific markers. a) Circulating EVs of healthy controls (n=10) and NS relapse patients (n=20) were stained with corresponding cell type specific markers. Data is represented as the mean±SD percentage (Unpaired t-test was used, ***p<0.001, **p<0.01, ns nonsignificant). b) Podocalyxin expression represented as MFI fold induction on the matched isotype control on NS relapse EVs (n=20) was compared to healthy controls (n=10) (p<0.001) (Mean±SD were shown, Unpaired Student's t test was performed.)*

3.2.4. Circulating EV particle and protein concentrations

The protein contents of the EVs were measured by BCA, and their individual particle sizes and numbers were measured by tunable resistive pulse sensing. The protein amount and the particle concentration per milliliter of plasma in the samples isolated during nephrotic relapse and remission were significantly higher than those in the samples from healthy controls (Figure 3.7.a and 3.7.b). Since the samples from the patients and healthy controls had different albumin levels and different plasma amounts during ultracentrifugation, the yields were also normalized based on plasma volume and albumin concentrations [121]. The protein amount and particle concentration per milliliter of plasma per gram albumin in the samples of isolated during nephrotic relapse were significantly higher than those in the samples isolated during remission and those in the samples from healthy controls (Figure 3.7.c and 3.7.d).

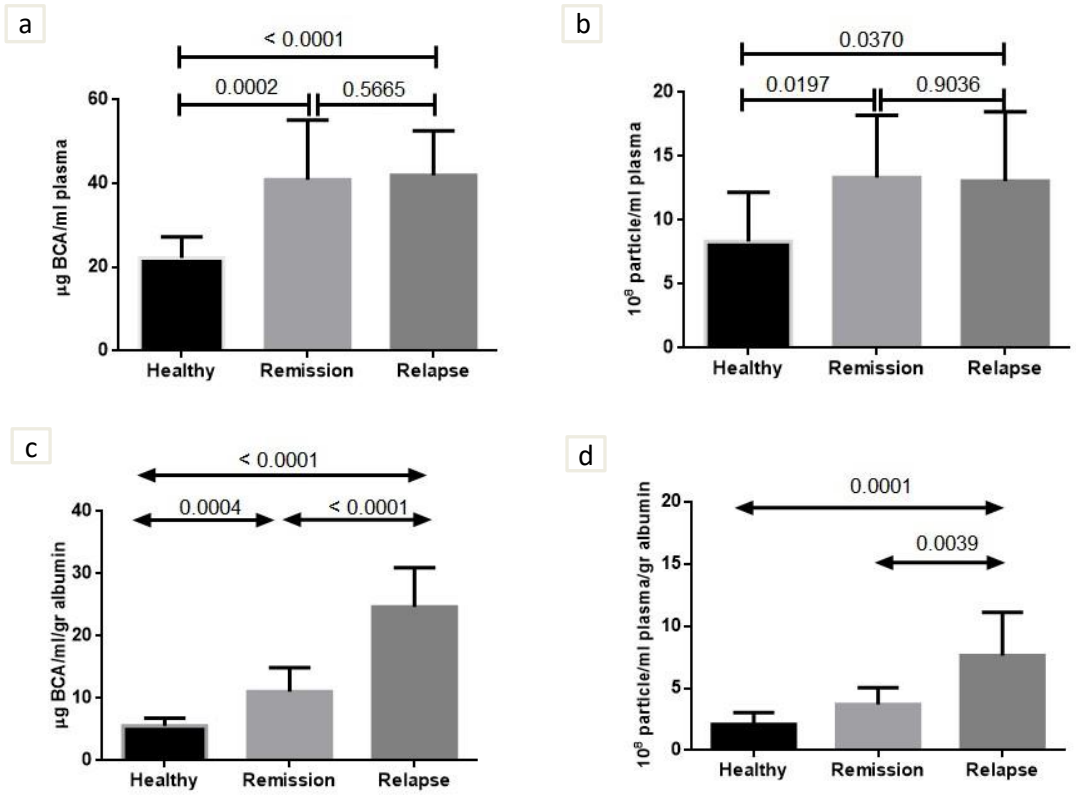

Figure 3.7 EV protein and particle concentration of relapse and remission NS patients and healthy controls a) The protein concentration of relapse and remission EVs (n=10) normalized to plasma volume were compared to healthy EVs (n=10). b) The particle concentration of relapse and remission EVs normalized to plasma volume were compared to healthy EVs. c) The protein concentration of relapse EVs (n=10) and remission EVs (n=10) normalized to albumin and plasma volume were compared to healthy EVs (n=10) d) The particle concentration of relapse EVs and remission EVs normalized to albumin and plasma volume were compared to healthy EVs. (Mean±SD were shown, Unpaired Student's t test was performed.)

3.2.5. EV size distribution and concentration

Representative images of particle size distribution and concentration of a healthy control, a relapse and a remission NS patient was shown in Figure 3.8.a. The median size of the particles was 205±31 nm in relapse patients, 209±25 nm in remission patients and 213±25 nm in healthy controls, suggesting that the sizes of the EVs in the different disease states were not significantly different from each other (Figure 3.8.b).

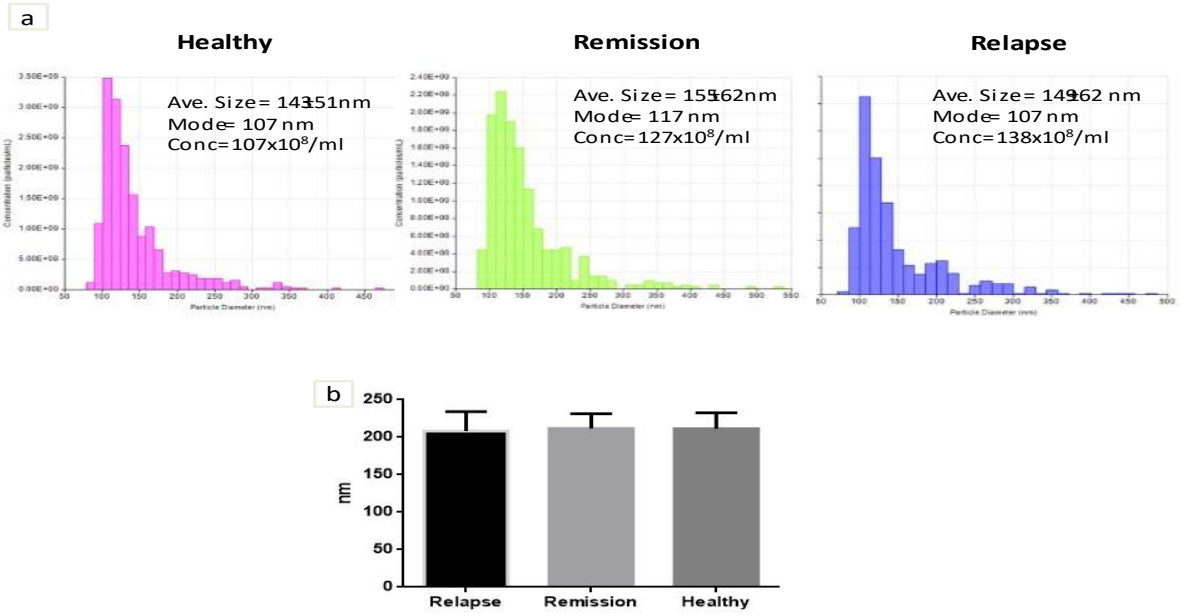

Figure 3.8. a) Representative images of particle size distribution and concentration of a healthy control, a relapse and remission NS patient EVs measured by tunable resistive pulse sensing (QNano, Izon Biosciences, USA). b) The mean sizes of EVs among patients and healthy controls were not significantly different (Kruskal-Wallis test p= 0.7521).

3.3. Effect of Extracellular Vesicles in PBMCs

Since we have observed a significant difference in T and B cell subsets, we planned to study the effects of EVs on healthy PBMCs and show if they transfer a pathological phenotype to the healthy PBMCs.

3.3.1. Supernatant cytokine measurement and T subset characterization after EV stimulation of healthy PBMCs

Five healthy PBMCs were stimulated with patient and healthy EVs for 24 hours and the supernatant cytokine levels were presented as fold induction normalized to unstimulated and autologous EV stimulated supernatant cytokine levels. As seen in Figure Figure 3.8.b SSNS relapse EVs induce significantly higher IFNɣ and IL13 levels compared to non-autologous healthy EVs. On the other hand, FSGS EVs induce higher IL10 production compared to healthy EVs.

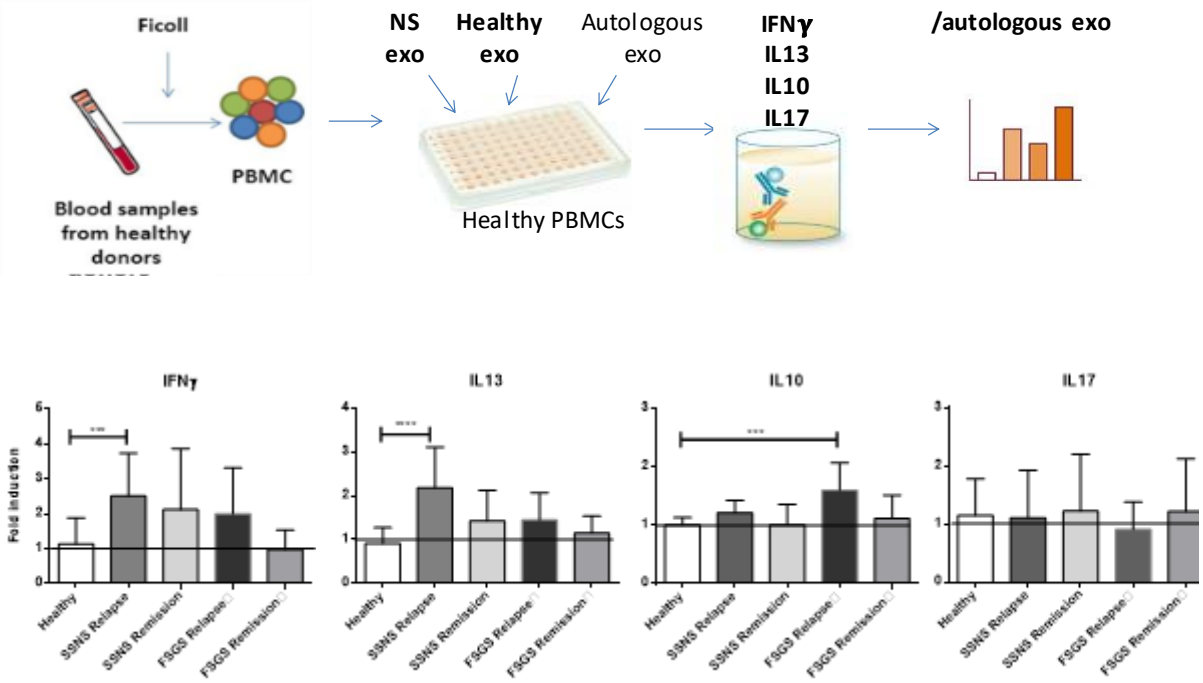

*Figure 3.9. Cytokine concentrations of healthy PBMC supernatants after stimulation with circulating EVs from patients and healthy controls. a) Representation of experimental plan b) Four healthy control PBMCs (4x10^5 cells pro well) were stimulated with healthy (n=8) and patient EVs (12 SSNS relapse, 6 SSNS remission, 8 FSGS relapse, 4 FSGS remission)(15 µ pro well) for 36 hours in U bottom duplicates. After 36 hours supernatants were collected and cytokine (IL13, IFNɣ, IL10 and IL17) concentrations were normalized to healthy autologous EV stimulation and represented as fold induction. Results are presented as mean±SEM. Two-way ANOVA with Dunnet's post hoc test was performed vs. healthy EV stimulated PBMCs. Data are presented as the mean ± SEM. ***P < 0.001.*

We have also characterized Th subsets after EV stimulation and showed that SSNS EVs induce more Th2 cells compared to healthy control and FSGS EVs. These results suggested that EVs surge healthy PBMCs to Th2 phenotype transferring NS phenotype to healthy cells (Figure 3.10).

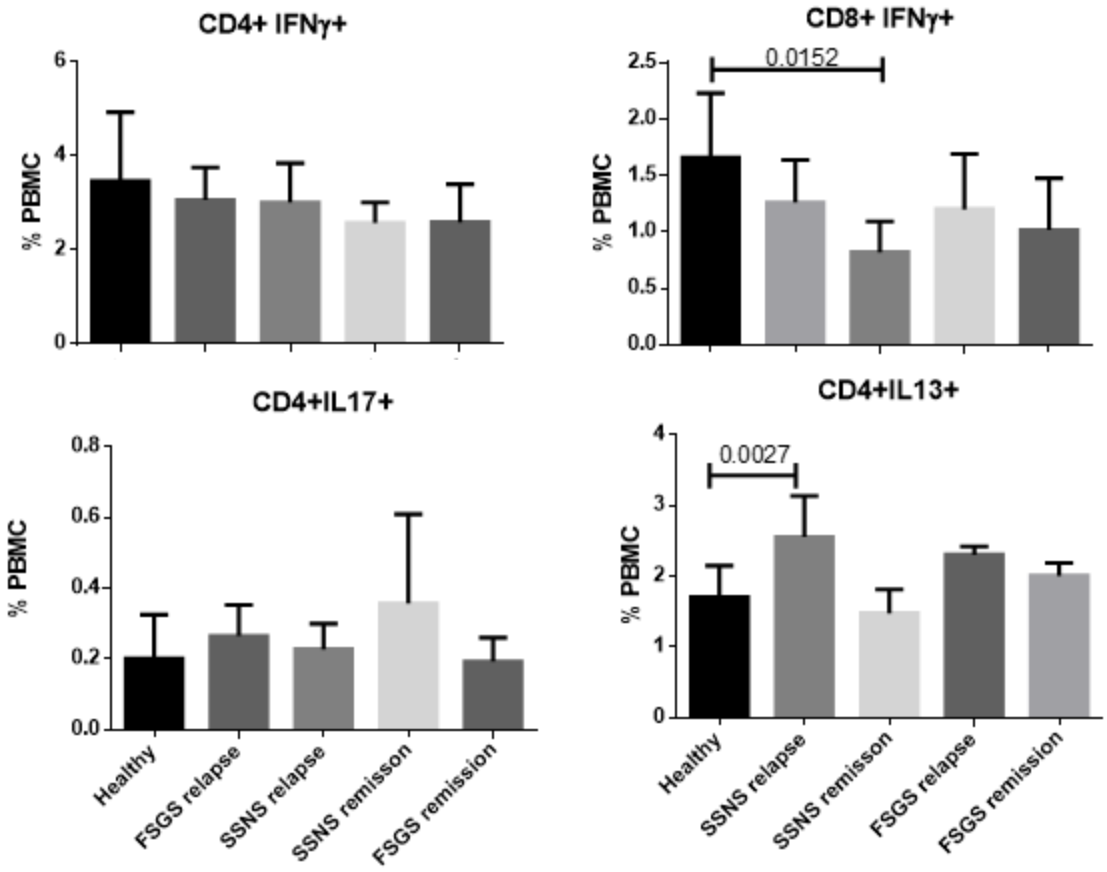

Figure 3.10. Healthy PBMC characterization after stimulation with circulating EVs from patients and healthy controls. Healthy PBMCs (4x10^5 cells pro well) were stimulated with healthy (n=8) and patient EVs (12 SSNS relapse, 6 SSNS remission, 8 FSGS relapse, 4 FSGS remission) (15 µ pro well) for 36 hours in U bottom duplicates. For intracellular staining and as positive control PBMCs were stimulated with PMA (50 ng/ml) at the 30th hour of stimulation. After 36 hours supernatants were collected from PMA unstimulated cells and the remaining PBMCs were fixed and stained with the antibodies against surface and intracellular markers. For statistical analysis Mann-Whitney U test were used. Data is represented as the mean±SD.

We planned to confirm our results with naïve CD4 cell stimulation. Naïve CD4 cells from healthy donors were isolated with magnetic depletion of memory CD4$^+$ T cells and non-CD4$^+$T cells and stimulated with patient EVs (Appendix Figure 4). We observed that a very small percent of EVs were internalized by naïve T cells (Appendix Figure 5) and there is no difference of Th2 percent compared to unstimulated cells (Figure 3.11). Then we concluded that EVs would be internalized with other cell types which may induce naïve T cells to differentiate to Th2 cells. Indeed, in another experimental setting with PKH stained EVs, the large part of EVs were internalized by macrophages (Appendix Figure 6).

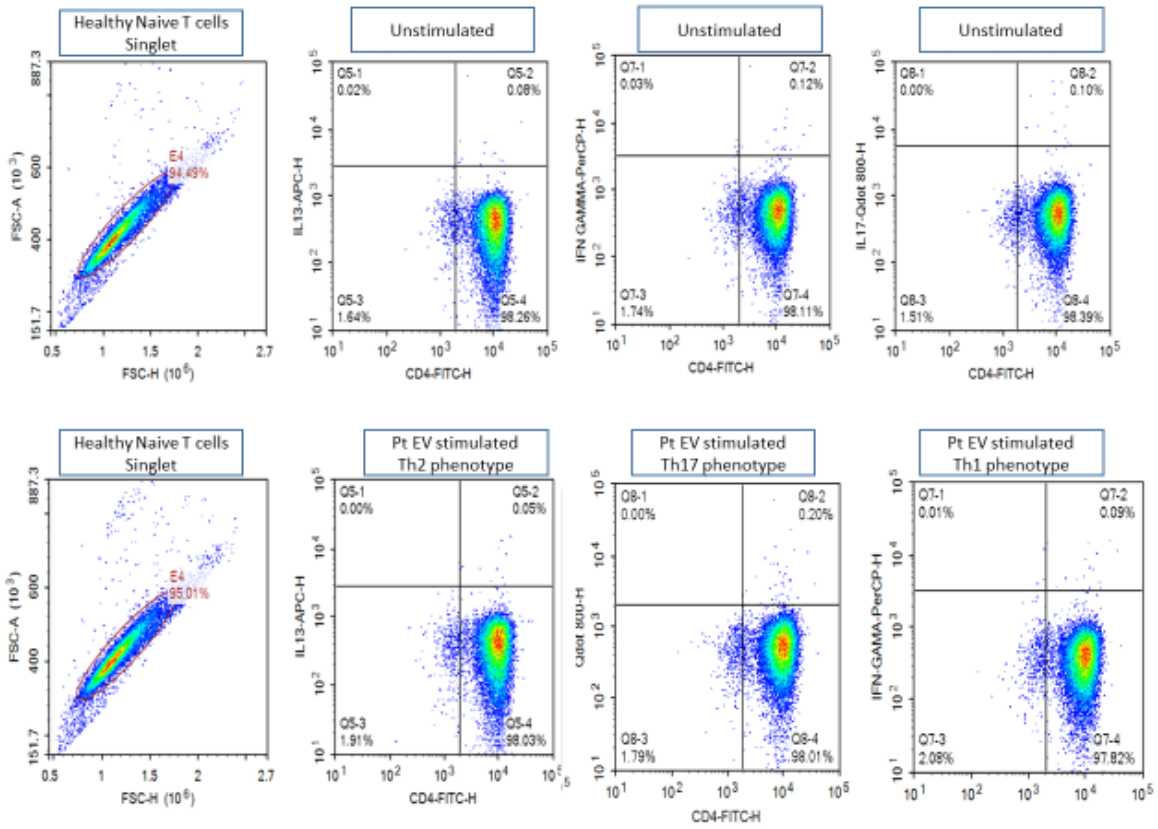

Figure 3.11. Representative histograms of naïve T cells before and after stimulation with circulating EVs from a SSNS relapse patient. Naïve CD4+ T cells were isolated with Human Naïve CD4+ T cell Isolation Kit,II (Miltenyi Biotec, USA) and subsequently were stimulated with SSNS relapse EV (5 µg EVs) for 6 days. Four hours before ending the stimulation and intracellular staining, the cells were stained with PMA (1 µg/ml) and ionomycin (1 µg/ml) then stained with antibodies against CD4, IL13, IFNγ and IL17.

3.4. Effect of Extracellular Vesicles in podocytes

The previous results suggested us that circulating plasma EVs of SSNS relapse patients are biologically active molecules. Since then, we analyzed the characteristics of SSNS EV during relapse and remission more deeply and studied the effect of these EVs on human immortalized podocyte culture.

3.4.1. Kinetics of extracellular vesicle binding and uptake by podocytes

The kinetics of EV binding and internalization by podocytes were assessed with the green lipophilic dye SP-DIOC and red lipophilic dye PKH26, and the samples were analyzed by flow cytometry and immunofluorescence. Live cell imaging of the podocytes cocultured with SP-DIOC-stained EVs showed increased uptake of the EVs over time (Figure 3.12).

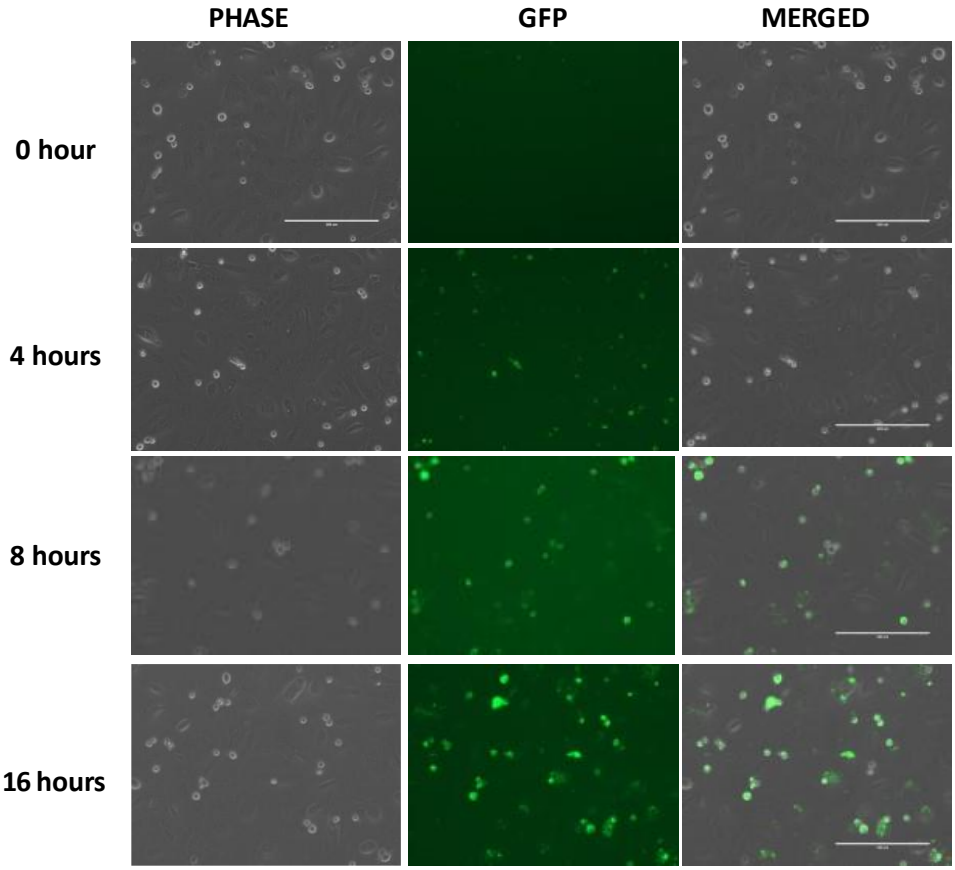

Figure 3.12. Representative photomicrograph images of EV uptake by podocytes. Time course (0, 4, 8 and 16 h EV incubation) representative images of EV uptake stained with green lipophilic dye SPDiOC visualized at GFP channel (Scale bar 1:200).

The kinetics of the binding and internalization of the patient and healthy EVs by podocytes were similar in the flow cytometry analysis (Figure 3.13 and Appendix Figure 7).

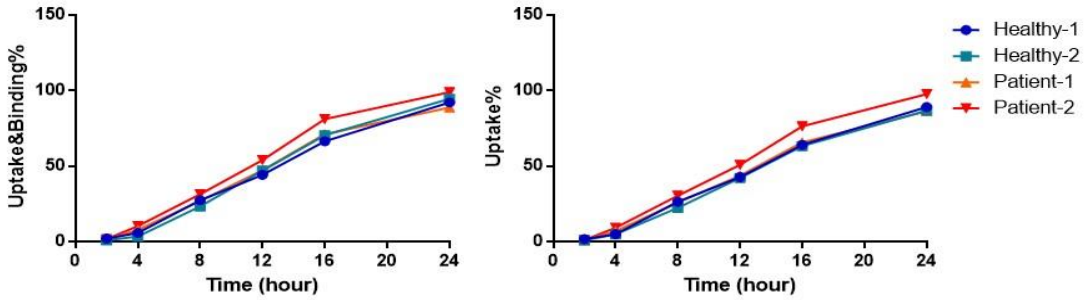

Figure 3.13. SPDiOC labeled EVs from 2 healthy controls and 2 relapse NS patients were incubated with podocytes and time course uptake&binding and uptake (internalization) kinetics were determined by FITC positive podocytes by flow cytometry. Nearly all SPDiOC labeled EVs were taken by podocytes in 24 hour. For uptake (internalization) kinetics, trypan blue (0.1%) was used to quench cell membrane-bound EVs.

At the end of 24 hours, the EVs stained with the red lipophilic dye PKH26 were located in the perinuclear region of the podocytes (Figure 3.14).

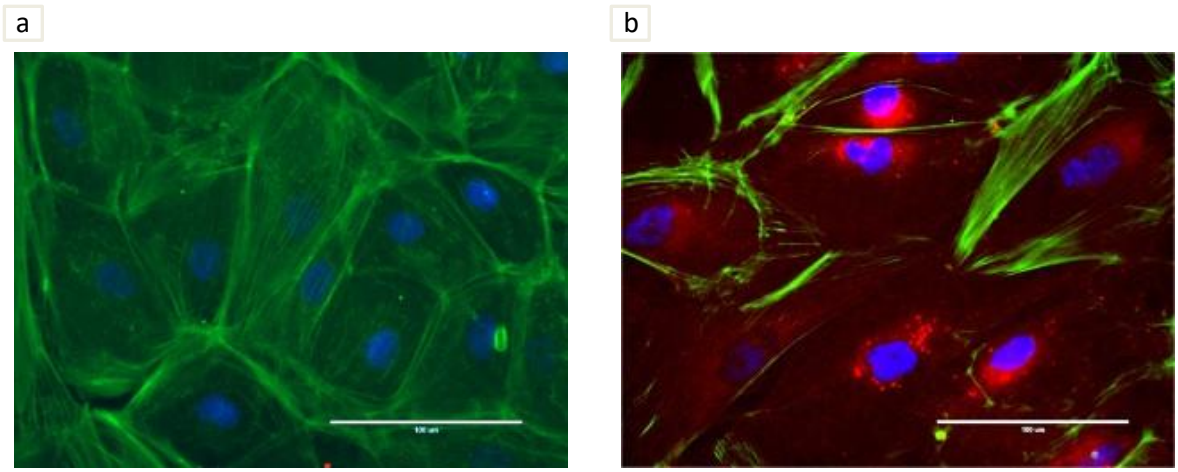

Figure 3.14. Images of podocytes a) not exposed and b) exposed to EVs. EVs stained with lipophilic red dye PKH26 were co-incubated with podocytes for 24 hours, and then podocytes were stained with actin dye phalloidin (green). EVs were mostly located around the nuclear region (DAPI, blue) at the end of 24 hour (Scale bar 1:100).

3.4.2. EVs isolated during relapse increase podocyte motility and albumin permeability *in vitro*

Foot process effacement and increased motility of podocytes are the key events in the development of nephrotic syndrome. *In vitro* podocyte motility was assessed by scratch assay. After scratching the well, the podocytes were stimulated with plasma, plasma fractions from which EVs were depleted (supernatant collected after ultracentrifugation at 100,000 *g*) and EVs from patients and healthy controls (Figure 3.15).

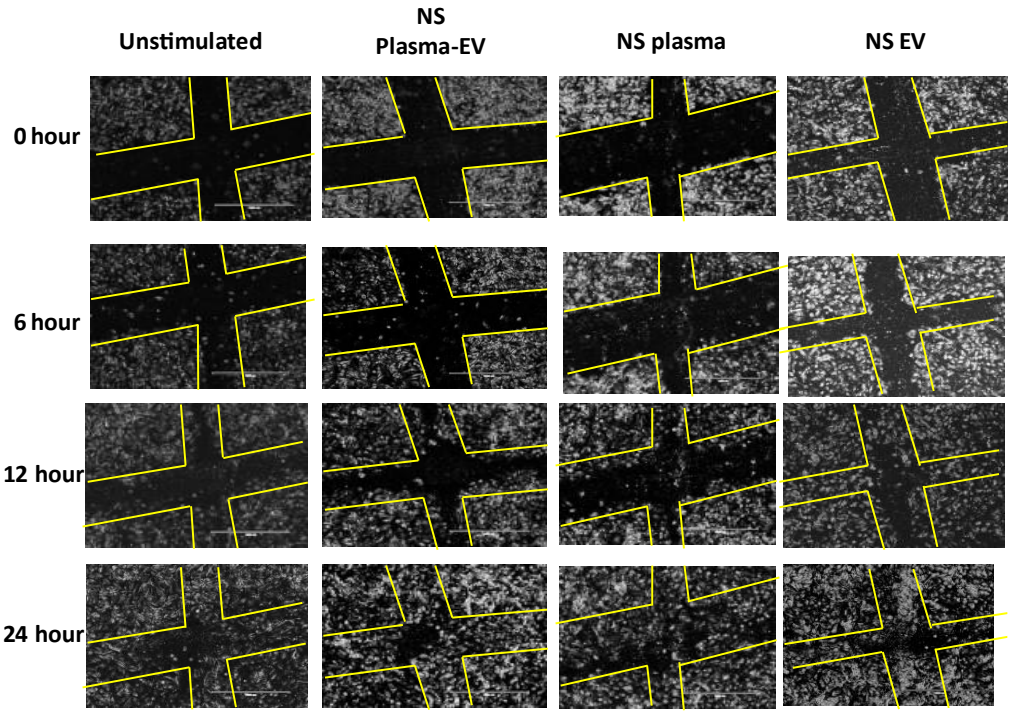

Figure 3.15. Representative set of well images showing the area of clear zone after scratch at 0 , 6, 12 and 24 hours.

Relapse NS EVs significantly increased the motility of the podocytes compared to NS plasma, healthy plasma and healthy EVs (Figure 3.16.a). Additionally, podocytes exposed to relapse NS EVs showed increased motility compared to podocytes exposed to disease control EVs (Figure 3.16.b).

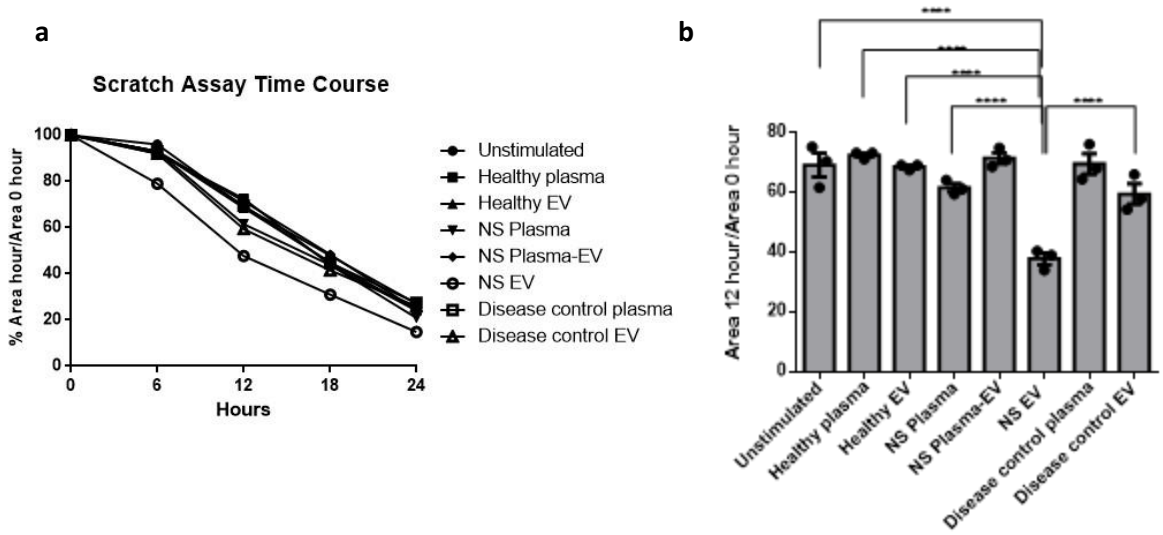

*Figure 3.16. a) Time course of scratch assay treated with %10 FBS (unstimulated), healthy plasma, healthy EV, relapse NS plasma, relapse NS EV and NS plasma depleted with EV, disease control plasma and disease control EVs. b) Comparison of the area of the clear zone after scratch assay. The area of the clear zone at post-scratch 12th hour is expressed as percent area of 0th hour. Each experiment was performed at least in duplicates, and repeated three times independently. Results are presented as mean±SEM. One-way ANOVA with Dunnet's post hoc test was performed vs. FBS treated podocytes. Data are presented as the mean ± SEM. ***P < 0.001.*

The albumin influx assay provides information about the integrity of the slit diaphragm *in vitro* [94]. Podocytes seeded on collagen-coated Transwells were exposed to EVs from NS patients and healthy controls for 4 hours, and then, the albumin influx was measured by BCA assay. At the second hour, the albumin concentrations were not significantly different among wells, but at the 4th hour, the wells treated with relapse NS EVs had higher albumin concentrations in the upper chamber than the wells treated with healthy EVs and remission NS EVs (p<0.001) (Figure 3.17).

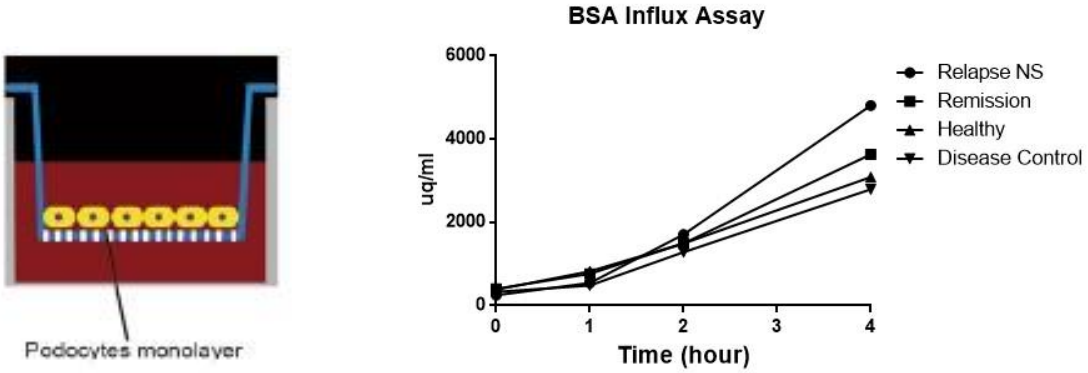

Figure 3.17. Albumin influx assay of podocytes treated with healthy (n=5), remission NS (n=5) and relapse NS plasma EVs (n=5). At the end of fourth hour, podocytes treated with NS relapse EVs had significantly higher albumin permeability compared to remission and healthy EVs and untreated controls (Two-way ANOVA, p<0.0001). Mean and standard errors of three independent experiments were shown.

Moreover, NS relapse EVs caused increased CD80 expression on podocytes compared to healthy EVs (p=0.001) (Figure 3.18) (Appendix Figure 8).

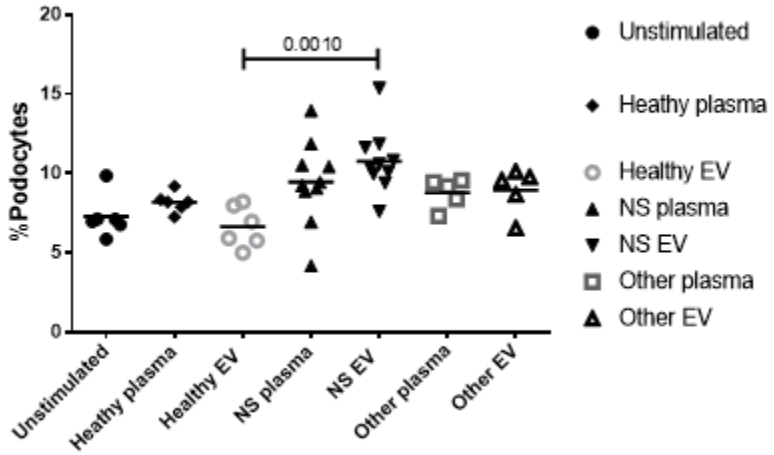

Figure 3.18. Comparison of CD80 positive podocyte percentage after healthy, NS relapse and other glomerular disease EV (20 µg(ml) and plasma (10%) stimulation. For statistical analysis Mann-Whitney U test were used. Data is represented as the mean.

3.5. Proteomic analysis of EVs isolated from NS patients and healthy controls

To determine the protein cargo of the EVs, the plasma EVs isolated from four NS patients in relapse, four NS patients in remission and four healthy controls were subjected to mass spectrometry analysis. A total of 925 proteins from remission EVs, 588 proteins from relapse EVs and 361 proteins from healthy control EVs were identified. Twenty-one of the 588 proteins identified during relapse were among the top 100 proteins identified in EVs in the Vesiclepedia database (Figure 3.19a)[150].

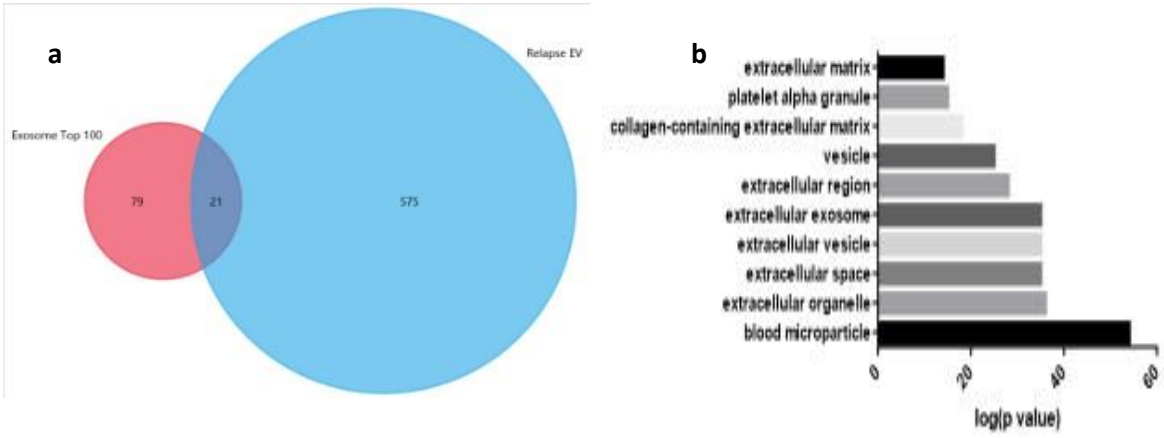

Figure 3.19. Proteomics analysis of plasma EVs from relapse, remission NS patients and healthy controls a) 21 of 588 proteins identified during relapse were among top 100 proteins identified in Vesiclepedia database. B) Gene ontology (GO) analysis of proteins expressed on relapse EVs showing ten most significantly expressed proteins according to cellular compartment.

The proteins that were most significantly expressed in the relapse EVs based on Gene Ontology (GO) analysis according to cellular compartment are shown in Figure 3.19b. One of the most common cellular compartments is the extracellular vesicle and exosome compartment, which confirms the source of these proteins.

Among the identified proteins, 272 proteins were only identified in the relapse NS EVs (Figure 3.20a). Ingenuity Pathway Analysis (IPA) Network Analaysis for the selectively expressed proteins in NS relapse patients was shown in Appendix Figure 10. The most significantly affected canonical pathways in these 272 selectively expressed proteins were RhoGD signaling, regulation of actin-based mobility by RHO, ERK/MAPK signaling, ILK signaling, integrin signaling, signaling by Rho family GTPases, HGF signaling and clathrin-mediated endocytosis signaling (Figure 3.20b). Additionally, annotations of disease analysis revealed that six proteins (ARHGDIA, CA1, CA2, ITGB1, PDE4B, and PDE8A) were significantly related to nephrosis (p=0.00496) (Table 3.1).

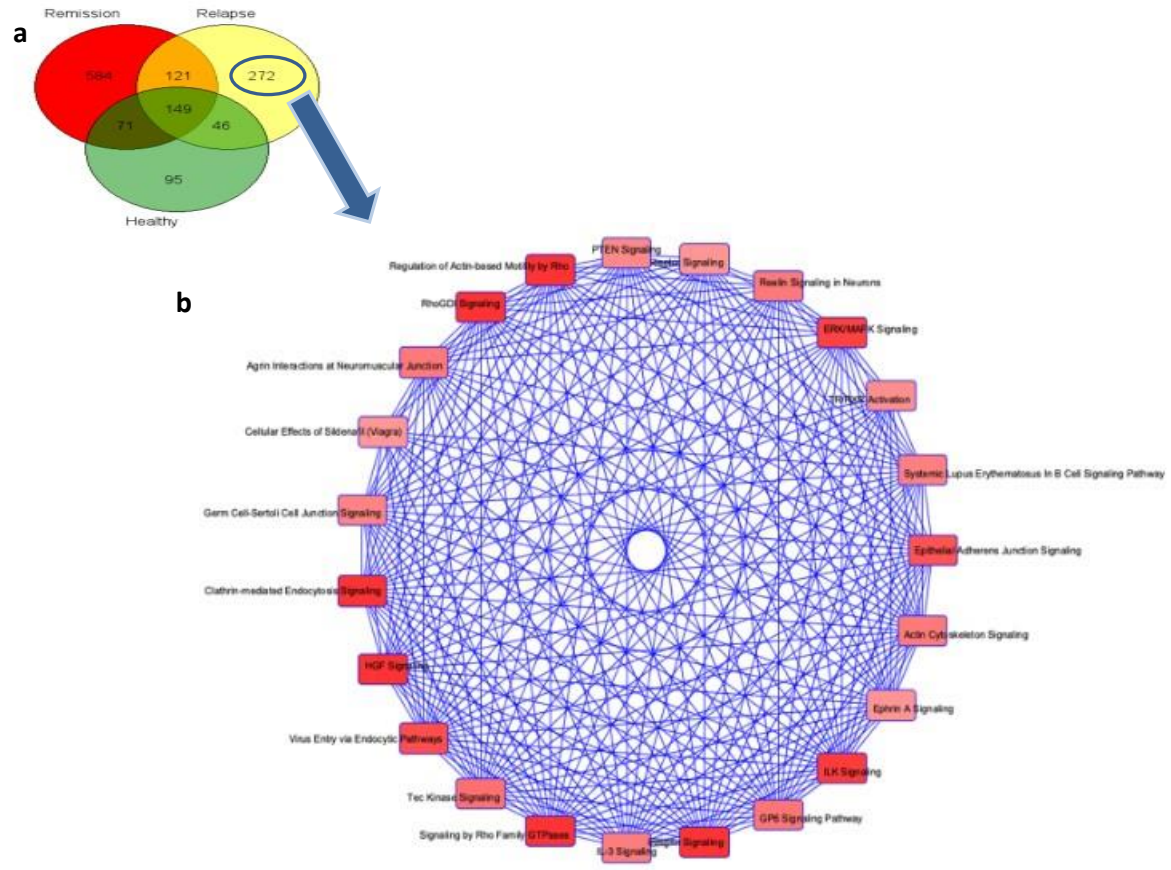

Figure 3.20. Ingenuity Pathway Analysis (IPA) software analysis of selectively expressed SSNS relapse proteins a) Venn diagram showing proteins expressed on EVs among NS patients and healthy controls. A total of 272 proteins were uniquely expressed on relapse EVs. b) The gene-gene interaction network was identified by Ingenuity Pathway Analysis (IPA) software. The input was the list of selectively expressed relapse NS EV protein genes described in Figure . Imported gene identifiers were mapped to corresponding gene objects and overlaid onto global molecular network identified by IPA algorithm. Edge relationship and node type symbols illustrate the nature of the relationship among genes, considering functionality of each gene supplied. Enrichment (FET) p-value threshold: 1e-03.

Table 3.1. Annotations of disease analysis of the selectively expressed NS relapse EV proteins by IPA Taxonomy Function.

Categories	Diseases or Functions Annotation	p-value	Molecules	# Molecules
Nephrosis	Nephrosis	0,00496	ARHGDIA, CA1, CA2, ITGB1, PDE4B, PDE8A	6
Nephrosis	Nephrotic syndrome type 8	0,0111	ARHGDIA	1
Nephrosis	Finnish congenital nephrotic syndrome	0,0436	ARHGDIA	1
Nephrosis	Familial nephrotic syndrome	0,159	ARHGDIA, ITGB1	2

3.6. Analysis of RAC expression on EVs and stimulated podocytes

3.6.1. RAC-GTP content of circulating plasma EVs and EVs derived from supernatants of podocytes

The protein cargo of NS relapse EVs was markedly different from that of NS remission EVs and healthy control EVs with respect to the ILK, MAPK, Rho and RhoGD pathways. The list of proteins from these pathways were shown in Appendix Figure 9. All these pathways converge at the Rac family small GTPase protein C3 botulinum toxin substrate 1 (RAC1). We measured the levels of active RAC1, RAC-GTP in the EVs by G-LISA after protein lysis and sonication and found that the RAC-GTP level normalized to EV particle number of relapse EVs was significantly higher than that of healthy EVs, remission EVs and disease control EVs (Figure 3.21a). Moreover, podocytes exposed to IL13 and LPS secreted EVs with significantly higher levels of RAC-GTP than those secreted by unstimulated podocytes (Figure 3.21b).

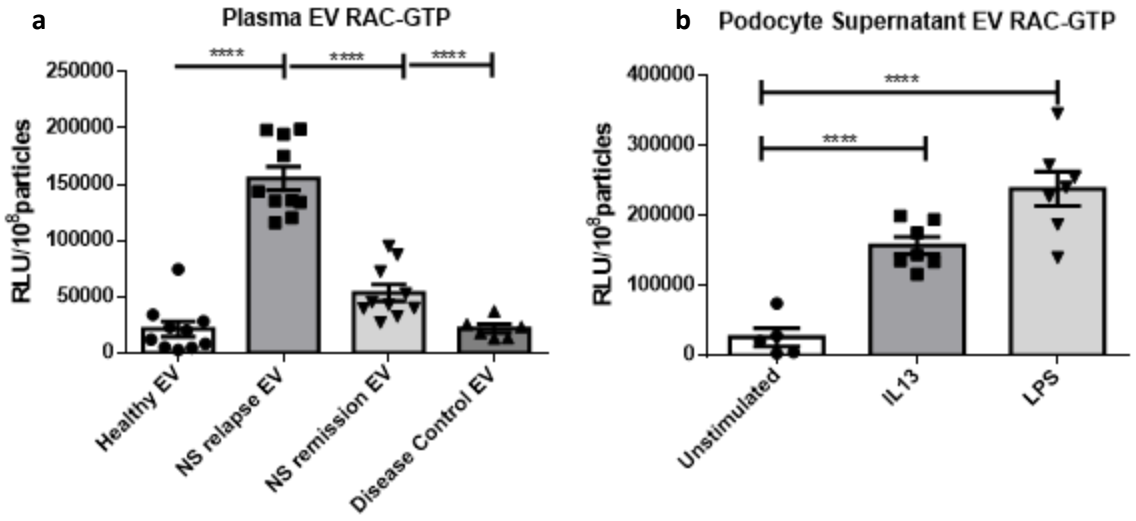

Figure 3.21. RAC-GTP content of circulating plasma EVs and EVs derived from supernatants of podocytes stimulated with IL13 and LPS. a) Plasma relapse NS EVs (n=10) RAC-GTP content normalized to EV particle number were compared those from healthy EVs (10), remission EVs (n=10) and disease control EVs (n=6) measured by G-LISA (Mean±SD were shown, Unpaired Student's t test was performed). b) EVs derived from supernatants of podocytes after 24 hour of IL13 (40 µg/ml) and LPS (25 µg/ml) stimulation caused significantly increased RAC-GTP luminescence normalized to EV particle number compared to unstimulated podocytes (Mean±SD were shown, Unpaired Student's t test was performed).

Based on the previous findings showing increased motility and albumin permeability of podocytes treated with NS relapse EVs, we measured the RAC-GTP levels in podocytes stimulated with EVs. In the podocytes exposed to IL13 (40 ng/ml), the peak RAC-GTP level was reached at T=15 mins (Figure 22a). The results showed that relapse NS EVs significantly increased the RAC-GTP levels in podocytes compared to healthy EVs, remission EVs and disease control EVs (Figure 3.22b).

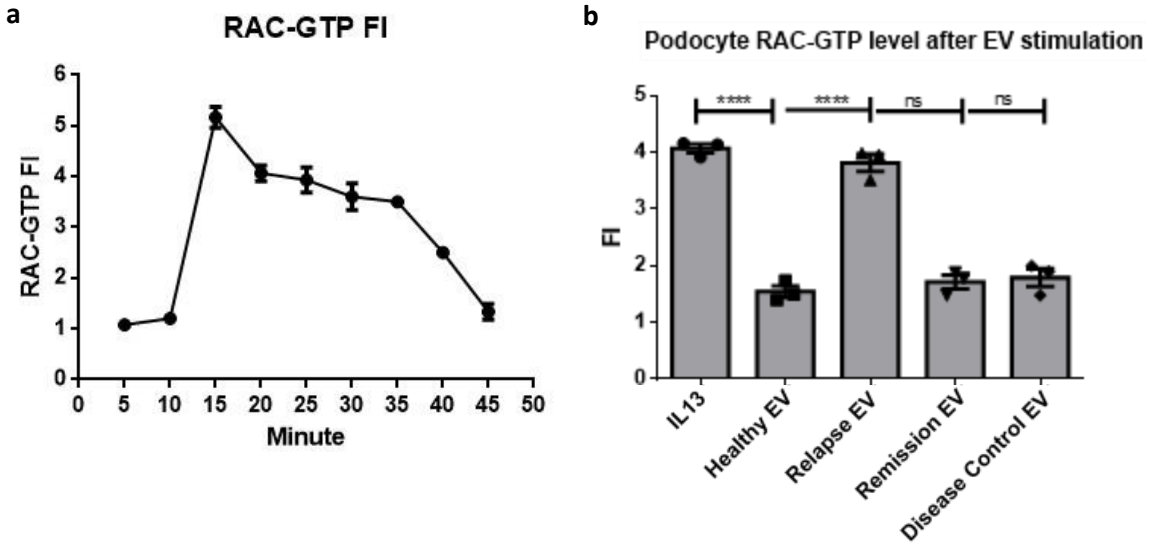

*Figure 3.22. Active RAC-GTP was measured by G-LISA assay in podocytes treated with IL-13 (40 ng/ml) (positive control), healthy EVs, NS relapse EVs and disease control NS remission EVs (20 µg/ml). a) Time course of RAC-GTP activation after IL13 (40 ng/ml) stimulation. RAC-GTP activation peaks at T=15 mins. b) RAC GTP levels were compared between NS relapse EVs, healthy EVs, NS remission EVs ($p<0.001$) and other disease control EVs. Anti-RAC1 antibody luminescence was normalized to untreated podocytes and presented as fold induction. Each experiment was performed at least in triplicates, and repeated three times independently. Results are presented as mean±SEM. Two-way ANOVA with Tukey's post hoc test was performed (***P < 0.001) (ns, nonsignificant).*

3.6.2. Phospho-p38 and synaptopodin expression of podocytes after SSNS plasma and EV stimulation

The mitogen-activated protein kinase (MAPK) phospho p38 (p-p38) has been shown to be downstream of RAC1 activation in podocytes [21]. In the podocytes exposed to IL13 (40 ng/ml), the peak RAC-GTP level was reached at T=15 mins and the peak p-p38 expression level was reached at T=20 mins (Figure 3.23a). Relapse NS EVs significantly induced higher p-p38 expression in podocytes compared to healthy, remission NS and disease control EVs, similar to the RAC-GTP levels (Figure 3.23b).

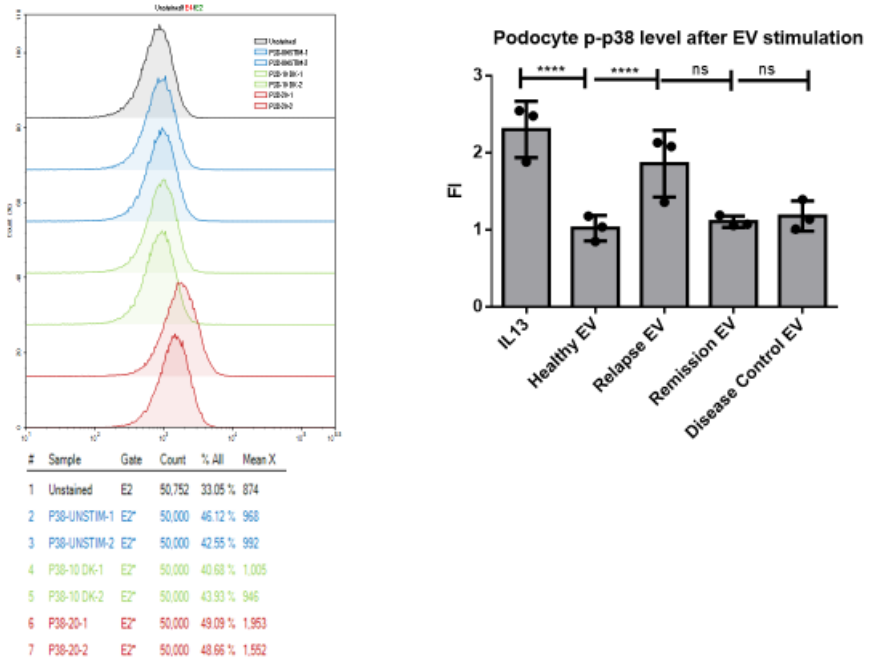

#	Sample	Gate	Count	% All	Mean X
1	Unstained	E2	50,752	33.05 %	874
2	P38-UNSTIM-1	E2*	50,000	46.12 %	968
3	P38-UNSTIM-2	E2*	50,000	42.55 %	992
4	P38-10 DK-1	E2*	50,000	40.68 %	1,005
5	P38-10 DK-2	E2*	50,000	43.93 %	946
6	P38-20-1	E2*	50,000	49.09 %	1,953
7	P38-20-2	E2*	50,000	48.66 %	1,552

*Figure 3.23. p-p38 expression of podocytes with IL13 (40 ng/ml), healthy and patient EVs (20 µg/ml). a) Representative histograms of time course p-p38 activation after IL13 (40 ng/ml) stimulation. Phosho-p38 activation peaks at T=20 mins.b) P-p38 expression levels were compared between NS relapse EVs, healthy EVs, NS remission EVs (p<0.001) and other disease control EVs. Anti-p-p38 antibody MFI was normalized to untreated podocytes and presented as fold induction. Each experiment was performed at least in triplicates, and repeated three times independently. Results are presented as mean±SEM. Two-way ANOVA with Tukey's post hoc test was performed (***P < 0.001) (ns, nonsignificant).*

Compared to relapse NS plasma, relapse NS EVs from the same patients induced significantly higher p-p38 stimulation (Figure 3.24 a-c). Moreover, plasma after 100,000 g ultracentrifugation, which was considered EV-free plasma, induced significantly lower p-p38 expression than relapse NS plasma from the same patients (Figure 3.24 c).

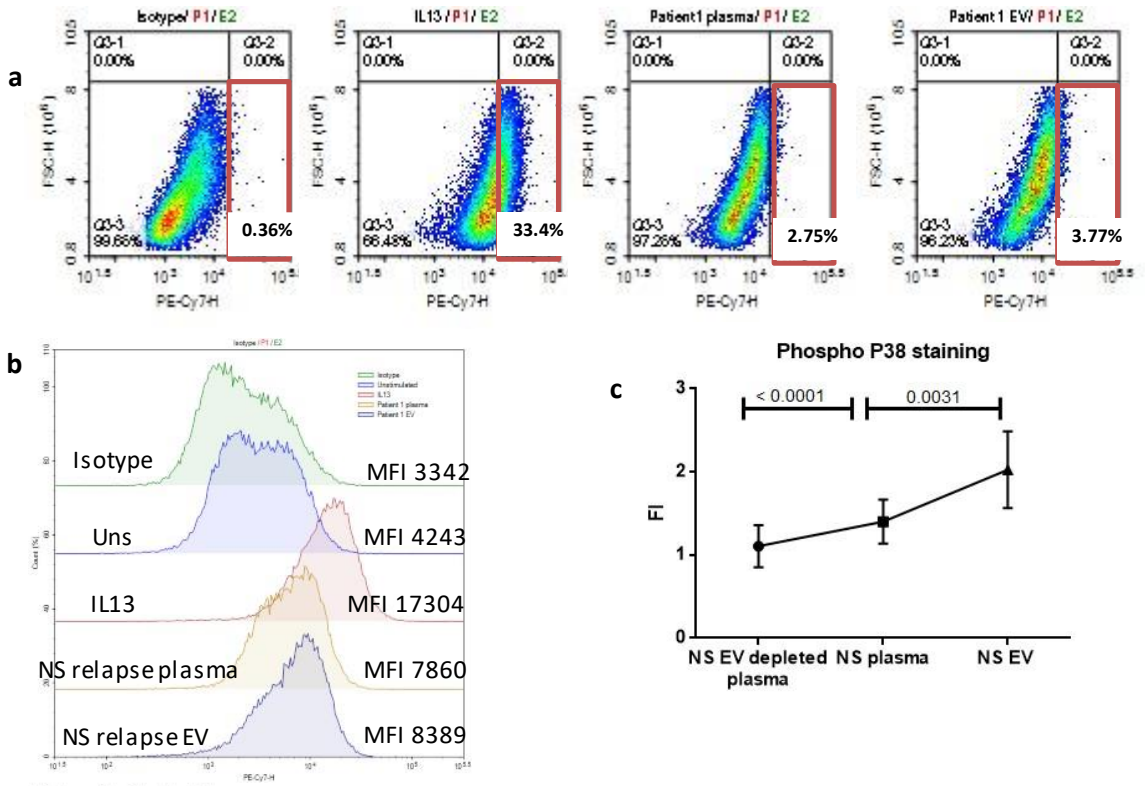

Figure 3.24. Representative images of flow cytometry plots displaying p-p38 expression. Anti-p-p38 labeled with PE-Cy7 and appropriate isotype control was used. Gating strategy after excluding cell aggregates with forward and side scatter parameters were shown. PE-Cy7 positive cells were prominently shifted with IL13 stimulation for 30 minutes. Both relapse NS plasma and relapse EV stimulation caused increase in p-p38 positive cell percentage (a) and mean fluorescent intensity (MFI) (b). c) MFI ratio of p-p38 on podocytes are significantly higher with relapse EV stimulation compared to NS plasma and NS EV-depleted plasma stimulation from the same patients (n=10) (Mean±SD were shown, Paired Student's t test was performed.)

We also assessed the time course of p-p38 and synaptopodin expression after stimulation with relapse NS EVs and plasma from the same patient (Figure 3.25). As seen in Figure 3.25, according to immunoblotting, relapse NS EVs and plasma led to increased p-p38 expression and decreased synaptopodin expression over time.

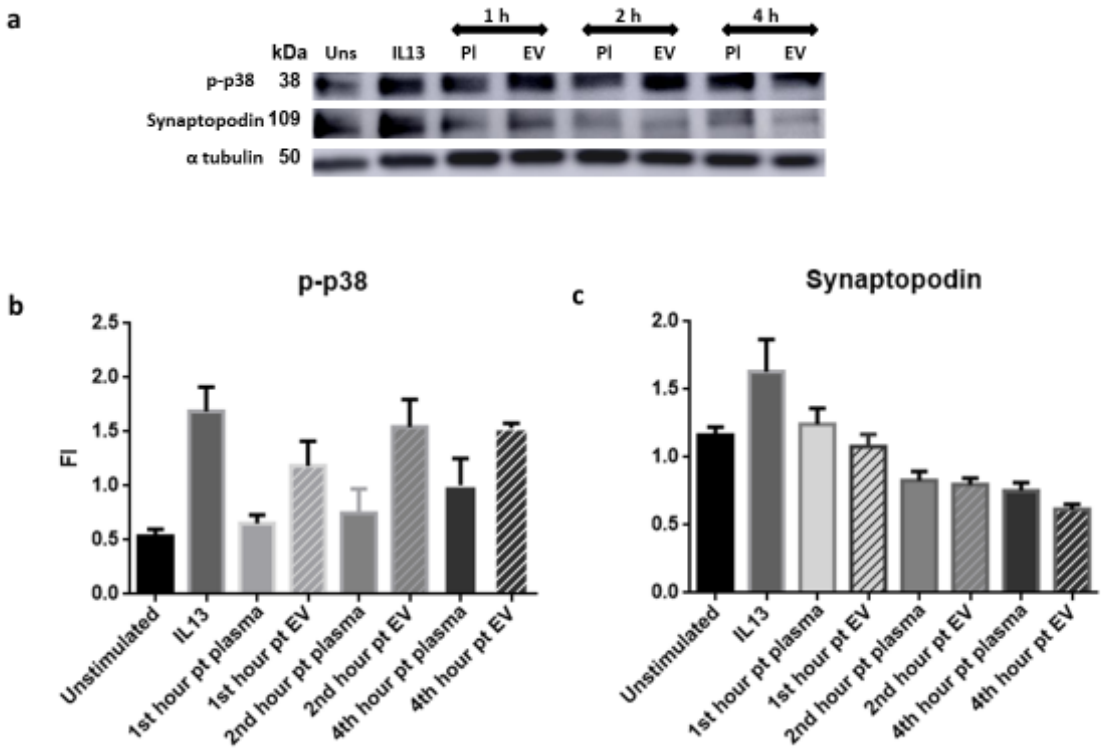

Figure 3.25. Western blot imaging has showed increased p-p38 expression and decreased synaptopodin expression at 1-4 hours of plasma and EV stimulation. a) Representative gel images of p-p-38, synaptopodin and α-tubulin expression in podocytes with IL13 (40 ng/ml), relapse plasma (10%) and EV (20 µg/ml) stimulation. b) Quantification of band intensity of p-p38 compared to α-tubulin by Image J analysis. Mean and standard errors of three independent experiments were shown. c) Quantification of band intensity of synaptopodin as fold induction (FI) to α-tubulin by Image J analysis. Mean and standard errors of three independent experiments were shown.

4. CHAPTER 4

DISCUSSION

Multiple studies proposed that an imbalance in T- and B cells has an important role in the pathogenesis of a nephrotic syndrome. Our findings support the findings of the previous studies that showed increased Th2/Th1 and Th17/Treg proportion [65, 69]. Moreover, we showed increased plasma IL13 levels that support prominent Th2 response during nephrotic syndrome attack. We also showed increased total B cell number and memory B cell number in SSNS relapse. This finding also supports the previous studies that showed increased total and memory B cell percentages [65, 72]. Rituximab which depletes B cells, is commonly used for treatment of SSNS with frequent relapses. Colucci et al. showed that earlier memory B cell reconstitution is associated with earlier relapse after rituximab therapy. In this study we have studied a relatively newly studied subset of B cells, regulatory B cells and showed that regulatory B cells are also increased during SSNS relapse[72]. Classically B cells are the main players of humoral immunity and secrete antibodies. But B cells act also as antigen-presenting cells and effect T cell priming via MHC molecules and costimulatory interactions [154]. The enhancement of T cell priming by B cells was shown to be mediated through a variety of cytokines, including IL-2, IL-4, IL-6, IFNγ, and TNF, which have essential roles in shaping the response from T cells. On the other hand, several groups of B cells have demonstrated to negatively regulate T-cell immune responses, and have been termed regulatory B cells [152]. PD-L1+ B cells are very rare in healthy individuals, but shown to be increased in SLE and melanoma patients in a manner that was positively associated with disease severity [155, 156]. In these studies, it was speculated that PD-L1 positive B cells can represent a class of abnormal activated B-cells, or B-cell subsets, that initiate a pathogenic effect [156]. Increased PD-L1 positive B cells in NS patients may reflect this abnormally activated B cells or reciprocally activated suppressor B cell response against immune activation. Further studies should be done to better delineate the role of these cells in NS patients. PD-L1 positive cells were shown to be increased with glucocorticoids which may explain the increased PD-L1 positive B cells in patient with remission [154].

Idiopathic nephrotic syndrome was postulated to be mediated by circulating factor(s) on the basis of observations that plasma collected from nephrotic subjects induced proteinuria in previously non-nephrotic subjects [122]. To date, many plasma permeability factors have been suggested as causes of NS; however, none has been validated yet [5, 94]. In this thesis, our hypothesis represents a new way of thinking about circulating permeability factors.

EVs are highly abundant in plasma and other body fluids, are highly stable and participate in important biological functions by acting as a mode of communication between cells [157]. Circulating EVs have been reported to be increased in many diseases and are widely accepted as ‘liquid biopsies’ in cancer

[158]. There is an increasing body of evidence that suggests that the cargo of circulating plasma EVs reflects the ongoing pathophysiological processes in organisms [159]. EV omics is increasingly considered a rich source of biomarkers for various disease states. However, there is no single method of plasma EV isolation, which causes confusion in the evaluation of study results [160]. Here, we took the approach of differential ultracentrifugation, which is the most well-studied method of EV isolation and is an appropriate approach for functional studies. Additionally, proteomics studies of plasma have shown that UC supplies fewer soluble proteins and lipoprotein complexes than newly developed isolation methods [161, 162]. Strategies are developed to decipher the purity of EVs. Nevertheless, none of these methods are accepted as a gold standard method and there is no consensus with regard to obtaining pure EVs employing a single method. One approach could be favored to the other in some studies, but always there is a trade of either from purity or from EV yield. The previous studies showed that plasma and/or serum-derived EVs using various isolation methods showed very similar proteome profile and conclude that certain plasma proteins as lipoproteins, immunoglobulins, and coagulation and complement proteins are tightly bound to the EV surface constituting a true protein corona rather than being mere co-isolating contaminants [163].Our focus was to isolate enough EVs with acceptable purity so that we could pursue our functional assays.

Prior to podocyte culture we tried to delineate the effects of EVs on healthy PBMCs. As shown in Figure 3.9 and 3.10, EVs act immune modulatory and transfer the pathologic phenotype characterized in NS PBMCs on to healthy PBMCs. Here we showed that NS EVs caused increased IL13, IFNɣ and IL10 secretion from healthy PBMCs and decreased Th2 cells. To our surprise these EVs do not express prominent immunologic factors in our proteomics study, but expressed proteins associated mainly cell motility. This can be caused due to several factors: Firstly, EVs are very heterogenous in nature. The mean size our EVs was 200 nm and can be characterized as medium sized EVs. Thery C has showed that different sized EVs from immature DCs stimulate naïve T cells differently that small EVs favor Th2 cytokine secretion while large EVs from the same cells favor Th1 cytokine secretion [164]. Secondly, the source of the circulating EVs are very heterogenous in nature that theoretically every cell in the body can secrete EVs into plasma [165].

Here, we showed that plasma EV numbers were also correlated with disease relapse and that their RAC content can be used as a potential biomarker. However, circulating EVs are very heterogeneous in nature and difficult to characterize [121].Vast majority of the human tissue contribute to the plasma EV pool which changes according to the disease. Our study confirmed the previous studies showing that platelet and endothelial EVs constitute the major part of the plasma EV pool and their percentages are significantly higher in relapse NS patients compared to healthy controls. This finding was also showed in patients with increased intravascular coagulation [166]. Moreover, the higher expression of podocalyxin which is found on podocytes and as well as endothelial cells may also reflect endothelial dysfunction and increased thrombosis risk in relapse NS patients. Here we used CD14 to reflect the EVs shed from monocytes. CD14 is a receptor of LPS and found on activated monocytes and to a lesser

extent on granulocytes. In a cohort of adult NS patients CD14 was found to be excreted in urine at higher levels from biopsy-proven MCD patients compared to FSGS and membranous glomerulopathy [167]. Increased CD19 positive EVs may also reflect the increased B cell pool in circulation of relapse NS patients [71]. The increased expression of podocalyxin in our patient cohort may also reflect podocyte injury that our proteomics study revealed specifically expressed proteins that suggest nephrosis.

Another argument is that under physiological conditions, the EVs would not be expected to pass the highly efficient and selective glomerular filtration barrier. Only molecular complexes below 6.4 nm in diameter and under 70 kDa could transit into the lumen of the nephron. Intriguingly fluorescently labeled EVs injected parentally into normal rats were shown in kidney sections and in urine [168]. Moreover, trans-renal EV passage may be facilitated under pathological conditions such as nephrotic syndrome characterized by injured glomerular filtration barrier [169]. Trans-renal EV release could depend on a process similar to transcytosis, i.e., vesicular uptake followed by transcellular release, a well-known process for the selective trans-endothelial transport of plasma albumin and low-density lipoproteins as well as the EV uptake and secretion from blood-brain barrier [170].

Cell motility, which is coordinated by actin and microtubules, is involved in the pathological events of NS, and enhanced migration was shown to be correlated with induced proteinuria [171]. Increased podocyte motility is one of the features of cultured podocytes induced by proteinuric factors [5, 171]. Cell motility and migration are complex processes, and recent studies in tumor models have shown that tumor EVs promote aggressive behavior and metastasis by modifying the complex interactions of the tumor microenvironment and promoting the motility and invasiveness of tumor cells (reviewed in [172, 173]). In particular, EVs were shown to deliver ECM components, such as fibronectin, to promote adhesion formation, and exosome secretion was found to be crucial for directional and efficient cell migration [174]. Moreover, EVs were shown to participate in the biogenesis and activity of invasive structures called invadopodia, which are cellular protrusions similar to lamellipodia, through the MVB-dependent delivery of metalloproteinases and other cargo molecules, including RAC1 [175].

In our study, the most significantly enriched pathways in the circulating EVs of relapsed NS patients were the ILK, MAPK, Rho and RhoGD pathways, which converge at the RAC1 protein. RAC1 is a member of the Rac family of guanosine triphosphate phosphohydrolases (GTPases), which is a subfamily of Rho small GTPases that regulates the actin cytoskeleton. RAC1 and Cdc42 activation was shown to increase lamellipodia formation and promote cell motility in podocytes [20]. The activation of RAC1 signaling in podocytes was shown to be a widespread cause of foot process effacement and proteinuria [176]. In a transgenic mouse model expressing a doxycycline-inducible active form of RAC1, transient activation of RAC1 caused transient proteinuria resembling SSNS, leading to p38-MAPK activation and β1-integrin redistribution [21]. Moreover, Robins *et al* showed that RAC1 was overexpressed in kidney biopsies from patients with MCD and idiopathic FSGS and that the sera of the same patients activated RAC1 downstream of p-p38 in cultured podocytes. These authors suggested RAC-p38 MAPK activation as a useful bioassay to assess the activity of potential permeability factors

[21]. In this report, we showed that relapse NS EVs had higher RAC-GTP than remission EVs and other proteinuric disease EVs and induced higher expression of RAC1 and its downstream molecule phospho p38 in cultured podocytes than EVs obtained from healthy controls, EVs from the same patients during the remission period and EVs from other proteinuric glomerular disease patients. Additionally, relapse NS EVs induced higher RAC1 and p-p38 expression in podocytes than plasma and EV-depleted plasma. Based on the higher RAC-GTP levels in the EVs of relapsed NS patients, EVs may be a mediator of podocyte dysfunction. Rho-GTP pathway and RAC1 also have role in biogenesis of EV formation and RAC1 was reported to be one of the most common top 100 proteins found in EVs [150, 177]. Increased RAC1 may also reflect increased number of EVs in plasma as we have shown in Figure 1B. However, LPS and IL13 stimulation of podocytes has also caused increased RAC-GTP content normalized to particle number supporting that the increased motility of podocytes and the increased RAC levels after stimulation with relapse EVs may be attributed to the active RAC1 contents in the EVs (Figure 6B). Recent studies have shown the effective transport of proteins by EVs including another GTP-bound enzyme, RAS, between tumor cells, which may induce the malignant transformation of recipient cells [178]. Gopal *et al.* showed that ovarian cancer cells undergoing epithelial to mesenchymal transition (EMT) specifically produce exosomes containing RAC1 and PAK2 and that these exosomes activate the RAC1 pathway in endothelial cells, promoting angiogenesis [179].

The major limitation of our study is that modeling NS *in vitro* is in its infancy and we have limited parameters to quantify changes in podocyte culture. However human immortalized podocyte culture which differentiates at 37 ^{o}C, expresses a slit diaphragm-like structure and the vast majority of the podocyte specific proteins [180]. Assessment of these proteins such as synaptopodin gives us important clues to podocyte injury which is the main pathological event in idiopathic nephrotic syndrome. However, an *in vitro* model representing the entire glomerular filtration barrier and the interactions between podocytes, the fenestrated endothelium and the GBM would better reflect the role EVs in crosstalk between cells and *in vivo* situation [104, 180]. But to the best of our knowledge, this study is the first to characterize the protein cargo of circulating EVs in nephrotic syndrome patients. Another limitation of our study is that EVs carry not only proteins but also many different types of cargo, such as mRNAs and miRNAs, and there is great potential for the discovery of potential pathological factors that play roles in the progression of kidney disease. This is a preliminary study with a small sample size but we conclude that circulating relapse EVs are biologically active molecules that carry elevated levels of RAC1 as cargo and induce recapitulation of the nephrotic syndrome phenotype in podocytes *in vitro*. Further studies are needed to completely characterize the cargo of EVs and their effects on the pathogenesis of NS.

CHAPTER 6.

APPENDICES

Appendix A

Additional Figures

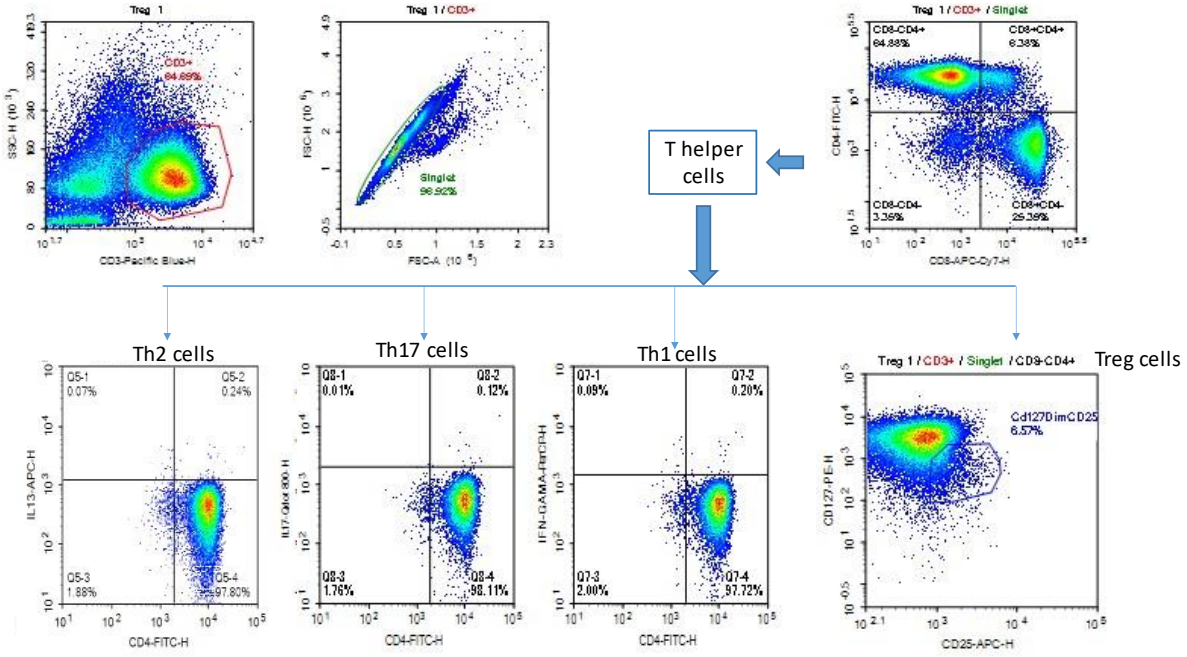

Appendix Figure 1. Gating strategy of T helper, cytotoxic T cells and T regs.

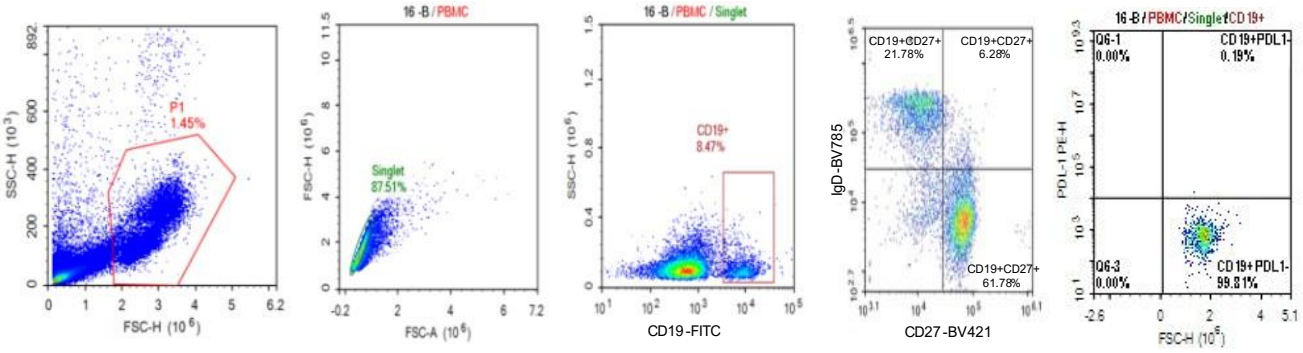

Appendix Figure 2. Gating strategy of B cells. Whole blood was stained with surface marker antibodies against CD19, CD27, IgD and PD-L1 to characterize total B cells ($CD19^+$) (a), memory B cells ($CD19^+CD27^+$) (b), switched memory B cells ($CD19^+CD27^+IgD^-$) (d) and regulatory B cells ($CD19^+PD\text{-}L1^+$) (c).

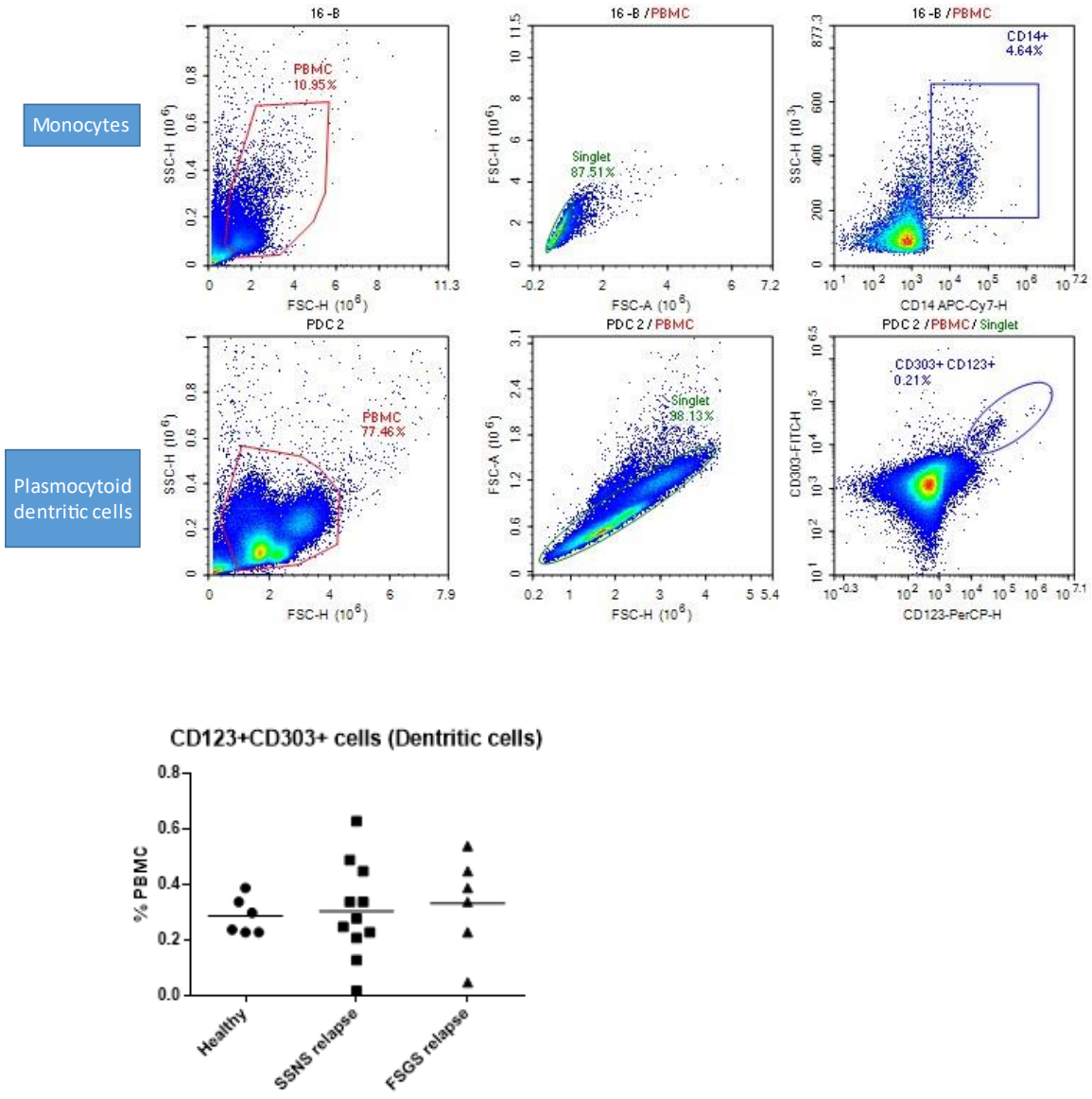

Appendix Figure 3. Gating strategy of monocytes and plasmocytoid dentritic cells. a) Whole blood was stained with surface marker antibodies CD14 for monocytes; CD303 and CD123 for plasmocytoid dentritic cells. b) Comparison of dentritic cell percentages from patients and controls.

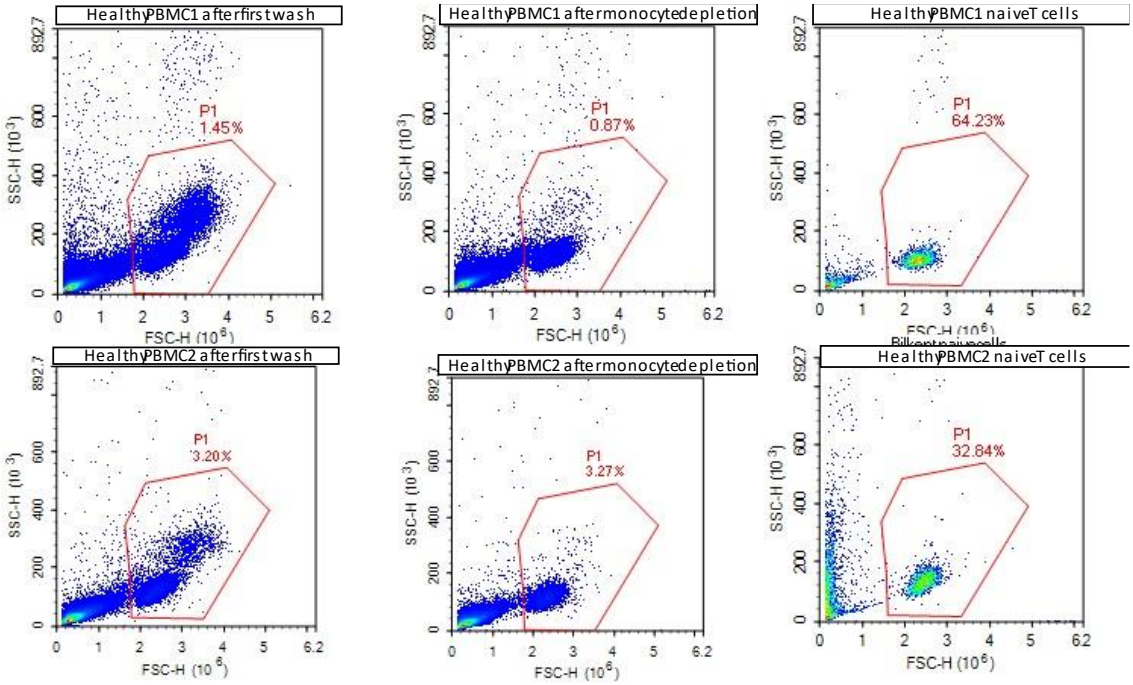

Appendix Figure 4. Strategy of Naive T cell isolation with Human Naïve CD4+ T cell Isolation Kit II (Miltenyi Biotec, USA) with magnetic depletion of memory CD4⁺ T cells and non-CD4⁺ T cells.

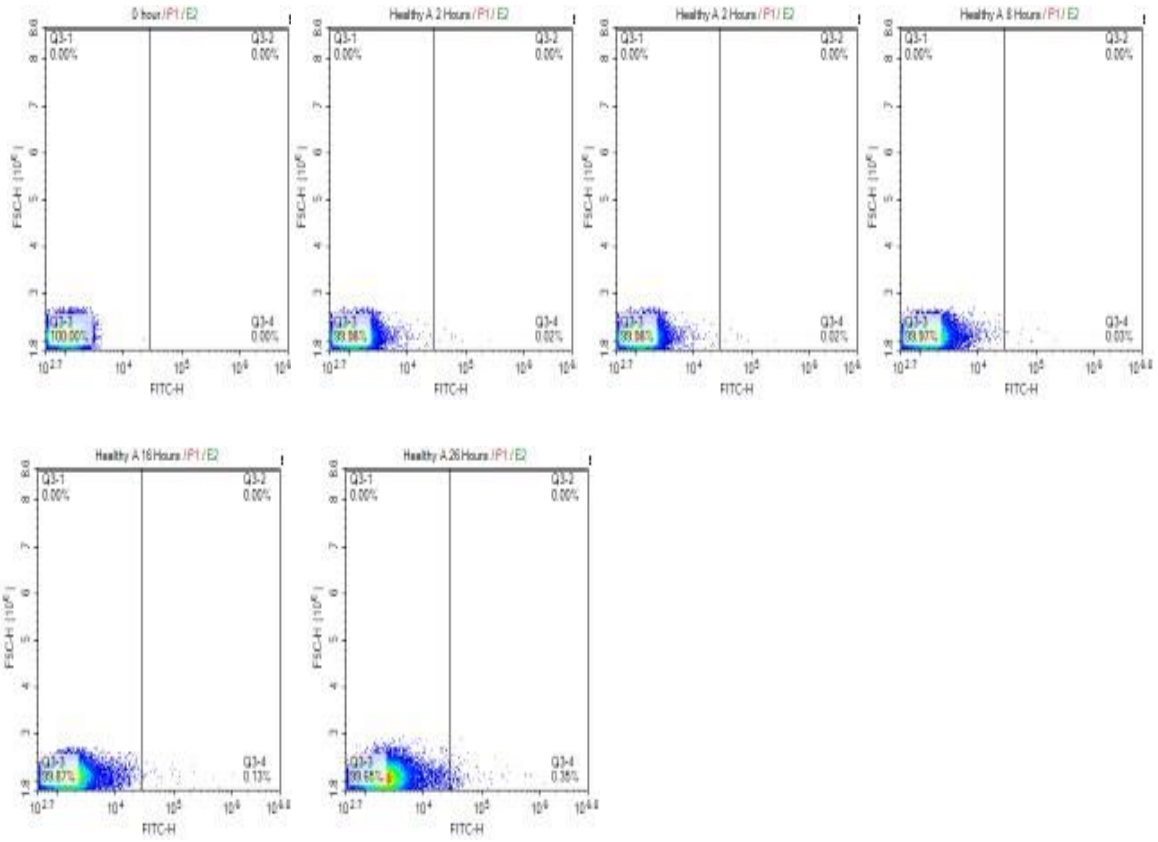

Appendix Figure 5. Time lapse representative histograms of naive T cells with SPDiOC stained EVs from a SSNS patient.

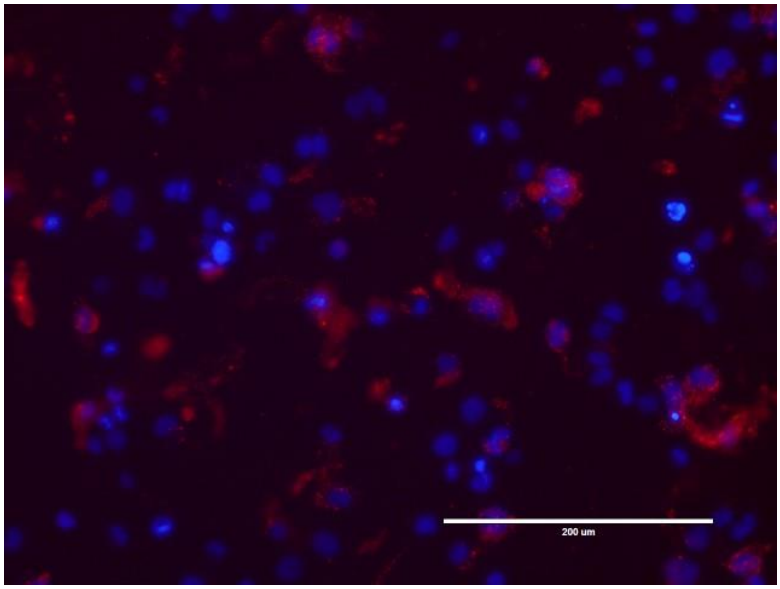

Appendix Figure 6. Representative photomicrograph images of EV uptake by THP macrophages after 8 hour.

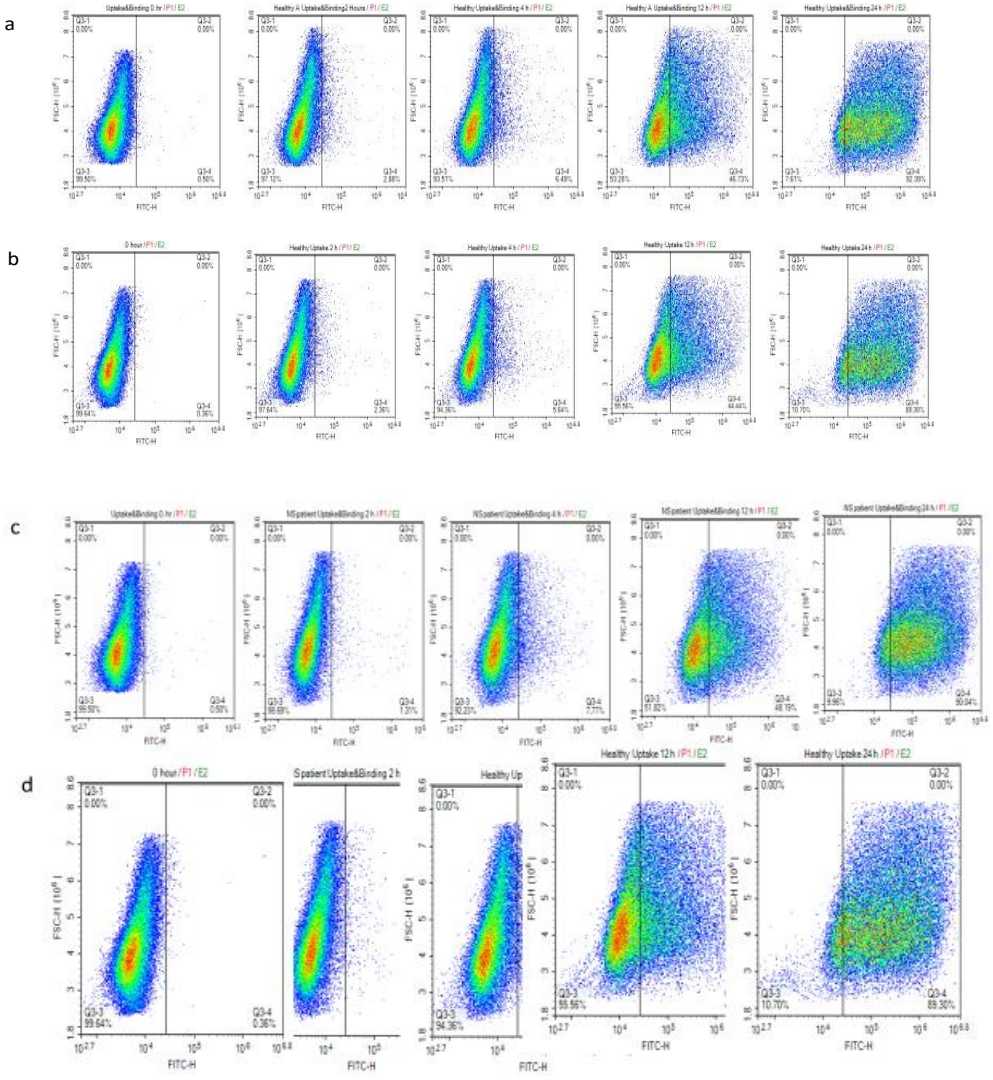

Appendix Figure 7. Representative histograms of podocytes with SPDIOC stained healthy (A,B) and relapse NS EVs (C,D) . In

first readings, FITC positive cells were acquired and reported as the level of EB binding and uptake by cells (a,c). To determine the internalized fraction, the remaining cells were mixed with 30 µl Trypan Blue and FITC gate was reanalyzed and this fraction was accepted as internalized EVs by cells (b,d).

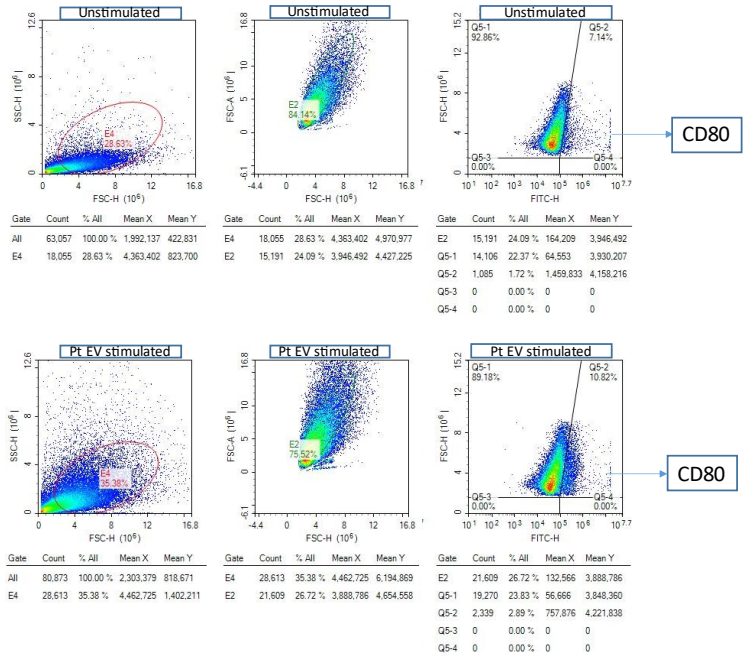

Appendix Figure 8. CD80 expression of podocytes before and after stimulation with EVs.

Symbol	Entrez Gene Name	Location	Type(s)
RHOGD Subset			
ACTC1	actin alpha cardiac muscle 1	Cytoplasm	enzyme
ACTR2	actin related protein 2	Plasma Membrane	other
ARHGDIA	Rho GDP dissociation inhibitor alpha	Cytoplasm	other
ARHGEF1	Rho guanine nucleotide exchange factor 1	Cytoplasm	other
CDH19	cadherin19	Plasma Membrane	other
ITGB1	integrinsubunitbeta 1	Plasma Membrane	receptor
RAC1	Racfamily small GTPase 1	Plasma Membrane	enzyme
RHO Subset			
ACTC1	actin alpha cardiac muscle 1	Cytoplasm	enzyme
ACTR2	actin related protein 2	Plasma Membrane	other
ARHGDIA	Rho GDP dissociation inhibitor alpha	Cytoplasm	other
ITGB1	integrin subunit beta 1	Plasma Membrane	receptor
RAC1	Racfamily small GTPase 1	Plasma Membrane	enzyme
MAPK Subset			
ELF5	E74 like ETS transcriptionfactor 5	Other	transcription regulator
ITGB1	integrin subunit beta 1	Plasma Membrane	transmembrane receptor
PIK3C2B	phosphatidylinositol-4-phosphate3-kinase catalytic subunittype 2 beta	Cytoplasm	kinase
RAC1	Rac family small GTPase 1	PlasmaMembrane	enzyme
RAPGEF1	Rap guanine nucleotide exchange factor 1	Cytoplasm	other
STAT3	signal transducer and activator of transcription 3	Nucleus	transcription regulator
YWHAB	tyrosine 3-monooxygenase/tryptophan 5-monooxygenase activation protein beta	Cytoplasm	other
ILK Subset			
ACTC1	actin alpha cardiac muscle 1	Cytoplasm	enzyme
ITGB1	integrin subunit beta 1	Plasma Membrane	transmembrane receptor
PARVB	parvin beta	Cytoplasm	other
PIK3C2B	phosphatidylinositol-4-phosphate 3-kinase catalytic subunit type 2 beta	Cytoplasm	kinase
RAC1	Rac family small GTPase 1	Plasma Membrane	enzyme
RSU1	Ras suppressor protein 1	Cytoplasm	other
TESK1	testis associated actin remodelling kinase 1	Nucleus	kinase

Appendix Figure 9. The list of proteins that was markedly different in NS relapse patients from that of NS remission EVs and healthy control EVs.

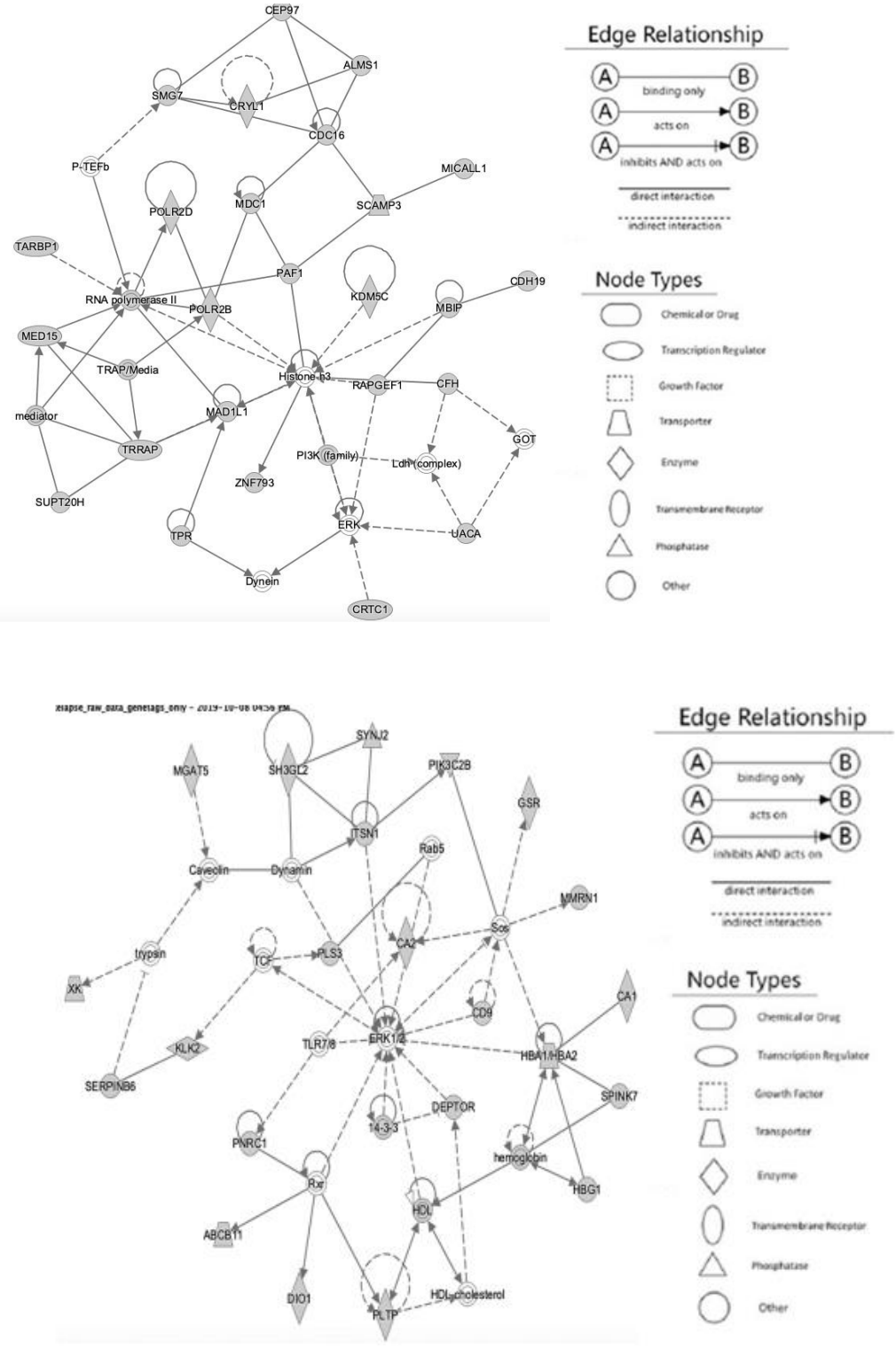

Appendix Figure 10. Ingenuity Pathway Analysis (IPA) Network Analsysis for the selectively expressed proteins in NS relapse patients. The protein list was analyzed to generate a network where all protein-protein interactions involved can be visually explored. The edge relationships and the node types were shown on the right side of the Figure.

Appendix B

Buffers for ELISA and Flow Cytometry

1. 10X Phosphate Buffered Saline (PBS):

• 80 g NaCl

• 2 g KCl

• 8.01 g Na2HPO4.2H2O

• 2 g KH2PO4

• 1 L dH2O

pH is set to 6.8 and the buffer is autoclaved before use.

2. 1X PBS:

• 100 ml 10X PBS

• 900 ml dH2O

pH is set to 7.4.

3. ELISA Blocking Buffer:

• 500 ml 1X PBS

• 25 g bovine serum albumin (BSA)

• 250 µl Tween-20

4. ELISA Washing Buffer:

• 500 ml 10X PBS

• 2.5 ml Tween-20

• 4.5 L dH2O

5. FACS Buffer for Flow Cytometry:

• 500 ml 1X PBS

• 5 g BSA

• 125 mg Na-Azide

6. **10X Running Buffer (SDS Page-Western Blot)**

- 144 g Glycine
- 30 g Tris-Base
- 10 g SDS

Completed to 1 liter with distilled water.

7. **10X Transfer Buffer (SDS Page-Western Blot)**

- 144 g Glycine
- 30 g Tris-Base

Complete to 1 liter with distilled water, store at +4 ^{0}C.

1X Transfer Buffer was prepared prior to each use: 700 ml distilled water, 200 ml Methanol, 100 ml 10X Transfer Buffer. Stored at -20 ^{0}C.

8. **Blocking Buffer (SDS Page-Western Blot)**

- 2.5 g Milk powder
- 50 µl Tween 20

Completed up to 50 ml with 1X PBS.

9. **PBS-T Buffer (SDS Page-Western Blot)**

- 999 ml 1X PBS
- 1 ml Tween20

10.**Antibody Dilution Buffer (SDS Page-Western Blot)**

- 2.5 g Milk Powder
- 25 µl Tween20

Completed up to 50 ml with 1X PBS.

5. CHAPTER 5

REFERENCES

1. Kopp, J.B., et al., *Podocytopathies.* Nat Rev Dis Primers, 2020. **6**(1): p. 68.
2. Agrawal, S., et al., *Dyslipidaemia in nephrotic syndrome: mechanisms and treatment.* Nat Rev Nephrol, 2018. **14**(1): p. 57-70.
3. Saleem, M.A., *Molecular stratification of idiopathic nephrotic syndrome.* Nat Rev Nephrol, 2019. **15**(12): p. 750-765.
4. *The primary nephrotic syndrome in children. Identification of patients with minimal change nephrotic syndrome from initial response to prednisone. A report of the International Study of Kidney Disease in Children.* J Pediatr, 1981. **98**(4): p. 561-4.
5. Vivarelli, M., et al., *Minimal Change Disease.* Clin J Am Soc Nephrol, 2017. **12**(2): p. 332-345.
6. Maas, R.J., et al., *The Clinical Course of Minimal Change Nephrotic Syndrome With Onset in Adulthood or Late Adolescence: A Case Series.* Am J Kidney Dis, 2017. **69**(5): p. 637-646.
7. Dossier, C., et al., *Epidemiology of idiopathic nephrotic syndrome in children: endemic or epidemic?* Pediatr Nephrol, 2016. **31**(12): p. 2299-2308.
8. Kikunaga, K., et al., *High incidence of idiopathic nephrotic syndrome in East Asian children: a nationwide survey in Japan (JP-SHINE study).* Clin Exp Nephrol, 2017. **21**(4): p. 651-657.
9. McKinney, P.A., et al., *Time trends and ethnic patterns of childhood nephrotic syndrome in Yorkshire, UK.* Pediatr Nephrol, 2001. **16**(12): p. 1040-4.
10. Rasheed Gbadegesin, W.E.S., *Nephrotic Syndrome*, in *Comphrehensive Pediatric Nephrology*, F.S. Denis F. Geary, Editor. 2008, Mosby Elsevier: Philadelphia.
11. Esezobor, C.I., A.U. Solarin, and R. Gbadegesin, *Changing epidemiology of nephrotic syndrome in Nigerian children: A cross-sectional study.* PLoS One, 2020. **15**(9): p. e0239300.
12. Riar, S.S., et al., *Prevalence of Asthma and Allergies and Risk of Relapse in Childhood Nephrotic Syndrome: Insight into Nephrotic Syndrome Cohort.* J Pediatr, 2019. **208**: p. 251-257 e1.
13. Eddy, A.A. and J.M. Symons, *Nephrotic syndrome in childhood.* Lancet, 2003. **362**(9384): p. 629-39.
14. Yoshimura, Y. and R. Nishinakamura, *Podocyte development, disease, and stem cell research.* Kidney Int, 2019. **96**(5): p. 1077-1082.
15. Carlton Bates, J.H., and Sunder Sims-Lucas, *Embryonic Development of the Kidney*, in *Pediatric Nephrology*, E.D. Avner, et al., Editors. 2016, Springer: Heidelberg.
16. Garg, P., *A Review of Podocyte Biology.* Am J Nephrol, 2018. **47 Suppl 1**: p. 3-13.
17. Blaine, J. and J. Dylewski, *Regulation of the Actin Cytoskeleton in Podocytes.* Cells, 2020. **9**(7).
18. Perico, L., et al., *Podocyte-actin dynamics in health and disease.* Nat Rev Nephrol, 2016. **12**(11): p. 692-710.

19. Schell, C. and T.B. Huber, *The Evolving Complexity of the Podocyte Cytoskeleton.* J Am Soc Nephrol, 2017. **28**(11): p. 3166-3174.
20. Matsuda, J., et al., *Rho GTPase regulatory proteins in podocytes.* Kidney Int, 2020.
21. Robins, R., et al., *Rac1 activation in podocytes induces the spectrum of nephrotic syndrome.* Kidney Int, 2017. **92**(2): p. 349-364.
22. Hackl, M.J., et al., *Tracking the fate of glomerular epithelial cells in vivo using serial multiphoton imaging in new mouse models with fluorescent lineage tags.* Nat Med, 2013. **19**(12): p. 1661-6.
23. Noone, D.G., K. Iijima, and R. Parekh, *Idiopathic nephrotic syndrome in children.* Lancet, 2018. **392**(10141): p. 61-74.
24. Kriz, W., et al., *The podocyte's response to stress: the enigma of foot process effacement.* Am J Physiol Renal Physiol, 2013. **304**(4): p. F333-47.
25. Kriz, W. and K.V. Lemley, *Mechanical challenges to the glomerular filtration barrier: adaptations and pathway to sclerosis.* Pediatr Nephrol, 2017. **32**(3): p. 405-417.
26. Barisoni, L. and P. Mundel, *Podocyte biology and the emerging understanding of podocyte diseases.* Am J Nephrol, 2003. **23**(5): p. 353-60.
27. Machuca, E., E.L. Esquivel, and C. Antignac, *Idiopathic Nephrotic Syndrome: Genetic Aspects*, in *Pediatric Nephrology*, E.D. Avner, et al., Editors. 2016, Springer: Berlin, Heidelberg.
28. Hinkes, B.G., et al., *Nephrotic syndrome in the first year of life: two thirds of cases are caused by mutations in 4 genes (NPHS1, NPHS2, WT1, and LAMB2).* Pediatrics, 2007. **119**(4): p. e907-19.
29. Trautmann, A., et al., *Spectrum of steroid-resistant and congenital nephrotic syndrome in children: the PodoNet registry cohort.* Clin J Am Soc Nephrol, 2015. **10**(4): p. 592-600.
30. Lane, B.M., et al., *Genetics of Childhood Steroid Sensitive Nephrotic Syndrome: An Update.* Front Pediatr, 2019. **7**: p. 8.
31. Boyer, O., G. Dorval, and A. Servais, *The genetics of steroid-resistant nephrotic syndrome in adults.* Nephrol Dial Transplant, 2021. **36**(9): p. 1600-1602.
32. Trautmann, A., et al., *Spectrum of steroid-resistant and congenital nephrotic syndrome in children: the PodoNet registry cohort.* Clin J Am Soc Nephrol, 2015. **10**(4): p. 592-600.
33. Watanabe, A., L.S. Feltran, and M.G. Sampson, *Genetics of Nephrotic Syndrome Presenting in Childhood: Core Curriculum 2019.* Am J Kidney Dis, 2019. **74**(4): p. 549-557.
34. Lipska-Zietkiewicz, B.S., et al., *Genetic aspects of congenital nephrotic syndrome: a consensus statement from the ERKNet-ESPN inherited glomerulopathy working group.* Eur J Hum Genet, 2020. **28**(10): p. 1368-1378.
35. Kitamura, A., et al., *A familial childhood-onset relapsing nephrotic syndrome.* Kidney Int, 2007. **71**(9): p. 946-51.
36. Lahdenkari, A.T., et al., *Nephrin gene (NPHS1) in patients with minimal change nephrotic syndrome (MCNS).* Kidney Int, 2004. **65**(5): p. 1856-63.
37. White, R.H., *The familial nephrotic syndrome. I. A European survey.* Clin Nephrol, 1973. **1**(4): p. 215-9.
38. Gee, H.Y., et al., *KANK deficiency leads to podocyte dysfunction and nephrotic syndrome.* J Clin Invest, 2015. **125**(6): p. 2375-84.

39. Gee, H.Y., et al., *Mutations in EMP2 cause childhood-onset nephrotic syndrome.* Am J Hum Genet, 2014. **94**(6): p. 884-90.
40. Roberts, I.S. and J.M. Gleadle, *Familial nephropathy and multiple exostoses with exostosin-1 (EXT1) gene mutation.* J Am Soc Nephrol, 2008. **19**(3): p. 450-3.
41. Dorval, G., et al., *Clinical and genetic heterogeneity in familial steroid-sensitive nephrotic syndrome.* Pediatr Nephrol, 2018. **33**(3): p. 473-483.
42. Banh, T.H., et al., *Ethnic Differences in Incidence and Outcomes of Childhood Nephrotic Syndrome.* Clin J Am Soc Nephrol, 2016. **11**(10): p. 1760-1768.
43. Gbadegesin, R.A., et al., *HLA-DQA1 and PLCG2 Are Candidate Risk Loci for Childhood-Onset Steroid-Sensitive Nephrotic Syndrome.* J Am Soc Nephrol, 2015. **26**(7): p. 1701-10.
44. Debiec, H., et al., *Transethnic, Genome-Wide Analysis Reveals Immune-Related Risk Alleles and Phenotypic Correlates in Pediatric Steroid-Sensitive Nephrotic Syndrome.* J Am Soc Nephrol, 2018. **29**(7): p. 2000-2013.
45. Jia, X., et al., *Strong Association of the HLA-DR/DQ Locus with Childhood Steroid-Sensitive Nephrotic Syndrome in the Japanese Population.* J Am Soc Nephrol, 2018. **29**(8): p. 2189-2199.
46. Karp, A.M. and R.A. Gbadegesin, *Genetics of childhood steroid-sensitive nephrotic syndrome.* Pediatr Nephrol, 2017. **32**(9): p. 1481-1488.
47. Ashraf, S., et al., *Mutations in six nephrosis genes delineate a pathogenic pathway amenable to treatment.* Nat Commun, 2018. **9**(1): p. 1960.
48. Shalhoub, R.J., *Pathogenesis of lipoid nephrosis: A disorder of T-cell function.* Lancet, 1974. **2**(7880): p. 556–560.
49. Koyama, A., et al., *A glomerular permeability factor produced by human T cell hybridomas.* Kidney Int, 1991. **40**(3): p. 453-60.
50. Lama, G., et al., *T-lymphocyte populations and cytokines in childhood nephrotic syndrome.* Am J Kidney Dis, 2002. **39**(5): p. 958-65.
51. Kemper, M.J., et al., *Changes of lymphocyte populations in pediatric steroid-sensitive nephrotic syndrome are more pronounced in remission than in relapse.* Am J Nephrol, 2005. **25**(2): p. 132-7.
52. Lapillonne, H., et al., *Stem cell mobilization in idiopathic steroid-sensitive nephrotic syndrome.* Pediatr Nephrol, 2008. **23**(8): p. 1251-6.
53. Shao, X.S., et al., *The prevalence of Th17 cells and FOXP3 regulate T cells (Treg) in children with primary nephrotic syndrome.* Pediatr Nephrol, 2009. **24**(9): p. 1683-90.
54. May, C.J., et al., *Human Th17 cells produce a soluble mediator that increases podocyte motility via signaling pathways that mimic PAR-1 activation.* Am J Physiol Renal Physiol, 2019. **317**(4): p. F913-F921.
55. Hashimura, Y., et al., *Minimal change nephrotic syndrome associated with immune dysregulation, polyendocrinopathy, enteropathy, X-linked syndrome.* Pediatr Nephrol, 2009. **24**(6): p. 1181-6.
56. Bertelli, R., et al., *Failure of regulation results in an amplified oxidation burst by neutrophils in children with primary nephrotic syndrome.* Clin Exp Immunol, 2010. **161**(1): p. 151-8.
57. Le Berre, L., et al., *Induction of T regulatory cells attenuates idiopathic nephrotic syndrome.* J Am Soc Nephrol, 2009. **20**(1): p. 57-67.
58. Bertelli, R., et al., *LPS nephropathy in mice is ameliorated by IL-2 independently of regulatory T cells activity.* PLoS One, 2014. **9**(10): p. e111285.

59. Tsuji, S., et al., *Idiopathic nephrotic syndrome in children: role of regulatory T cells and gut microbiota.* Pediatr Res, 2021. **89**(5): p. 1185-1191.
60. Tsuji, S. and K. Kaneko, *The long and winding road to the etiology of idiopathic nephrotic syndrome in children: Focusing on abnormalities in the gut microbiota.* Pediatr Int, 2021.
61. Yamaguchi, T., et al., *Clinical Significance of Probiotics for Children with Idiopathic Nephrotic Syndrome.* Nutrients, 2021. **13**(2).
62. Lai, K.W., et al., *Overexpression of interleukin-13 induces minimal-change-like nephropathy in rats.* J Am Soc Nephrol, 2007. **18**(5): p. 1476-85.
63. Le Berre, L., et al., *Renal macrophage activation and Th2 polarization precedes the development of nephrotic syndrome in Buffalo/Mna rats.* Kidney Int, 2005. **68**(5): p. 2079-90.
64. Park, S.J., et al., *Effects of interleukin-13 and montelukast on the expression of zonula occludens-1 in human podocytes.* Yonsei Med J, 2015. **56**(2): p. 426-32.
65. Colucci, M., et al., *Immunology of idiopathic nephrotic syndrome.* Pediatr Nephrol, 2018. **33**(4): p. 573-584.
66. Podesta, M.A. and C. Ponticelli, *Autoimmunity in Focal Segmental Glomerulosclerosis: A Long-Standing Yet Elusive Association.* Front Med (Lausanne), 2020. **7**: p. 604961.
67. Colucci, M., et al., *Atypical IgM on T cells predict relapse and steroid dependence in idiopathic nephrotic syndrome.* Kidney Int, 2019. **96**(4): p. 971-982.
68. Datta, S.K., *Anti-CD20 antibody is an efficient therapeutic tool for the selective removal of autoreactive T cells.* Nat Clin Pract Rheumatol, 2009. **5**(2): p. 80-2.
69. Bhatia, D., et al., *Rituximab modulates T- and B-lymphocyte subsets and urinary CD80 excretion in patients with steroid-dependent nephrotic syndrome.* Pediatr Res, 2018. **84**(4): p. 520-526.
70. Kemper, M.J., et al., *Combined T- and B-cell activation in childhood steroid-sensitive nephrotic syndrome.* Clin Nephrol, 2003. **60**(4): p. 242-7.
71. Colucci, M., et al., *B cell phenotype in pediatric idiopathic nephrotic syndrome.* Pediatr Nephrol, 2019. **34**(1): p. 177-181.
72. Colucci, M., et al., *B Cell Reconstitution after Rituximab Treatment in Idiopathic Nephrotic Syndrome.* J Am Soc Nephrol, 2016. **27**(6): p. 1811-22.
73. Sellier-Leclerc, A.L., et al., *Rituximab in steroid-dependent idiopathic nephrotic syndrome in childhood--follow-up after CD19 recovery.* Nephrol Dial Transplant, 2012. **27**(3): p. 1083-9.
74. Kim, A.H., et al., *B cell-derived IL-4 acts on podocytes to induce proteinuria and foot process effacement.* JCI Insight, 2017. **2**(21).
75. Jamin, A., et al., *Autoantibodies against podocytic UCHL1 are associated with idiopathic nephrotic syndrome relapses and induce proteinuria in mice.* J Autoimmun, 2018. **89**: p. 149-161.
76. Delville, M., et al., *A circulating antibody panel for pretransplant prediction of FSGS recurrence after kidney transplantation.* Sci Transl Med, 2014. **6**(256): p. 256ra136.
77. Akilesh, S., et al., *Podocytes use FcRn to clear IgG from the glomerular basement membrane.* Proc Natl Acad Sci U S A, 2008. **105**(3): p. 967-72.
78. Goldwich, A., et al., *Podocytes are nonhematopoietic professional antigen-presenting cells.* J Am Soc Nephrol, 2013. **24**(6): p. 906-16.

79. Krummey, S.M. and M.L. Ford, *Braking bad: novel mechanisms of CTLA-4 inhibition of T cell responses.* Am J Transplant, 2014. **14**(12): p. 2685-90.
80. Wing, K., et al., *CTLA-4 control over Foxp3+ regulatory T cell function.* Science, 2008. **322**(5899): p. 271-5.
81. Reiser, J. and P. Mundel, *Danger signaling by glomerular podocytes defines a novel function of inducible B7-1 in the pathogenesis of nephrotic syndrome.* J Am Soc Nephrol, 2004. **15**(9): p. 2246-8.
82. Yu, C.C., et al., *Abatacept in B7-1-positive proteinuric kidney disease.* N Engl J Med, 2013. **369**(25): p. 2416-23.
83. Garin, E.H., et al., *Urinary CD80 excretion increases in idiopathic minimal-change disease.* J Am Soc Nephrol, 2009. **20**(2): p. 260-6.
84. Garin, E.H., et al., *Urinary CD80 is elevated in minimal change disease but not in focal segmental glomerulosclerosis.* Kidney Int, 2010. **78**(3): p. 296-302.
85. Ling, C., et al., *Urinary CD80 levels as a diagnostic biomarker of minimal change disease.* Pediatr Nephrol, 2015. **30**(2): p. 309-16.
86. Bertelli, R., et al., *Regulatory T cells and minimal change nephropathy: in the midst of a complex network.* Clin Exp Immunol, 2016. **183**(2): p. 166-74.
87. Cara-Fuentes, G., et al., *Minimal change disease: a dysregulation of the podocyte CD80-CTLA-4 axis?* Pediatr Nephrol, 2014. **29**(12): p. 2333-40.
88. Shimada, M., et al., *Minimal change disease: a "two-hit" podocyte immune disorder?* Pediatr Nephrol, 2011. **26**(4): p. 645-9.
89. Delville, M., et al., *B7-1 Blockade Does Not Improve Post-Transplant Nephrotic Syndrome Caused by Recurrent FSGS.* J Am Soc Nephrol, 2016. **27**(8): p. 2520-7.
90. Garin, E.H., et al., *Case series: CTLA4-IgG1 therapy in minimal change disease and focal segmental glomerulosclerosis.* Pediatr Nephrol, 2015. **30**(3): p. 469-77.
91. Salant, D.J., *Podocyte Expression of B7-1/CD80: Is it a Reliable Biomarker for the Treatment of Proteinuric Kidney Diseases with Abatacept?* J Am Soc Nephrol, 2016. **27**(4): p. 963-5.
92. Ishimoto, T., et al., *Toll-like receptor 3 ligand, polyIC, induces proteinuria and glomerular CD80, and increases urinary CD80 in mice.* Nephrol Dial Transplant, 2013. **28**(6): p. 1439-46.
93. Uffing, A., et al., *Recurrence of FSGS after Kidney Transplantation in Adults.* Clin J Am Soc Nephrol, 2020. **15**(2): p. 247-256.
94. Maas, R.J., J.K. Deegens, and J.F. Wetzels, *Permeability factors in idiopathic nephrotic syndrome: historical perspectives and lessons for the future.* Nephrol Dial Transplant, 2014. **29**(12): p. 2207-16.
95. Matsumoto, K. and K. Kanmatsuse, *Transforming growth factor-beta1 inhibits vascular permeability factor release by T cells in normal subjects and in patients with minimal-change nephrotic syndrome.* Nephron, 2001. **87**(2): p. 111-7.
96. Cheung, P.K., et al., *Induction of experimental proteinuria in vivo following infusion of human plasma hemopexin.* Kidney Int, 2000. **57**(4): p. 1512-20.
97. Lennon, R., et al., *Hemopexin induces nephrin-dependent reorganization of the actin cytoskeleton in podocytes.* J Am Soc Nephrol, 2008. **19**(11): p. 2140-9.
98. Bakker, W.W., et al., *Altered activity of plasma hemopexin in patients with minimal change disease in relapse.* Pediatr Nephrol, 2005. **20**(10): p. 1410-5.

99. Bakker, W.W., et al., *Protease activity of plasma hemopexin.* Kidney Int, 2005. **68**(2): p. 603-10.
100. Wei, C., et al., *Circulating urokinase receptor as a cause of focal segmental glomerulosclerosis.* Nat Med, 2011. **17**(8): p. 952-60.
101. Meijers, B., et al., *The soluble urokinase receptor is not a clinical marker for focal segmental glomerulosclerosis.* Kidney Int, 2014. **85**(3): p. 636-40.
102. Wada, T., et al., *A multicenter cross-sectional study of circulating soluble urokinase receptor in Japanese patients with glomerular disease.* Kidney Int, 2014. **85**(3): p. 641-8.
103. Sinha, A., et al., *Serum-soluble urokinase receptor levels do not distinguish focal segmental glomerulosclerosis from other causes of nephrotic syndrome in children.* Kidney Int, 2014. **85**(3): p. 649-58.
104. Veissi, S., et al., *Nephrotic syndrome in a dish: recent developments in modeling in vitro.* Pediatr Nephrol, 2020. **35**(8): p. 1363-1372.
105. Rico, M., et al., *WT1-interacting protein and ZO-1 translocate into podocyte nuclei after puromycin aminonucleoside treatment.* Am J Physiol Renal Physiol, 2005. **289**(2): p. F431-41.
106. Koshikawa, M., et al., *Role of p38 mitogen-activated protein kinase activation in podocyte injury and proteinuria in experimental nephrotic syndrome.* J Am Soc Nephrol, 2005. **16**(9): p. 2690-701.
107. Trautmann, A., et al., *IPNA clinical practice recommendations for the diagnosis and management of children with steroid-resistant nephrotic syndrome.* Pediatr Nephrol, 2020. **35**(8): p. 1529-1561.
108. www.kdigo.org/clinical_practice_guidelines/pdf/KDIGO-GN-Guideline.pdf.
109. Schonenberger, E., et al., *The podocyte as a direct target of immunosuppressive agents.* Nephrol Dial Transplant, 2011. **26**(1): p. 18-24.
110. Sever, S. and M. Schiffer, *Actin dynamics at focal adhesions: a common endpoint and putative therapeutic target for proteinuric kidney diseases.* Kidney Int, 2018. **93**(6): p. 1298-1307.
111. Mallipattu, S.K. and J.C. He, *The podocyte as a direct target for treatment of glomerular disease?* Am J Physiol Renal Physiol, 2016. **311**(1): p. F46-51.
112. Lowenberg, M., et al., *Novel insights into mechanisms of glucocorticoid action and the development of new glucocorticoid receptor ligands.* Steroids, 2008. **73**(9-10): p. 1025-9.
113. Thaunat, O., et al., *Effect of Immunosuppressive Drugs on Humoral Allosensitization after Kidney Transplant.* J Am Soc Nephrol, 2016. **27**(7): p. 1890-900.
114. Ransom, R.F., et al., *Glucocorticoids protect and enhance recovery of cultured murine podocytes via actin filament stabilization.* Kidney Int, 2005. **68**(6): p. 2473-83.
115. Yu, S. and Y. Li, *Dexamethasone inhibits podocyte apoptosis by stabilizing the PI3K/Akt signal pathway.* Biomed Res Int, 2013. **2013**: p. 326986.
116. Azzi, J.R., M.H. Sayegh, and S.G. Mallat, *Calcineurin inhibitors: 40 years later, can't live without.* J Immunol, 2013. **191**(12): p. 5785-91.
117. Faul, C., et al., *The actin cytoskeleton of kidney podocytes is a direct target of the antiproteinuric effect of cyclosporine A.* Nat Med, 2008. **14**(9): p. 931-8.
118. Shengyou, Y., et al., *Influence of tacrolimus on podocyte injury inducted by angiotensin II.* J Renin Angiotensin Aldosterone Syst, 2015. **16**(2): p. 260-6.
119. Kemper, M.J., et al., *Is rituximab effective in childhood nephrotic syndrome? Yes and no.* Pediatr Nephrol, 2014. **29**(8): p. 1305-11.

120. Fornoni, A., et al., *Rituximab targets podocytes in recurrent focal segmental glomerulosclerosis.* Sci Transl Med, 2011. **3**(85): p. 85ra46.
121. Thery, C., et al., *Minimal information for studies of extracellular vesicles 2018 (MISEV2018): a position statement of the International Society for Extracellular Vesicles and update of the MISEV2014 guidelines.* J Extracell Vesicles, 2018. **7**(1): p. 1535750.
122. Kalluri, R. and V.S. LeBleu, *The biology, function, and biomedical applications of exosomes.* Science, 2020. **367**(6478).
123. Hessvik, N.P. and A. Llorente, *Current knowledge on exosome biogenesis and release.* Cell Mol Life Sci, 2018. **75**(2): p. 193-208.
124. Lv, L.L., et al., *New insight into the role of extracellular vesicles in kidney disease.* J Cell Mol Med, 2019. **23**(2): p. 731-739.
125. Lv, L.L., et al., *Therapeutic application of extracellular vesicles in kidney disease: promises and challenges.* J Cell Mol Med, 2018. **22**(2): p. 728-737.
126. Street, J.M., et al., *Exosomal transmission of functional aquaporin 2 in kidney cortical collecting duct cells.* J Physiol, 2011. **589**(Pt 24): p. 6119-27.
127. Pathare, G., et al., *Changes in V-ATPase subunits of human urinary exosomes reflect the renal response to acute acid/alkali loading and the defects in distal renal tubular acidosis.* Kidney Int, 2018. **93**(4): p. 871-880.
128. Corbetta, S., et al., *Urinary exosomes in the diagnosis of Gitelman and Bartter syndromes.* Nephrol Dial Transplant, 2015. **30**(4): p. 621-30.
129. Gildea, J.J., et al., *Exosomal transfer from human renal proximal tubule cells to distal tubule and collecting duct cells.* Clin Biochem, 2014. **47**(15): p. 89-94.
130. Oosthuyzen, W., et al., *Vasopressin Regulates Extracellular Vesicle Uptake by Kidney Collecting Duct Cells.* J Am Soc Nephrol, 2016. **27**(11): p. 3345-3355.
131. Gracia, T., et al., *Urinary Exosomes Contain MicroRNAs Capable of Paracrine Modulation of Tubular Transporters in Kidney.* Sci Rep, 2017. **7**: p. 40601.
132. Feigerlova, E., et al., *Extracellular vesicles as immune mediators in response to kidney injury.* Am J Physiol Renal Physiol, 2018. **314**(1): p. F9-F21.
133. Liu, X., et al., *Tubule-derived exosomes play a central role in fibroblast activation and kidney fibrosis.* Kidney Int, 2020. **97**(6): p. 1181-1195.
134. Wen, J., et al., *Decreased secretion and profibrotic activity of tubular exosomes in diabetic kidney disease.* Am J Physiol Renal Physiol, 2020. **319**(4): p. F664-F673.
135. Guan, H., et al., *Injured tubular epithelial cells activate fibroblasts to promote kidney fibrosis through miR-150-containing exosomes.* Exp Cell Res, 2020. **392**(2): p. 112007.
136. Jing, H., et al., *The role of extracellular vesicles in renal fibrosis.* Cell Death Dis, 2019. **10**(5): p. 367.
137. Borges, F.T., et al., *TGF-beta1-containing exosomes from injured epithelial cells activate fibroblasts to initiate tissue regenerative responses and fibrosis.* J Am Soc Nephrol, 2013. **24**(3): p. 385-92.
138. Lv, L.L., et al., *Exosomal CCL2 from Tubular Epithelial Cells Is Critical for Albumin-Induced Tubulointerstitial Inflammation.* J Am Soc Nephrol, 2018. **29**(3): p. 919-935.
139. Feng, Y., et al., *Urinary Exosomes and Exosomal CCL2 mRNA as Biomarkers of Active Histologic Injury in IgA Nephropathy.* Am J Pathol, 2018. **188**(11): p. 2542-2552.

140. Li, Z.L., et al., *HIF-1alpha inducing exosomal microRNA-23a expression mediates the cross-talk between tubular epithelial cells and macrophages in tubulointerstitial inflammation.* Kidney Int, 2019. **95**(2): p. 388-404.
141. Ding, C., et al., *Exosomal MicroRNA-374b-5p From Tubular Epithelial Cells Promoted M1 Macrophages Activation and Worsened Renal Ischemia/Reperfusion Injury.* Front Cell Dev Biol, 2020. **8**: p. 587693.
142. Li, M., et al., *High glucose provokes microvesicles generation from glomerular podocytes via NOX4/ROS pathway.* Biosci Rep, 2019. **39**(11).
143. Munkonda, M.N., et al., *Podocyte-derived microparticles promote proximal tubule fibrotic signaling via p38 MAPK and CD36.* J Extracell Vesicles, 2018. **7**(1): p. 1432206.
144. Huang, Y., et al., *Extracellular Vesicles From High Glucose-Treated Podocytes Induce Apoptosis of Proximal Tubular Epithelial Cells.* Front Physiol, 2020. **11**: p. 579296.
145. Chen, S.J., et al., *Crosstalk between tubular epithelial cells and glomerular endothelial cells in diabetic kidney disease.* Cell Prolif, 2020. **53**(3): p. e12763.
146. Wu, X., et al., *Exosomes from high glucose-treated glomerular endothelial cells trigger the epithelial-mesenchymal transition and dysfunction of podocytes.* Sci Rep, 2017. **7**(1): p. 9371.
147. Chen, T., et al., *Increased urinary exosomal microRNAs in children with idiopathic nephrotic syndrome.* EBioMedicine, 2019. **39**: p. 552-561.
148. Zhou, H., et al., *Urinary exosomal Wilms' tumor-1 as a potential biomarker for podocyte injury.* Am J Physiol Renal Physiol, 2013. **305**(4): p. F553-9.
149. Tang, T.T., et al., *Extracellular vesicle-encapsulated IL-10 as novel nanotherapeutics against ischemic AKI.* Sci Adv, 2020. **6**(33): p. eaaz0748.
150. Kalra, H., et al., *Vesiclepedia: a compendium for extracellular vesicles with continuous community annotation.* PLoS Biol, 2012. **10**(12): p. e1001450.
151. Perez-Riverol, Y., et al., *The PRIDE database and related tools and resources in 2019: improving support for quantification data.* Nucleic Acids Res, 2019. **47**(D1): p. D442-D450.
152. Khan, A.R., et al., *PD-L1hi B cells are critical regulators of humoral immunity.* Nat Commun, 2015. **6**: p. 5997.
153. Li, Y., et al., *EV-origin: Enumerating the tissue-cellular origin of circulating extracellular vesicles using exLR profile.* Comput Struct Biotechnol J, 2020. **18**: p. 2851-2859.
154. Adorisio, S., et al., *Glucocorticoid and PD-1 Cross-Talk: Does the Immune System Become Confused?* Cells, 2021. **10**(9).
155. Wu, H., et al., *PD-L1(+) regulatory B cells act as a T cell suppressor in a PD-L1-dependent manner in melanoma patients with bone metastasis.* Mol Immunol, 2020. **119**: p. 83-91.
156. Jia, X.Y., et al., *The role and clinical significance of programmed cell death-ligand 1 expressed on CD19(+)B-cells and subsets in systemic lupus erythematosus.* Clin Immunol, 2019. **198**: p. 89-99.
157. Tkach, M. and C. Thery, *Communication by Extracellular Vesicles: Where We Are and Where We Need to Go.* Cell, 2016. **164**(6): p. 1226-1232.
158. Kosaka, N., et al., *Exploiting the message from cancer: the diagnostic value of extracellular vesicles for clinical applications.* Exp Mol Med, 2019. **51**(3): p. 1-9.

159. Martinez del Hoyo, G., et al., *CD81 controls immunity to Listeria infection through rac-dependent inhibition of proinflammatory mediator release and activation of cytotoxic T cells.* J Immunol, 2015. **194**(12): p. 6090-101.
160. Pitt, J.M., G. Kroemer, and L. Zitvogel, *Extracellular vesicles: masters of intercellular communication and potential clinical interventions.* J Clin Invest, 2016. **126**(4): p. 1139-43.
161. Tian, Y., et al., *Quality and efficiency assessment of six extracellular vesicle isolation methods by nano-flow cytometry.* J Extracell Vesicles, 2020. **9**(1): p. 1697028.
162. Brennan, K., et al., *A comparison of methods for the isolation and separation of extracellular vesicles from protein and lipid particles in human serum.* Sci Rep, 2020. **10**(1): p. 1039.
163. Palviainen, M., et al., *Extracellular vesicles from human plasma and serum are carriers of extravesicular cargo-Implications for biomarker discovery.* PLoS One, 2020. **15**(8): p. e0236439.
164. Tkach, M., et al., *Qualitative differences in T-cell activation by dendritic cell-derived extracellular vesicle subtypes.* EMBO J, 2017. **36**(20): p. 3012-3028.
165. Tkach, M., J. Kowal, and C. Thery, *Why the need and how to approach the functional diversity of extracellular vesicles.* Philos Trans R Soc Lond B Biol Sci, 2018. **373**(1737).
166. Iba, T. and H. Ogura, *Role of extracellular vesicles in the development of sepsis-induced coagulopathy.* J Intensive Care, 2018. **6**: p. 68.
167. Choi, Y.W., et al., *Potential urine proteomics biomarkers for primary nephrotic syndrome.* Clin Proteomics, 2017. **14**: p. 18.
168. Cheng, Y., et al., *A translational study of urine miRNAs in acute myocardial infarction.* J Mol Cell Cardiol, 2012. **53**(5): p. 668-76.
169. Uil, M., et al., *Cellular origin and microRNA profiles of circulating extracellular vesicles in different stages of diabetic nephropathy.* Clin Kidney J, 2021. **14**(1): p. 358-365.
170. Simeone, P., et al., *Extracellular Vesicles as Signaling Mediators and Disease Biomarkers across Biological Barriers.* Int J Mol Sci, 2020. **21**(7).
171. Harris, J.J., et al., *Active proteases in nephrotic plasma lead to a podocin-dependent phosphorylation of VASP in podocytes via protease activated receptor-1.* J Pathol, 2013. **229**(5): p. 660-71.
172. Mashouri, L., et al., *Exosomes: composition, biogenesis, and mechanisms in cancer metastasis and drug resistance.* Mol Cancer, 2019. **18**(1): p. 75.
173. Sung, B.H. and A.M. Weaver, *Exosome secretion promotes chemotaxis of cancer cells.* Cell Adh Migr, 2017. **11**(2): p. 187-195.
174. Sung, B.H., et al., *Directional cell movement through tissues is controlled by exosome secretion.* Nat Commun, 2015. **6**: p. 7164.
175. Hoshino, D., et al., *Exosome secretion is enhanced by invadopodia and drives invasive behavior.* Cell Rep, 2013. **5**(5): p. 1159-68.
176. Yu, H., et al., *Rac1 activation in podocytes induces rapid foot process effacement and proteinuria.* Mol Cell Biol, 2013. **33**(23): p. 4755-64.
177. Antonyak, M.A., K.F. Wilson, and R.A. Cerione, *R(h)oads to microvesicles.* Small GTPases, 2012. **3**(4): p. 219-24.
178. Sexton, R.E., et al., *Ras and exosome signaling.* Semin Cancer Biol, 2019. **54**: p. 131-137.

179. Gopal, S.K., et al., *Oncogenic epithelial cell-derived exosomes containing Rac1 and PAK2 induce angiogenesis in recipient endothelial cells.* Oncotarget, 2016. **7**(15): p. 19709-22.
180. Shankland, S.J., et al., *Podocytes in culture: past, present, and future.* Kidney Int, 2007. **72**(1): p. 26-36.

Copyright Permissions

Order Summary

Licensee:	Dr. Fehime Kara Eroğlu
Order Date:	Sep 21, 2021
Order Number:	5153860339407
Publication:	Nature Reviews Disease Primers
Title:	Podocytopathies
Type of Use:	Thesis/Dissertation
Order Total:	0.00 EUR

View or print complete details of your order and the publisher's terms and conditions.

Sincerely,

Copyright Clearance Center

Tel: +1-855-239-3415 / +1-978-646-2777
customercare@copyright.com
https://myaccount.copyright.com

Thank you for placing your order through Copyright Clearance Center's RightsLink® service.

Order Summary

Licensee:	Dr. Fehime Kara Eroğlu
Order Date:	Sep 21, 2021
Order Number:	5153870250693
Publication:	Nature Reviews Nephrology
Title:	Podocyte–actin dynamics in health and disease
Type of Use:	Thesis/Dissertation
Order Total:	0.00 EUR

View or print complete details of your order and the publisher's terms and conditions.

Sincerely,

Copyright Clearance Center

Tel: +1-855-239-3415 / +1-978-646-2777
customercare@copyright.com
https://myaccount.copyright.com

Dear Dr. Fehime Kara Eroğlu,

Thank you for placing your order through Copyright Clearance Center's RightsLink® service.

Order Summary

Licensee:	Dr. Fehime Kara Eroğlu
Order Date:	Sep 21, 2021
Order Number:	5153870524774
Publication:	Kidney International
Title:	Rho GTPase regulatory proteins in podocytes
Type of Use:	reuse in a thesis/dissertation
Order Total:	0.00 EUR

View or print complete details of your order and the publisher's terms and conditions.

Sincerely,

Copyright Clearance Center

Tel: +1-855-239-3415 / +1-978-646-2777
customercare@copyright.com
https://myaccount.copyright.com

Thank you for placing your order through Copyright Clearance Center's RightsLink® service.

Order Summary

Licensee:	Dr. Fehime Kara Eroğlu
Order Date:	Sep 21, 2021
Order Number:	5153870629799
Publication:	The Lancet
Title:	Idiopathic nephrotic syndrome in children
Type of Use:	reuse in a thesis/dissertation
Order Total:	0.00 EUR

View or print complete details of your order and the publisher's terms and conditions.

Sincerely,

Copyright Clearance Center

Tel: +1-855-239-3415 / +1-978-646-2777
customercare@copyright.com
https://myaccount.copyright.com

Dear Dr. Fehime Kara Eroğlu,

Thank you for placing your order through Copyright Clearance Center's RightsLink® service.

Order Summary

Licensee:	Dr. Fehime Kara Eroğlu
Order Date:	Sep 21, 2021
Order Number:	5153880289458
Publication:	Science
Title:	The biology, function, and biomedical applications of exosomes
Type of Use:	Thesis / Dissertation
Order Total:	0.00 EUR

View or print complete details of your order and the publisher's terms and conditions.

Sincerely,

Copyright Clearance Center

Tel: +1-855-239-3415 / +1-978-646-2777
customercare@copyright.com
https://myaccount.copyright.com

Marketplace

This is a License Agreement between Fehime Kara Erğlu ("User") and Copyright Clearance Center, Inc. ("CCC") on behalf of the Rightsholder identified in the order details below. The license consists of the order details, the CCC Terms and Conditions below, and any Rightsholder Terms and Conditions which are included below.

All payments must be made in full to CCC in accordance with the CCC Terms and Conditions below.

Order Date	22-Sep-2021	Type of Use	Republish in a thesis/dissertation
Order License ID	1149245-1		
ISSN	1533-3450	Publisher	AMERICAN SOCIETY OF NEPHROLOGY
		Portion	Image/photo/illustration

LICENSED CONTENT

Publication Title	Journal of the American Society of Nephrology	Country	United States of America
		Rightsholder	American Society of Nephrology
Author/Editor	American Society of Nephrology.	Publication Type	e-Journal
Date	01/01/1990	URL	https://jasn.asnjournals.org/
Language	English		

REQUEST DETAILS

Portion Type	Image/photo/illustration	Distribution	Worldwide
Number of images / photos / illustrations	1	Translation	Original language of publication
Format (select all that apply)	Print	Copies for the disabled?	No
		Minor editing privileges?	Yes
Who will republish the content?	Academic institution	Incidental promotional use?	No
Duration of Use	Life of current edition	Currency	EUR
Lifetime Unit Quantity	Up to 499		
Rights Requested	Main product		

NEW WORK DETAILS

Title	CHARACTERIZATION OF FUNCTIONAL AND MOLECULAR PROPERTIES OF CIRCULATING EXTRACELLULAR VESICLES OF CHILDHOOD IDIOPATHIC NEPHROTIC SYNDROME PATIENTS	Institution name	Bilkent University
		Expected presentation date	2021-10-01
Instructor name	Fehime Kara Eroğlu		

ADDITIONAL DETAILS

Thank you for placing your order through Copyright Clearance Center's RightsLink® service.

Order Summary

Licensee:	Dr. Fehime Kara Eroğlu
Order Date:	Sep 21, 2021
Order Number:	5153870800295
Publication:	Pediatric Nephrology
Title:	Immunology of idiopathic nephrotic syndrome
Type of Use:	Thesis/Dissertation
Order Total:	0.00 EUR

View or print complete details of your order and the publisher's terms and conditions.

Sincerely,

Copyright Clearance Center

Tel: +1-855-239-3415 / +1-978-646-2777
customercare@copyright.com
https://myaccount.copyright.com

RightsLink®

Rights Requested	Main product		
NEW WORK DETAILS			
Title	CHARACTERIZATION OF FUNCTIONAL AND MOLECULAR PROPERTIES OF CIRCULATING EXTRACELLULAR VESICLES OF CHILDHOOD IDIOPATHIC NEPHROTIC SYNDROME PATIENTS	Institution name	Bilkent University
		Expected presentation date	2021-10-01
Instructor name	Fehime Kara Eroğlu		
ADDITIONAL DETAILS			
The requesting person / organization to appear on the license	Fehime Kara Eroğlu		
REUSE CONTENT DETAILS			
Title, description or numeric reference of the portion(s)	Figure 1	Title of the article/chapter the portion is from	The Evolving Complexity of the Podocyte Cytoskeleton
Editor of portion(s)	Christoph Schell	Author of portion(s)	American Society of Nephrology.
Volume of serial or monograph	28	Publication date of portion	2017-01-18
Page or page range of portion	3167		

RightsLink®

Help | Email Support

SPRINGER NATURE

Current knowledge on exosome biogenesis and release

Author: Nina Pettersen Hessvik et al

Publication: Cellular and Molecular Life Sciences

Publisher: Springer Nature

Date: Jul 21, 2017

Contact

E-mail
fehimekara@yahoo.com

Languages

English
German (Intermediate)

Education

1999/09 – 2005/06	**M.D.** *Hacettepe University, Faculty of Medicine* - Ankara
2005/09 – 2011/05	**Pediatrician** *Hacettepe University, Department of Pediatrics* - Ankara
2011/11 – 2015/05	**Pediatric Nephrologist** *Hacettepe University, Div. of Pediatric Nephrology*
2011/09 – 2015/06	**Master of Science: Hereditary Autoinflammatory Diseases** *Hacettepe Uni. Graduate School of Health Sciences* - Ankara
2014/09 - Current	**Ph.D.: Molecular Immunology** *Bilkent Uni., Molecular Biolology and Genetics* - Ankara

Academic Title

From **Associate Professor of Pediatrics**

23.10.2019

Working Experience

2016/01 – 2020/08 **Pediatric Nephrology Consultant**

Dr. Sami Ulus Maternity and Children's Hospital, Ankara

Publications

1. Ozen S, **Eroglu FK**. Pediatric onset Behçet's Disease. CURRENT OPINION IN RHEUMATOLOGY 2013, 25(5), 636-642.
2. Ozantürk A, Marshall JD, Collin GB, Düzenli S, Marshall RP, Candan Ş, Tos T, Esen İ, Taşkesen M, Çayır A, Öztürk Ş, Üstün İ, Ataman E,Karaca E, Özdemir TR, Erol İ, **Eroğlu FK**, ..., Naggert JK, Özgül RK. The phenotypic and molecular spectrum of Alström syndrome in 44 Turkish kindreds and a literature review of Alström syndrome in Turkey. JOURNAL OF HUMAN GENETICS 2015, 60(1), 1-9.
3. Eroglu FK, Besbas N, Ozaltin F, Topaloglu R, Ozen S. Lupus in a patient with cystinosis: is it drug induced? LUPUS 2015, 24(13), 1452-1454.
4. Eroglu FK, Beşbaş N, Topaloglu R, Ozen S. Treatment of colchicine-resistant Familial Mediterranean fever in children and adolescents. RHEUMATOLOGY INTERNATIONAL 2015, 35(10), 1733-1737.
5. Chia J, **Eroglu FK**, Özen S, et al. Failure to thrive, interstitial lung disease, and progressive digital necrosis with onset in infancy. JOURNAL OF THE AMERICAN ACADEMY OF DERMATOLOGY 2016, 74(1), 186-189.
6. Eroglu FK, Kasapcopur O, Beşbaş N, et al. Genetic and clinical features of cryopyrin-associated periodic syndromes in Turkish children. Clin Exp Rheumatol. 2016 Sep-Oct;34(6 Suppl 102): S115-S120.
7. Isiyel E, Ezgu SA, Caliskan S, Akman S, Akil I, Tabel Y, Akinci N, Ozdogan EB, Ozel A, **Eroglu FK**, Ezgu FS. Molecular analysis of the AGXT gene in patients suspected with hyperoxaluria type 1 and three novel mutations from Turkey. MOLECULAR GENETICS AND METABOLISM 2016, 119(4), 311-316.
8. Gul E, Sayar EH, Gungor B, **Eroglu FK**, ..., Gursel I, Ozen S, Reisli I, Gursel M. Type I IFN-related NETosis in ataxia telangiectasia and

Artemis deficiency. JOURNAL OF ALLERGY AND CLINICAL IMMUNOLOGY 2018, 142(1), 246-257.
9. Akkaya-Ulum YZ, Balci-Peynircioglu B, Karadag O, **Eroglu FK**, Kalyoncu U, Kiraz S, Ertenli AI, Özen S, Yilmaz E. Alteration of the microRNA expression profile in familial Mediterranean fever patients. CLINICAL AND EXPERIMENTAL RHEUMATOLOGY 2017, 35(6), 90-94.
10. Çakıcı EK, **Eroğlu FK**, Yazılıtaş F, Bülbül M, Gür G, Aydoğ Ö, Güngör T, Erel Ö, Alışık M, Elhan AH. Evaluation of the level of dynamic thiol/disulphide homeostasis in adolescent patients with newly diagnosed primary hypertension. PEDIATRIC NEPHROLOGY 2018, 33(5), 847-853.
11. Yazılıtaş F, Aydoğ Ö, Özlü SG, Çakıcı EK, Güngör T, Eroğlu FK, Gür G, Bülbül M. Canakinumab treatment in children with familial Mediterranean fever: report from a single center. RHEUMATOLOGY INTERNATIONAL 2018, 38(5), 879-885.
12. Eroglu FK, Aerts Kaya F, Cagdas D, Özgür TT, Yılmaz T, Tezcan İ, Sanal Ö. B lymphocyte subsets and outcomes in patients with an initial diagnosis of transient hypogammaglobulinemia of infancy. SCANDINAVIAN JOURNAL OF IMMUNOLOGY 2018, 88(4), Doi: 10.1111/sji.12709
13. Eroglu FK, Kargın Çakıcı E, Can Gür G, et al. Retrospective Analysis of Simple and Stage II Renal Cysts: Pediatric Nephrology Point of View. PEDIATRICS INTERNATIONAL 2018, 60(12), 1068-1072.
14. Eroglu FK, Ozaltin F, Gönç N, ..., Topaloğlu R, Düzova A. Response to Early Coenzyme Q10 Supplementation Is not Sustained in CoQ10 Deficiency Caused by CoQ2 Mutation. PEDIATRIC NEUROLOGY 2018, 88, 71-74.
15. Cakici EK, Aydog O, **Eroglu FK**, et al. Value of renal pelvic diameter and urinary tract dilation classification in the prediction of urinary tract anomaly. PEDIATRICS INTERNATIONAL 2019 Mar;61 (3):271-277.
16. Cakici EK, Şükür EDK, Özlü SG, Yazılıtaş F, Özdel S, Gür G, **Eroğlu FK**, Güngör T, Çelikkaya E, Bağlan E, Bülbül M. MEFV gene mutations in children with Henoch-Schönlein purpura and their correlations-do mutations matter? CLINICAL RHEUMATOLOGY 2019 Jul;38(7):1947-1952
17. Çakıcı EK, Gür G, Yazılıtaş F, **Eroğlu FK**, Güngör T, Arda N, Orhan D, Özalp Ateş FS, Bülbül M. A retrospective analysis of children with Henoch-Schonlein purpura and re-evaluation of renal pathologies using Oxford classification. CLINICAL and EXPERIMENTAL NEPHROLOGY Clin Exp Nephrol. 2019 Jul;23(7):939-947.
18. Eroglu FK, Orhan D, İnözü M, Duzova A, Gulhan B, Ozaltin F, Topaloglu R. CD80 expression and infiltrating regulatory T cells in idiopathic nephrotic syndrome of childhood. PEDIATRICS INTERNATIONAL 2019 Sep 12. doi: 10.1111/ped.14005.
19. Güngör T, Çakıcı EK, Yazılıtaş F, **Eroğlu FK**, Özdel S, Kurt-Sukur ED, Çelikkaya E, Karakaya D, Bağlan E, Bülbül M. Clinical Characteristics of Childhood Acute Tubulointerstitial Nephritis. PEDIATRİCS INT. 2020 Oct 5. doi: 10.1111/ped.14495.
20. Ozdemir G, Gulhan B, Atayar E, Saygılı S, Soylemezoglu O, Ozcakar ZB, **Eroglu FK**, …, Topaloglu R. COL4A3 mutation is an independent risk factor for poor prognosis in children with Alport

syndrome. PEDİATR. NEPHROL. 2020 Oct;35(10):1941-1952. doi: 10.1007/s00467-020-04574-8.
21. Güngör T, **Eroğlu FK**, Yazılıtaş F, Gür G, Çakıcı EK, Ludwig M, Bülbül M. A case of Type 1 Dent disease presenting with isolated persistent proteinuria. Turk Pediatri Ars. 2020 Mar 9;55(1):72-75. doi: 10.5152/TURKPEDİATRİARS2018.6540.
22. Güngör T, **Eroğlu FK**, Kargın Çakıcı E, Yazılıtaş F, Can G, Çelikkaya E, Karakaya D, Kurt Şükür ED, Özaltın F, Yağız B, Bülbül M. Gastric duplication cyst in an infant with Finnish-type congenital nephrotic syndrome: concurrence or coincidence? ACTA CLIN BELG. 2019 Oct 5:1-3. doi: 10.1080/17843286.2019.1675333.
23. Balat A, Kilic BD, Aksu B, Kara MA, Buyukcelik M, Agbas A, **Eroglu FK**, Gungor T, …, Sonmez F. Kidney disease profile and encountered problems during follow-up in Syrian refugee children: a multicenter retrospective study. PEDIATR NEPHROL. 2021 Jul 31. doi: 10.1007/s00467-021-05046-3.

PhD Thesis

Eroglu FK, Yazar V, Guler U, Yıldırım M, Yildirim T, Gungor T, Celikkaya E, Karakaya D, Turay N, Ciftci Dede E, Korkusuz P, Salih B, Bulbul M, Gursel I. Circulating extracellular vesicles of steroid sensitive nephrotic syndrome patients have higher RAC1 and induce recapitulation of nephrotic syndrome phenotype in podocytes. AM J PHYSIOL Renal Physiol. 2021 Sep 27. doi: 10.1152/ajprenal.00097.2021.

Oral Presentations

51th ESPN Congress, Antalya, Turkey

Eroglu, F. K., Yildirim, M., Kaya, G., Gungor, T., Can, G. G., Cakici, E. K., ... & Gursel, I. (2018, October). EXOSOMES FROM IDIOPATHIC NEPHROTIC SYNDROME PATIENTS EXACERBATES IMMUNE DYSREGULATION. In PEDIATRIC NEPHROLOGY (Vol. 33, No. 10, pp. 1822-1822).

50th ESPN Congress, Glasgow, UK

Eroglu, F. K., Topaloglu, R., Karagoz, T., Oguz, B., Ozaltin, F., Gulhan, B., & Duzova, A. (2017, September). RISK FACTORS FOR CARDIOVASCULAR COMORBIDITIES IN CHILDREN WITH STEROID-SENSITIVE AND STEROID-RESISTANT NEPHROTIC SYNDROME. In PEDIATRIC NEPHROLOGY (Vol. 32, No. 9, pp. 1661-1661).

14th ISSAID Congress, Dresden, Germany
F Kara Eroglu, I Gursel, M Gursel, A Duzova, AA de Jesus, RT Goldbach-Mansky, S Ozen. STING-associated vasculopathy with onset in infancy: new clinical findings and mutation in three Turkish children. In Pediatric Rheumatology 13 (S1), O85.

Research Experiences

2008 Observership Supervisor: Fatma Dedeoglu. Boston's Children Hospital, Division of Pediatric Rheumatology

Membership

2017- European Society of Pediatric Nephrology

Certifications

2015-01 Board Certificate of Turkish Pediatric Nephrology Society

Certificate for Use of Experimental Animals

2017-09

Board Certificate of European Society of Pediatric

2021-01 Nephrology

Leadership Experience

2009-2010 Chief Residency, Hacettepe University, Department of Pediatrics (Elected by department members among 12 residents, given responsibility of all teaching activities, inpatient care and intensive care patients)